Characterization in Cochlea of *KCTD12/PFET1*, An Intronless Gene with Predominant Fetal Expression

by

Sharon Fan Kuo

B.S. Biochemistry, Tufts University, 1997
B.M. Piano Performance, New England Conservatory of Music, 1997

Submitted to the Harvard-MIT Division of Health Sciences and Technology
in partial fulfillment of the requirements for the degree of

Doctor of Philosophy

in the Program of Speech and Hearing Bioscience and Technology

Massachusetts Institute of Technology
Cambridge, Massachusetts
[February 2006]
December 2005

Signature of Author.....
Speech and Hearing Bioscience and Technology
Feb. 13, 2006

Certified by.....
Cynthia C. Morton
William Lambert Richardson Professor of Obstetrics, Gynecology and Reproductive Biology
and Professor of Pathology, Harvard Medical School
Thesis Supervisor

Accepted by.....
Martha L. Gray, Ph.D.
Edward Hood Taplin Professor on Medical & Electrical Engineering
Director, Harvard-MIT Division of Health Sciences and Technology

Characterization in Cochlea of *KCTD12/PFET1*, An Intronless Gene with Predominant Fetal Expression

by

Sharon Fan Kuo

Submitted to the Harvard-MIT Division of Health Sciences and Technology
in December 2005 in partial fulfillment of the requirements for the degree of
Doctor of Philosophy in Speech and Hearing Bioscience and Technology

Abstract

The prevalence of severe to profound bilateral congenital hearing loss is estimated at 1 in 1000 births, at least half of which can be attributed to a genetic cause. To date, mutations in at least 67 genes have been associated with hearing loss. Discovery of these genes has revealed fundamental processes within the ear, and enabled diagnosis and implementation of genetic counseling in affected patients. As a part of the continuing effort to study genes important for hearing and deafness, a novel cochlear transcript with predominantly fetal expression containing a single tetramerization domain (*PFET1*, HUGO-approved symbol *KCTD12*) was identified from the Morton fetal cochlear cDNA library. *KCTD12/Kctd12* is an evolutionarily conserved intronless gene encoding a 6 kb transcript in human and three transcripts of approximately 4, 4.5 and 6 kb in mouse. The protein, pfetin, is predicted to contain a voltage-gated potassium channel tetramerization (T1) domain. This thesis reports characterization of this novel human gene and its encoded protein pfetin in relation to its role in auditory function. Experimental data from tissue and cellular expression profiling, and genetic and functional analyses suggests *KCTD12* and its orthologs playing a crucial role in the developmental of the auditory sense organ.

Thesis Supervisor: **Cynthia C. Morton**
Title: William Lambert Richardson Professor of Obstetrics, Gynecology and Reproductive Biology and Professor of Pathology, Harvard Medical School; Director of Cytogenetics, Brigham and Women's Hospital

For my family

ACKNOWLEDGEMENTS

I would like to thank my thesis committee: David Corey, Douglas Cotanche, Stefan Heller, and Charles Liberman for their guidance and support over the last few years.

My heartfelt thanks to Cynthia Morton my research advisor for her unwavering support and encouragement through my exploration in the field of genetic hearing loss and my pursuit of clinical certification in speech and language pathology.

I was fortunate through this joint program to have directly worked with so many wonderful individuals from different areas of expertise. This thesis would not have been possible with out their generosity and kindness.

To my parents, thank you for your love, understanding and support through this incredible journey.

SK's Interaction and Functional Domain

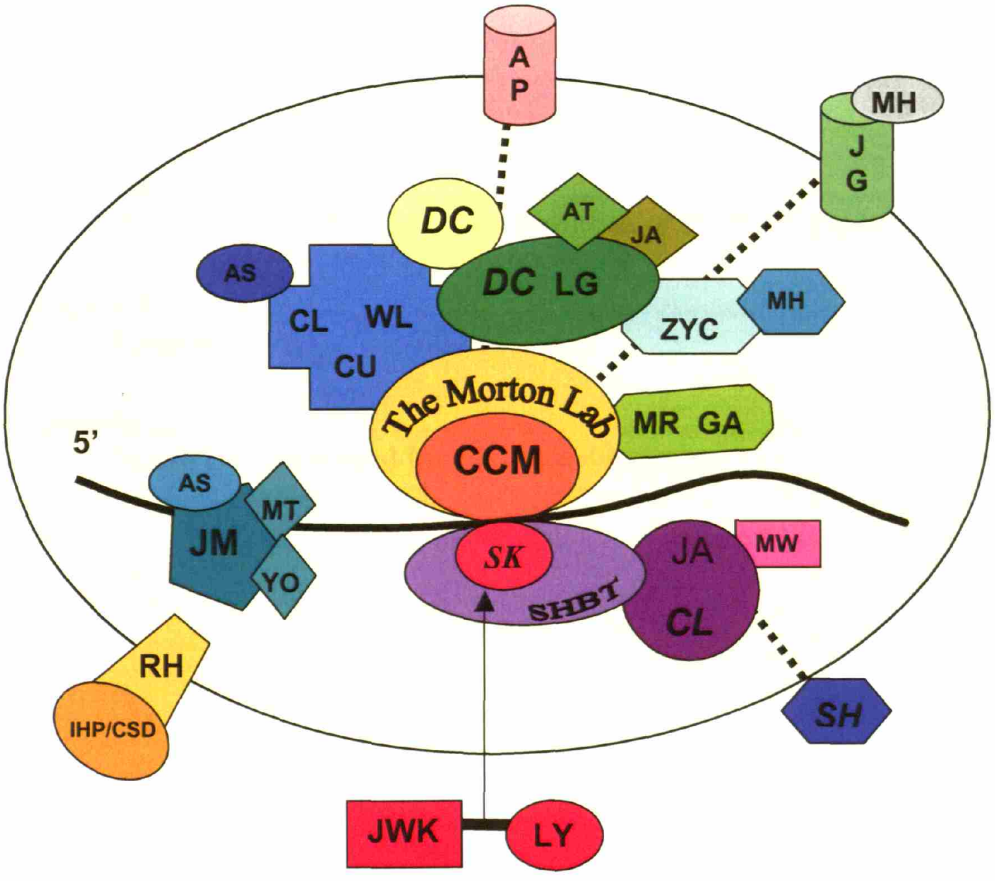

AP: Arti Pandya
AS: Andria Schibler
AS: Amanda Smith
AT: Andrew Tucker
CL: Charles Lee
CL: Charles Liberman
CM: Cynthia Morton
CU: Chinweike Ukomadu
DC: David Corey
DC: Douglas Cotanche
GA: Gil Alterovitz
JA: Jessica Appler
JA: Joe Adams
JG: Joshua Gamse
JM: Jarema Malicki
LG: Lisa Goodrich
MH: Marnie Halpern
MH: Mingqian Huang
MR: Marco Ramoni
MT: Motokazu Tsujikawa
MW: Melissa Wood
RH: Robert Hillman
SH: Stefan Heller
WL: Weining Lu
YO: Yoshihiro Omori
ZYC: Zheng-Yi Chen

LY +JWK: Mom + Dad

SHBT:
Speech and Hearing Bioscience and Technology

IHP/CSD:

TABLE OF CONTENTS

LIST OF FIGURES AND TABLES

CHAPTER 1

Hearing loss is the most common sensory disorder in the human population with the incidence of congenital hearing loss estimated at 1 in 1000 births (Morton 1991). It is estimated that 50% to 75% of all childhood deafness is due to hereditary causes (Gorlin 1995). The remainder is due to environmental factors including acoustic trauma, ototoxic drugs (*e.g.*, aminoglycosides), bacterial and viral infections. Of the hearing disorders with a genetic contribution, roughly 70% are classified as nonsyndromic and 30% as syndromic, depending on the presence or absence of other clinical features (http://webhost.ua.ac.be/hhh/). To date, mutations in at least 67 genes have been associated with hearing loss. Discovery of these genes has revealed fundamental processes within the ear, and enabled diagnosis and implementation of more accurate genetic counseling for families and affected patients.

The auditory apparatus consists of three major compartments, the external, middle and inner ear. The external ear consists of the auricle and the external auditory canal. It is bounded at the external-middle ear junction by the tympanic membrane. The middle ear is an air-filled cavity containing a chain of three ossicles (malleus, incus, stapes). The inner ear resides in the temporal bone of the skull, and is a complex membranous labyrinth filled with endolymph housed inside a perilymph-filled bony labyrinth. The snail-like portion of this labyrinth is called the cochlea, the auditory sense organ. It resides in the inner ear along with the vestibule. The human cochlea detects sound frequencies between 20 Hz and 20 kHz and the vestibule (saccule, utricle, three semicircular canals) responds to linear and angular accelerations. The cochlea and the vestibule both derive embryologically from the otic placode (Fekete 1996) and share several structural and functional features.

Briefly, the mammalian hearing process functions as follows. Sound waves travel through the external ear canal to the tympanic membrane (TM) where sound pressure sets the

TM into vibration. The ossicular chain, attached at one end to the TM, contacts the cochlea via the oval window. Vibration creates a traveling wave in the endolymph down the length of the cochlea, and the traveling wave sets into motion the basilar membrane (on which rests a cellular layer known as the organ of Corti lined with auditory hair cells), inducing movement of these hair cells relative to the tectorial membrane. Deflection of the hair cells leads to their depolarization, triggering neurotransmitter release, and creating an action potential traveling along the auditory nerve to the brain which encodes different characteristics of the sound stimulus including intensity, time course, and frequency.

Genes Involved in Hearing Disorders

Gene mutations have been found affecting almost every part of the auditory system from the shape of the ear lobe, to the middle ear and the auditory neurons in the brain. However, many encoded protein of genes responsible for deafness have been found to be expressed in the cochlea. The cochlea is a most intricate and complex organ consisting of dozens of cell types and specialized regions required for normal auditory function. Therefore, genes underlying the molecular development, structure, function and maintenance of these cell types and regions are crucial to the hearing process. As mentioned previously, mutations in at least 67 genes have been identified to show association with hearing loss. These genes encode a wide variety of proteins, including gap junctions, ion channels, extracellular matrix components and transcription factors.

Hair Cell Organization and Function

One of the most important structures in the cochlea is the auditory hair cells. These hair cells are highly organized and convert mechanical vibration into nerve impulses, and require precise structural maintenance for proper function. Mouse mutant studies have been instrumental in identifying a number of deafness-associated genes that are required for the proper organization and maintenance of hair cell stereocilia such as *Myo7a*, *Myo6*, *Cdh23*, *Pcdh15*, *Itga8*, *Espn* and *Tmie*. Most of the human orthologs when mutated result in hearing disorders: *MYO7A* for DFNB2, DFNA11 and USH1B (Liu et al. 1997); *MYO15A* for DFNB3 (Wang et al. 1998); *CDH23* for both DFNB12 and USH1D (Bolz et al. 2001); *PCDH15* for USH1F (Ahmed et al. 2001); *ESPN* for DFNB36 (Naz et al. 2004); and *TMIE* for DFNB6 (Naz et al. 2002). In addition, mutation in *MYO6* results in the disorganization and fusion of stereocilia and accounts for the nonsyndromic autosomal dominant hearing loss in an Italian family (Melchionda et al. 2001). A defect in harmonin, a PDZ domain-containing protein expressed in the inner ear sensory hair cells, underlies USH1C (Verpy et al. 2000) and defects in whirlin, a PDZ domain molecule involved in stereocilia elongation, cause deafness in the whirler mouse and families with DFNB31 (Mburu et al. 2003).

Extracellular Matrix

The extracellular matrix (ECM) is a complex structural entity surrounding and supporting cells that are found within mammalian tissues. The ECM is composed of three major classes of biomolecules: structural proteins like collagen and elastin; specialized proteins such as fibrillin, fibronectin, and laminin; and proteoglycans.

Collagens are crucial for the structural integrity of many organ systems including the inner ear. Several collagens responsible for deafness include *COL4A5, COL4A3* and *COL4A4* for both X-linked and autosomal forms of Alport syndrome; *COL1A1* and *COL1A2* for osteogenesis imperfecta (OI); *COL2A1* for Stickler syndrome type I (STL1); *COL11A2* for Stickler syndrome type II (STL2) and DFNA13; *COL11A1* for Stickler syndrome type III (STL3) (reviewed in Resendes et al. 2001 and Smith et al. 2005). Mutations in *COL9A3* have recently been identified in patients with nonsyndromic hearing impairment with moderate progressive bilateral sensorineural hearing loss in all frequencies (Asamura et al. 2005). Other extracellular matrix proteins like usherin that is responsible for Usher syndrome type 2A (USH2A) (Eudy et al. 1998) contain both laminin epidermal growth factor and fibronectin type III motifs, which are most commonly observed in proteins comprising components of the basal lamina and extracellular matrixes and in cell adhesion molecules. The tectorial membrane is also an extracellular matrix of the inner ear that contacts the stereocilia bundles of specialized sensory hair cells. Mutations in *TECTA* causing defects in the membrane are etiologic for hearing disorders DFNA8 and DFNA12 (Verhoeven et al. 1998) and DFNB21 (Mustapha et al. 1999). The cause of DFNA9 is mutations in *COCH* (Robertson et al. 1998) which encodes a secreted protein that becomes part of the extracellular matrix. The mutant form of the protein leads to the loss of cells in the spiral ligament and limbus and accumulation of acidophilic deposits in the nerve channels and supporting tissues of the organ of Corti.

Ion Homeostasis

For proper auditory signal transduction, it is critical to maintain ion homeostasis, especially regarding the high potassium concentration in endolymph. Potassium recycling begins with an efflux of potassium from the outer hair cells through the potassium channel. Ions migrate to the stria vascularis through gap junctions between supporting cells and are finally pumped back into the endolymph.

Potassium channels *KCNQ4*, *KCNQ1*, and *KCNE1* have all been shown to play fundamental roles in the potassium recycling pathway. Mutations in these genes lead to the hearing disorders DFNA2, Jervell and Lange-Nielsen syndrome (loci 1 and 2) (Schulze-Bahr et al. 1997, Neyroud et al. 1997). Mutations in an anion transporter protein like pendrin, encoded by *SLC26A4*, are postulated to disrupt transport of negatively charged particles, thus upsetting fluid balance in the inner ear, and causing Pendred syndrome and DFNB4 (Li et al. 1998).

Gap junction subunits are called connexins and four connexins have been implicated in at least six types of both dominant and recessive nonsyndromic hearing loss, and they are connexin 26 (*GJB2*), connexin 31 (*GJB3*), connexin 30 (*GJB6*), and connexin 43 (*GJA1*). *GJB2* alone is estimated to account for 50% or more of recessive congenital nonsyndromic hearing loss in some populations (Rabionet et al. 2000). In addition to ion recycling, ion concentration must be strictly maintained within the two separate compartments of cochlea, one containing perilymph and the other endolymph. Tight junctions in the cochlea are thought to compartmentalize endolymph by controlling the permeability of the paracellular pathway. Mutations in the tight junction gene *CLDN14* may cause loss of endolymphatic potential

leading to degeneration of cochlear hair cells, and is etiologic in the autosomal recessive hearing loss DFNB20 (Wilcox et al. 2001).

Transcription Factors

Transcription factors regulate the spatio-temporal expression of thousands of genes and the control of cellular proliferation, differentiation, and regulation of cellular function to ensure proper development and functioning of an organism, and the inner ear is no exception. Four transcription factor genes have been identified (*POU3F4*, *POU4F3, EYA4*, and *TFCP2L3)* to be etiologic for the nonsyndromic hearing disorders DFN3, DFNA15, DFNA10 and DFNA28, respectively (de Kok et al. 1995, Vahava et al. 1998, Wayne et al. 2001, Peters et al. 2002).

POU3F4 is a member of a larger family of genes called POU domain genes, which play a role in determining cell types in the central nervous system during early development and are likely to be involved in the development of the middle and inner ear. Mutations in or near *POU3F4* probably lead to insufficiency of POU3F4 protein, thus disrupting the normal development of structures in the middle and inner ear and leading to hearing loss (de Kok et al. 1995). *POU4F3*, a class IV POU domain transcription factor, has a central function in the development of all hair cells in the human and mouse inner ear sensory epithelia. Mutations in *POU4F3* affect protein stability, localization, and transcriptional activity (Hertzano et al. 2004).

Mutations in *EYA4* lead to production of abnormal EYA4 protein, lacking some or all of the Eya domain and thus impairing interactions with other proteins. Impaired protein interactions probably disrupt control of gene activities that are important for the development

of the inner ear and maintenance of normal hearing (Wayne et al. 2001). Transcription factor *TFCP2L3* was shown to be highly expressed in epithelial cells lining the cochlear duct. The predicted translation product of *TFCP2L3* has sequence similarity to a group of proteins comprising the transcription factor cellular promoter 2 (TFCP2) family. However, its exact function remains to be elucidated (Peter et al. 2002).

Often times, transcription factors work in synchrony during the development and maintenance of mammalian inner ear (Corey and Breakefield 1994, Cantos et al. 2000), an example being the interactions between MITF, PAX3, and SOX10. Mutations in these genes result in the various subtypes of Waardenburg syndrome: *PAX3* (Waardenburg syndrome types I, III and craniofacial–deafness–hand syndrome), *MITF* (Waardenburg syndrome type II), and *SOX10* (Waardenburg syndrome type IV). It has been shown that *SOX10* and *PAX3* synergistically regulate *MITF* expression in transfection assays and mutant SOX10 and PAX3 proteins failed to bind to the *MITF* promoter region to commence induction (Bondurand et al. 2000).

Modifiers

In addition to genes that directly causing hearing loss, there also exist modifier genes that can contribute to hearing disorders through their influence on the expression or function of other genes. Notable examples include *tub* (tubby) and *moth1*, *dwf* and *mdfw* in mice and DFNB26 and *DRNM1* in humans. *Tub* encodes a transcription factor with expression in the outer and inner hair cells and the spiral ganglion cells. *Moth1*, a modifier of tubby hearing, can either worsen or prevent the hearing impairment in tubby, depending on the type of *moth1* allele and on whether one or both copies of the allele are present (Ikeda et al. 1999). *Dfw*

encodes an ATPase pump that is necessary for maintenance of low cytosolic calcium ions (Kozel et al. 1998; Street et al. 1998). *Mdfw* as a modifier of *dfw* (deaf wobbler) can protect *dfw* heterozygotes from hearing loss with one allele and is permissive of hearing loss with the other (Noben-Trauth et al. 1997). In the autosomal recessive, nonsyndromic sensorineural hearing loss DFNB26, a dominant modifier gene (*DFNM1*) has been mapped to 1q24 and is thought to suppress deafness in individuals with DFNB26 (Riazuddin et al. 1999).

Approaches to Gene Discovery and Characterization in the Auditory System

The traditional method for identification of genes involved in deafness begins by collection of DNAs from kindreds segregating a hearing impairment. It is then followed by genetic linkage analysis to identify the region of genome in which a gene involved in hearing is likely to reside. Once the region is discovered, positional cloning is then performed. When successful, it can reveal the identity of the gene involved in the deafness. This process has been very successful in identifying a number of human deafness genes such as *NDP*, *TCOF1*, *DDP*, *SLC26A4*, *USH2A* and *DFNA5* (Morton 2002). However due to the complex genetic nature of deafness, linkage analysis is a less than optimum method in gene discovery efforts for hearing disorders. Successful use of genetic linkage for mapping hearing disorders in autosomal recessive nonsyndromic loci has been fruitful largely in consanguineous kindreds or populations in which there has been limited admixture. Even in families in which a heritable hearing disorder is successfully mapped, there may be insufficient numbers of recombination events to narrow a chromosomal interval, resulting in a candidate region in the megabase scale.

A complementary method to the genetic linkage analysis for gene identification is one that utilizes tissues or organ-specific cDNA libraries to provide candidate genes (Hedrick et al. 1984, Jones et al. 1989, Gurish et al 1992). Presently, cochlear libraries are available for human, mouse, rat and chicken. These libraries have provided valuable tools for gene discovery in hearing and deafness. Almost 15,000 human (Morton fetal cochlear cDNA library) and 1,600 mouse (Soares mouse NMIE cDNA library) inner ear ESTs are currently available in the GenBank (http://www.ncbi.nlm.nih.gov/gquery/gquery.fcgi). ESTs from the human cochlear cDNA clones have already elucidated thousands of potential positional candidate genes for hearing disorders. Some of the human ESTs are genes already known to be involved in deafness: *COL4A5* (Alport syndrome), *EDNRB* (Waardenburg syndrome, type IV), *EYA1A* (BOR syndrome), *GJB2* (DFNB1 and DFNA3), *GJB6* (DFNA3), *KVLQT1* (Jervelle and Lange-Nielsen syndrome), and *MYO6* (DFNA22). Several genes preferentially expressed in the cochlea, namely *COCH* (Robertson et al. 1997), *OTOR* (Roberton et al. 2000) and *KCTD12/PFET1* (Resendes and Kuo, 2004) have been identified from the human fetal cochlea cDNA library. *COCH* was further shown to be responsible for the sensorineural deafness and vestibular disorder, DFNA9 (Robertson et al. 1998). Using a similar approach, a number of genes implicated in murine auditory function have been identified from mouse inner ear transcripts, such as *Otog*, *Ocn95*, *Fdp* (mouse homolog of *OTOR*), *Strc* and *Ush1c*, and (Morton 2002). The human ortholog of *Strc* was found to be etiologic in DFNB16 (Verpy et al. 2001) and mutations found in the human ortholog of *Ush1c* underlie USH1C and DFNB18 (Ahmed et al. 2002).

In addition to inner ear cDNA libraries, microarray technology offers a rapid and efficient way of identifying new deafness genes. It is a highly sensitive assay that requires

very little starting material. It was instrumental in the identification of *CRYM* (Abe et al. 2003) and *COL9A3* (Asamura et al. 2005), which were then studied as candidate genes for nonsyndromic deafness. With the completion of the DNA sequence of the human and mouse genomes, the sequence can be used to determine the expression pattern of thousands of genes from the inner ear. Cross-tissue comparisons facilitate identification of genes that are preferentially expressed in the inner ear. Microdissection and subtraction between data sets can help identify cell-type specific and structural-specific genes important for the function of the inner ear and expedite identification of genes that interact with deafness genes (Corey and Chen, 2002).

Model Organisms for Hearing and Deafness

Genes discussed in the previous section constitute just a fraction of what is involved in the process of hearing. Animal models have been invaluable in understanding how mutations or changes in these genes affect the function and development of the ear. Model organisms, genetically altered or pharmacologically treated, have been employed in the study of human diseases for many years. Animal models have made available a wide variety of studies including gene expression during development, anatomical and physiological experimentation, and various kinds of genetic manipulation that are not possible or ethical with human subjects. These have helped elucidate important questions such as whether candidate genes actually cause disease and by what mechanisms a gene mutation underlies a disorder.

Many considerations are taken into account when choosing an animal model, such as a researcher's familiarity with and accessibility to the animal. In addition, the time required to produce an animal model is critical, which is determined partly by the animal's generation

time, and in part by the ease of disease gene modification (lower eukaryotes being faster than higher eukaryotes). The potential resemblance of the phenotype observed in the animal model compared to that in human is an important criterion; this choice is dependent upon the disease gene under study and the affected organ. In general, the lowest eukaryote containing an ortholog of the human disease gene and the organ system is the preferred model organism.

Mouse Models

The mouse is a great model for studying human genetic deafness and genes essential for the auditory system because the anatomy, function, and hereditary abnormalities of the mouse ear have been shown to be highly similar to that of humans (Probst and Camper 1997). There are two general approaches to the utilization of mouse models in the analysis of human disease, one being the disease-driven directed genetic approach and the other mutagenesis-driven non-directed approach. In the direct approach, the disease-causing genes are already identified and the mutation characterized in the human population. Then, the mouse ortholog is identified and manipulation performed for functional gene alteration. Specifically, genetic modification may be introduced via transgenic animals where multiple copies of a foreign mutant gene were are inserted into its genome, or gene targeting where one or both normal alleles of the animal's ortholog are mutated typically via homologous recombination. In the non-directed approach, the process begins with the genetic modification and phenotype characterization in the mice followed by genetic and molecular studies of the disease. This is exemplified by chemically induced mutations via N-ethyl-N-nitrosourea (ENU) where mice are treated with ENU and screened for hearing and balance phenotypes. There are multiple centers performing mouse ENU mutagenesis including Harwell in the UK; Neuherberg in

Germany; Ricken in Japan; and Brigham and Women's Hospital, The Jackson Laboratory, Baylor College of Medicine, McLaughlin Research Institute and Oak Ridge National Laboratory in the United States. Both spontaneous and chemically induced mutations provide an array of naturally occurring and randomly induced mouse mutations to study. Advantages and limitations are associated with each approach and technique (reviewed in Chapter 15 of *Current Protocols in Human Genetics*, and Brown and Hardisty, 2003).

In addition to these genetically engineered and chemically induced mutations, there are also mutations that spontaneously arise in the mice (Johnson 2001). Spontaneous mutations have occurred naturally in large inbred populations of mice and they constitute a large portion of the mouse mutations now being used as models for human deafness. These mutations are identified often through behavioral abnormalities. Mice displaying hyperactivity, head bobbing, and circling behavior typical of vestibular dysfunction are frequently found to be deaf or hearing impaired. Other abnormalities in pigmentation and development can be associated with a hearing deficit as well. Certain inbred strains of mice exhibit a late-onset, progressive hearing loss, providing valuable models for the study of human age-related hearing loss (AHL), or presbycusis. In both humans and mice, AHL occurs earliest at high frequencies with loss of sensory hair cells from the base to the apex of the cochlea. Thus far, three AHL loci have been mapped, *Ahl3*(AHL-resistant) (Nemoto et al. 2004), *Ahl* and *Ahl2* (AHL-sensitive) (Johnson and Zheng 2002).

Deaf mouse mutants are posted on the Sanger Institute website (http://www.sanger.ac.uk/PostGenomics/mousemutants/deaf/). This site contains a current listing of genes or loci identified thus far known to be involved in deafness and/or balance defects in mice with a wide array of abnormalities from the periphery to the central auditory

system. Numerous human hearing disorders with mouse models can be found at The Jackson Laboratory website (http://www.jax.org/hmr/models.html). There are currently at least 22 nonsyndromic and 30 syndromic human deafness genes with corresponding mouse mutations.

Zebrafish Models

Zebrafish (*Danio rerio*) has become an important model system for the study of development and function of the vertebrate inner ear. The vertebrate inner ear is a complex system involving many sensory organs. It can be divided into two major compartments, dorsal and ventral. The dorsal part containing the utricle macula and three cristae for the semicircular canals is highly conserved structurally and functionally amongst all vertebrates. The ventral part becomes more specific to each vertebrate class and contains the macular organs of the saccule and lagena, which function in balance, audition or both. In the case of zebrafish, the primary auditory organ is the saccule. Sound is detected through the fish's air-filled swim bladder and transmitted via a series of bones called the Weberian ossicles connecting the swim bladder to the sensory patch in the saccule. There are also additional auditory inputs from the lagena and macula neglecta that are developed later during the juvenile stage (Fekete and Wu 2002). In addition to the inner ear, zebrafish also possess another sensory organ called the lateral line that allows for the detection of low-frequency stimuli such as water movements.

There are several advantages to using zebrafish as a model for studying hearing. Embryogenesis is rapid, and monitoring and manipulation of auditory organs in *vivo* during development are possible. Although zebrafish do not possess the equivalent of the mammalian cochlea, the organization and morphology of the zebrafish inner ear sensory epithelium cristae

and maculae are highly similar to that of higher vertebrates, including human. Genetic mechanisms governing the development and function of the zebrafish ear also appear well conserved (Whitfield et al. 2002). Nonetheless, there are exceptions including the formation of the otocyst by cavitation in zebrafish rather than by invagination as in chicks and mice.

Utilizing the classical forward genetic approach, many random mutations have been generated in zebrafish through ENU mutagenesis. Mutants can be screened initially for defects in morphology. Behavioral assays are also employed to search for mutants with aberrant swimming patterns that are indicative of vestibular defects. Functional assays such as generation of microphonic potentials and apical endocytosis, which is highly active in normal hair cells, are also effective screening tools. One may also measure the startle response of adult mutants to an auditory stimulus. This is a high throughput and automated screening that can elicit a rapid tail-flip from zebrafish with "normal" hearing in response to a tone burst. It can detect subtle behavioral defects that might have been missed by human observation. *In situ* hybridization may also be used as a high-throughput method to identify genes with specific or restricted temporal and spatial expression patterns, which is ideal for studying organ specific processes.

Reverse genetic approaches have also been useful in determining the importance of individual genes or a combination of genes' involvement in development and function of the inner ear via suppression of expression for targeted genes (morpholino knockdown), overexpression of a targeted gene (ectopic expression), and fluorescent reporting of targeted genes (transgenesis). At least 22 genes have been identified so far to be necessary for inner ear development and function in zebrafish (Nicolson 2005). Mutations in these genes can cause defects affecting many aspects of normal hair cell specification, survival and function,

development of otic induction and formation of the otic vesicle. At least five forms of syndromic or nonsyndromic human hearing disorders are known to have zebrafish models (Whitfield 2002).

In the past decade, tremendous progress has been made in auditory research. With the sequence completion of both human and mouse genomes and the zebrafish genome over three-fifths complete, gene discovery and functional analysis shall proceed at an ever rapid pace facilitated by advances in new genomic and proteomics technologies. To this end, we are ever closer to an enhanced understanding of the hearing process that will assist in better treatment, prevention and diagnosis of this complex disease.

REFERENCES

Abe S, Katagiri T, Saito-Hisaminato A, Usami S, Inoue Y, Tsunoda T, Nakamura Y (2003) Identification of CRYM as a candidate responsible for nonsyndromic deafness, through cDNA microarray analysis of human cochlear and vestibular tissues. Am J Hum Genet 72(1):73-82

Ahmed ZM, Riazuddin S, Bernstein SL, Ahmed Z, Khan S, Griffith AJ, Morell RJ, Friedman TB, Riazuddin S, Wilcox ER (2001) Mutations of the protocadherin gene PCDH15 cause Usher syndrome type 1F. Am J Hum Genet 69(1):25-34

Ahmed ZM, Smith TN, Riazuddin S, Makishima T, Ghosh M, Bokhari S, Menon PS, Deshmukh D, Griffith AJ, Riazuddin S, Friedman TB, Wilcox ER (2002) Nonsyndromic recessive deafness DFNB18 and Usher syndrome type IC are allelic mutations of USHIC. Hum Genet 110(6):527-31

Asamura K, Abe S, Fukuoka H, Nakamura Y, Usami S (2005) Mutation analysis of COL9A3, a gene highly expressed in the cochlea, in hearing loss patients. Auris Nasus Larynx 32(2):113-7

Bolz H, von Brederlow B, Ramirez A, Bryda EC, Kutsche K, Nothwang HG, Seeliger M, del C-Salcedo Cabrera M, Vila MC, Molina OP, Gal A, Kubisch C (2001) Mutation of CDH23, encoding a new member of the cadherin gene family, causes Usher syndrome type 1D. Nat Genet 27(1):108-12

Bondurand N, Pingault V, Goerich DE, Lemort N, Sock E, Caignec CL, Wegner M, Goossens M (2000) Interaction among SOX10, PAX3 and MITF, three genes altered in Waardenburg syndrome. Hum Mol Genet 9(13):1907-17

Brown SD, Hardisty RE (2003) Mutagenesis strategies for identifying novel loci associated with disease phenotypes. Semin Cell Dev Biol 14(1):19-24

Cantos R, Cole LK, Acampora D, Simeone A, Wu DK (2000) Patterning of the mammalian cochlea. Proc Natl Acad Sci USA 97(22):11707-13

Corey DP, Breakefield XO (1994) Transcription factors in inner ear development. Proc Natl Acad Sci USA 91(2):433-6

Chen ZY, Corey DP (2002) Understanding inner ear development with gene expression profiling. J Neurobiol 53(2):276-85

de Kok YJ, Merkx GF, van der Maarel SM, Huber I, Malcolm S, Ropers HH, Cremers FP (1995) A duplication/paracentric inversion associated with familial X-linked deafness (DFN3) suggests the presence of a regulatory element more than 400 kb upstream of the POU3F4 gene. Hum Mol Genet 4(11):2145-50

Eudy JD, Weston MD, Yao S, Hoover DM, Rehm HL, Ma-Edmonds M, Yan D, Ahmad I, Cheng JJ, Ayuso C, Cremers C, Davenport S, Moller C, Talmadge CB, Beisel KW, Tamayo M, Morton CC, Swaroop A, Kimberling WJ, Sumegi J (1998) Mutation of a gene encoding a protein with extracellular matrix motifs in Usher syndrome type IIa. Science 280(5370):1753-7

Fekete DM (1996) Cell fate specification in the inner ear. Curr Opin Neurobiol 6(4):533-41

Fekete DM, Wu DK (2002) Revisiting cell fate specification in the inner ear. Curr Opin Neurobiol 12(1):35-42

Gorlin RJ, Toriello HV, Cohen MM (1995) Hereditary hearing loss and its syndromes. Oxford, Oxford University Press.

Gurish MF, Bell AF, Smith TJ, Ducharme LA, Wang RK, Weis JH (1992) Expression of murine beta 7, alpha 4, and beta 1 integrin genes by rodent mast cells. J Immunol 149:1964-72

Hedrick SM, Cohen DI, Nielsen EA, Davis MM (1984) Isolation of cDNA clones encoding T cell-specific membrane-associated proteins. Nature 308:149-53

Hertzano R, Montcouquiol M, Rashi-Elkeles S, Elkon R, Yucel R, Frankel WN, Rechavi G, Moroy T, Friedman TB, Kelley MW, Avraham KB (2004) Transcription profiling of inner ears from Pou4f3(ddl/ddl) identifies Gfi1 as a target of the Pou4f3 deafness gene. Hum Mol Genet 13(18):2143-53

Ikeda A, Zheng QY, Rosenstiel P, Maddatu T, Zuberi AR, Roopenian DC, North MA, Naggert JK, Johnson KR, Nishina PM (1999) Genetic modification of hearing in tubby mice: evidence for the existence of a major gene (moth1) which protects tubby mice from hearing loss. Hum Mol Genet 8(9):1761-7

Johnson KR (2001) Mouse Models of Human Hearing Disorders. Curr Genomics 2:55-69

Johnson KR, Zheng QY (2002) Ahl2, a second locus affecting age-related hearing loss in mice. Genomics 80(5):461-4

Jones DT, Reed RR (1989) Golf: an olfactory neuron specific-G protein involved in odorant signal transduction. Science 244:790-5

Kozel PJ, Friedman RA, Erway LC, Yamoah EN, Liu LH, Riddle T, Duffy JJ, Doetschman T, Miller ML, Cardell EL, Shull GE (1998) Balance and hearing deficits in mice with a null mutation in the gene encoding plasma membrane Ca2+-ATPase isoform 2. J Biol Chem 273(30):18693-6

Li XC, Everett LA, Lalwani AK, Desmukh D, Friedman TB, Green ED, Wilcox ER (1998) A mutation in PDS causes non-syndromic recessive deafness. Nat Genet 18(3):215-7

Liu XZ, Walsh J, Mburu P, Kendrick-Jones J, Cope MJ, Steel KP, Brown SD (1997) Mutations in the myosin VIIA gene cause non-syndromic recessive deafness. Nat Genet 16(2):188-90

Mburu P, Mustapha M, Varela A, Weil D, El-Amraoui A, Holme RH, Rump A, Hardisty RE, Blanchard S, Coimbra RS, Perfettini I, Parkinson N, Mallon AM, Glenister P, Rogers MJ, Paige AJ, Moir L, Clay J, Rosenthal A, Liu XZ, Blanco G, Steel KP, Petit C, Brown SD (2003) Defects in whirlin, a PDZ domain molecule involved in stereocilia elongation, cause deafness in the whirler mouse and families with DFNB31. Nat Genet 34(4):421-8

Melchionda S, Ahituv N, Bisceglia L, Sobe T, Glaser F, Rabionet R, Arbones ML, Notarangelo A, Di Iorio E, Carella M, Zelante L, Estivill X, Avraham KB, Gasparini P (2001) MYO6, the human homologue of the gene responsible for deafness in Snell's waltzer mice, is mutated in autosomal dominant nonsyndromic hearing loss. Am J Hum Genet 69(3):635-40

Morton NE (1991) Genetic epidemiology of hearing impairment. Ann N Y Acad Sci 630:16-31

Morton CC (2002) Genetics, genomics and gene discovery in the auditory system. Hum Mol Genet 11(10):1229-40

Mustapha M, Weil D, Chardenoux S, Elias S, El-Zir E, Beckmann JS, Loiselet J, Petit C (1999) An alpha-tectorin gene defect causes a newly identified autosomal recessive form of sensorineural pre-lingual non-syndromic deafness, DFNB21. Hum Mol Genet 8(3):409-12

Naz S, Giguere CM, Kohrman DC, Mitchem KL, Riazuddin S, Morell RJ, Ramesh A, Srisailpathy S, Deshmukh D, Riazuddin S, Griffith AJ, Friedman TB, Smith RJ, Wilcox ER (2002) Mutations in a novel gene, TMIE, are associated with hearing loss linked to the DFNB6 locus. Am J Hum Genet 71(3):632-6

Naz S, Griffith AJ, Riazuddin S, Hampton LL, Battey JF Jr, Khan SN, Riazuddin S, Wilcox ER, Friedman TB (2004) Mutations of ESPN cause autosomal recessive deafness and vestibular dysfunction. J Med Genet 41(8):591-5

Nemoto M, Morita Y, Mishima Y, Takahashi S, Nomura T, Ushiki T, Shiroishi T, Kikkawa Y, Yonekawa H, Kominami R (2004) Ahl3, a third locus on mouse chromosome 17 affecting age-related hearing loss. Biochem Biophys Res Commun 324(4):1283-8

Neyroud N, Tesson F, Denjoy I, Leibovici M, Donger C, Barhanin J, Faure S, Gary F, Coumel P, Petit C, Schwartz K, Guicheney P (1997) A novel mutation in the potassium channel gene KVLQT1 causes the Jervell and Lange-Nielsen cardioauditory syndrome. Nat Genet 15(2):186-9

Nicolson T (2005) The genetics of hearing and balance in zebrafish. Annu Rev Genet 39:9-22

Noben-Trauth K, Zheng QY, Johnson KR, Nishina PM (1997) mdfw: a deafness susceptibility locus that interacts with deaf waddler (dfw). Genomics 44(3):266-72

Peters LM, Anderson DW, Griffith AJ, Grundfast KM, San Agustin TB, Madeo AC, Friedman TB, Morell RJ (2002) Mutation of a transcription factor, TFCP2L3, causes progressive autosomal dominant hearing loss, DFNA28. Hum Mol Genet 11(23):2877-85

Probst, F.J., and Camper, S.A. 1999. The role of mouse mutants in the identification of human hereditary hearing loss genes. Hear Res 130:1-6

Rabionet R, Gasparini P, Estivill X (2000) Molecular genetics of hearing impairment due to mutations in gap junction genes encoding beta connexins. Hum Mutat 16(3):190-202

Resendes BL, Williamson RE, Morton CC (2001) At the speed of sound: gene discovery in the auditory system. Am J Hum Genet 69(5):923-35

Resendes BL, Kuo SF, Robertson NG, Giersch AB, Honrubia D, Ohara O, Adams JC, Morton CC (2004) Isolation from cochlea of a novel human intronless gene with predominant fetal expression. J Assoc Res Otolaryngol 5(2):185-202

Riazuddin S, Castelein CM, Friedman TB, Lalwani AK, Liburd NA, Naz S, Smith TN, Riazuddin S, Wilcox ER (1999) A novel nonsyndromic recessive form of deafness maps to 4q28 and demonstrates incomplete penetrance. Am J Hum Genet Suppl 65:A101

Robertson NG, Skvorak AB, Yin Y, Weremowicz S, Johnson KR, Kovatch KA, Battey JF, Bieber FR, Morton CC (1997) Mapping and characterization of a novel cochlear gene in human and in mouse: a positional candidate gene for a deafness disorder, DFNA9. Genomics 46(3):345-54

Robertson NG, Lu L, Heller S, Merchant SN, Eavey RD, McKenna M, Nadol JB Jr, Miyamoto RT, Linthicum FH Jr, Lubianca Neto JF, Hudspeth AJ, Seidman CE, Morton CC, Seidman JG (1998) Mutations in a novel cochlear gene cause DFNA9, a human nonsyndromic deafness with vestibular dysfunction. Nat Genet 20(3):299-303

Robertson NG, Heller S, Lin JS, Resendes BL, Weremowicz S, Denis CS, Bell AM, Hudspeth AJ, Morton CC (2000) A novel conserved cochlear gene, OTOR: identification, expression analysis, and chromosomal mapping. Genomics 66(3):242-8

Schulze-Bahr E, Wang Q, Wedekind H, Haverkamp W, Chen Q, Sun Y, Rubie C, Hordt M, Towbin JA, Borggrefe M, Assmann G, Qu X, Somberg JC, Breithardt G, Oberti C, Funke H (1997) KCNE1 mutations cause jervell and Lange-Nielsen syndrome. Nat Genet 17(3):267-8

Smith RJH, Green GE, Van Camp G (2005) Deafness and Hereditary Hearing Loss Overview. In: GeneReviews at GeneTests: Medical Genetics Information Resource (database online). Copyright, University of Washington, Seattle. 1997-2005. Available at http://www.genetests.org

Street VA, McKee-Johnson JW, Fonseca RC, Tempel BL, Noben-Trauth K (1998) Mutations in a plasma membrane Ca2+-ATPase gene cause deafness in deafwaddler mice. Nat Genet 19(4):390-4

Vahava O, Morell R, Lynch ED, Weiss S, Kagan ME, Ahituv N, Morrow JE, Lee MK, Skvorak AB, Morton CC, Blumenfeld A, Frydman M, Friedman TB, King MC, Avraham KB (1998) Mutation in transcription factor POU4F3 associated with inherited progressive hearing loss in humans. Science 279(5358):1950-4

Verhoeven K, Van Laer L, Kirschhofer K, Legan PK, Hughes DC, Schatteman I, Verstreken M, Van Hauwe P, Coucke P, Chen A, Smith RJ, Somers T, Offeciers FE, Van de Heyning P, Richardson GP, Wachtler F, Kimberling WJ, Willems PJ, Govaerts PJ, Van Camp G (1998) Mutations in the human alpha-tectorin gene cause autosomal dominant non-syndromic hearing impairment. Nat Genet 19(1):60-2

Verpy E, Leibovici M, Zwaenepoel I, Liu XZ, Gal A, Salem N, Mansour A, Blanchard S, Kobayashi I, Keats BJ, Slim R, Petit C (2000) A defect in harmonin, a PDZ domain-containing protein expressed in the inner ear sensory hair cells, underlies Usher syndrome type 1C. Nat Genet 26(1):51-5

Verpy E, Masmoudi S, Zwaenepoel I, Leibovici M, Hutchin TP, Del Castillo I, Nouaille S, Blanchard S, Laine S, Popot JL, Moreno F, Mueller RF, Petit C (2001) Mutations in a new gene encoding a protein of the hair bundle cause non-syndromic deafness at the DFNB16 locus. Nat Genet 29(3):345-9

Wang A, Liang Y, Fridell RA, Probst FJ, Wilcox ER, Touchman JW, Morton CC, Morell RJ, Noben-Trauth K, Camper SA, Friedman TB (1998) Association of unconventional myosin MYO15 mutations with human nonsyndromic deafness DFNB3. Science 280(5368):1447-51

Wayne S, Robertson NG, DeClau F, Chen N, Verhoeven K, Prasad S, Tranebjarg L, Morton CC, Ryan AF, Van Camp G, Smith RJ (2001) Mutations in the transcriptional activator EYA4 cause late-onset deafness at the DFNA10 locus. Hum Mol Genet 10(3):195-200

Whitfield TT (2002) Zebrafish as a model for hearing and deafness. J Neurobiol 53(2):157-71

Whitfield TT, Riley BB, Chiang MY, Phillips B (2002) Development of the zebrafish inner ear. Dev Dyn 223(4):427-58

Wilcox ER, Burton QL, Naz S, Riazuddin S, Smith TN, Ploplis B, Belyantseva I, Ben-Yosef T, Liburd NA, Morell RJ, Kachar B, Wu DK, Griffith AJ, Riazuddin S, Friedman TB

(2001) Mutations in the gene encoding tight junction claudin-14 cause autosomal recessive deafness DFNB29. Cell 104(1):165-72

CHAPTER 2

Isolation from Cochlea of a Novel Human Intronless Gene with Predominant Fetal Expression

Barbara L. Resendes[1, 4]*, Sharon F. Kuo[1, 3]*, Nahid G. Robertson[1], Anne B. S. Giersch[2, 4], Dynio Honrubia[4, 5], Osamu Ohara[7, 8], Joe C. Adams[4, 6], Cynthia C. Morton[1, 2,4#]

[1]Departments of Obstetrics, Gynecology and Reproductive Biology, and [2]Pathology, Brigham and Women's Hospital; [3]Speech and Hearing Bioscience and Technology Program, Harvard-MIT Division of Health Sciences and Technology; [4]Harvard Medical School, Boston, MA 02115; and [5]Department of Neonatal Care, Children's Hospital, Boston, MA 02115; [6]Massachusetts Eye and Ear Infirmary, Boston, MA 02114; [7]Kazusa DNA Research Institute, Chiba 292-0812 Japan; [8]Laboratory of Immunogenomics, RIKEN Research Center for Allergy and Immunology, 1-7-22 Suehiro-cho, Tsurumi-ku, Yokohama, Kanagawa 230-0045, Japan.

* Co-first authors
# Correspondence should be addressed to:
Cynthia C. Morton, Ph.D.
Brigham and Women's Hospital
77 Avenue Louise Pasteur, Boston, MA 02115
Tel: (617) 525 4532
Fax: (617) 525 4533
Email: cmorton@partners.org

Nucleotide sequences have been deposited in the GenBank database under accession numbers AF359381 for human and AY267461 for mouse.

ACKNOWLEDGMENTS

We thank Steve Herrick for help with preparation of chromosome spreads and Dr. Charles Lee for assistance with the fluorescence *in situ* hybridization and chromosome analysis. We thank Robert Blaustein for critical reading of this manuscript. This work was supported by the NIH Grants DC03402 (C.C.M.), DC00405 (B.L.R.), T32DC0019 (S.F.K.), and DC03929 (J.C.A.)

ABSTRACT

We have cloned a novel human gene, designated *PFET1* (predominantly fetal expressed T1 domain) (HUGO approved symbol *KCTD12* or *C13orf2*), by subtractive hybridization and differential screening of human fetal cochlear cDNA clones. Also, we have identified the mouse homolog, designated *Pfet1*. *PFET1/Pfet1* encode a single transcript of approximately 6 kb in human, and three transcripts of approximately 4, 4.5 and 6 kb in mouse with a 70% GC-rich open reading frame (ORF) consisting of 978 bp in human and 984 bp in mouse. Both genes have unusually long 3' untranslated (3' UTR) regions (4996 bp in human *PFET1*, 3700 bp in mouse *Pfet1*) containing 12 and five putative polyadenylation consensus sequences, respectively. Pfetin, the protein encoded by *PFET1/Pfet1,* is predicted to have 325 amino acids in human and 327 amino acids in mouse and to contain a voltage-gated potassium (K+) channel tetramerization (T1) domain. Otherwise, to date these genes have no significant homology to any known gene. *PFET1* maps to the long arm of human chromosome 13, in band q21 as shown by FISH analysis and STS mapping. *Pfet1* maps to mouse chromosome 14 near the markers D14Mit8, D14Mit93 and D14Mit145.1. The human 6 kb transcript is present in a variety of fetal organs, with highest expression levels in the cochlea and brain and in stark contrast, is detected only at extremely low levels in adult organs, such as brain and lung. Immunohistochemistry with a polyclonal antibody raised against a synthetic peptide to *PFET1* sequence (pfetin) reveals immunostaining in a variety of cell types in human, monkey, mouse, and guinea pig cochleas and the vestibular system, including type I vestibular hair cells.

KEYWORDS: novel gene, intronless, GC-rich, cochlea, predominant fetal expression, tetramerization domain, unusually long 3' UTR, hair cells

INTRODUCTION

The prevalence of severe to profound bilateral congenital hearing loss is estimated at 1 in 1000 births (Gorlin et al. 1995). About 50% of congenital deafness is thought to be due to environmental factors, such as acoustic trauma, ototoxicity (*e.g.*, aminoglycoside antibiotics), and viral or bacterial infections (*e.g.*, rubella, bacterial meningitis). The remaining 50% are attributed to genetic causes and are categorized as syndromic or nonsyndromic hearing loss. Approximately 77% of hereditary deafness is estimated to show autosomal recessive inheritance, 22% is autosomal dominant, 1% is X-linked, and less than 1% segregates through the maternal lineage via mitochondria mutations (Morton 1991). Hundreds of syndromes are recognized in which hearing loss is among the clinical findings (Gorlin et al. 1995); over 90 loci have been mapped for nonsyndromic hearing loss (51 autosomal dominant, 39 autosomal recessive, 1 modifier, and 6 X-linked), and to date (Van Camp and Smith, 2003) mutations in at least 53 genes that cause deafness have been identified (Resendes et al. 2001).

We undertook an organ-specific cDNA library approach to identify genes important for hearing, a method that has been used successfully to identify various genes including auditory genes (Hedrick et al. 1984; Jones and Reed 1989; Gurish et al. 1992; Cohen-Salmon et al. 1997; Soto-Prior et al. 1997; Heller et al. 1998; Jacob et al. 1998; Robertson et al. 1998) . To this end, we made a human fetal cochlear cDNA library (Robertson et al. 1994) and have used two complementary methods to identify genes within the cochlear library. The first strategy, sequencing of the cDNA library, resulted in over 14,000 ESTs, revealed the presence of over greater than 1,200 known genes, over 2,200 EST clusters also expressed in other libraries, and 700 EST clusters unique to the cochlear library (Skvorak et al. 1999; Resendes et al. 2002). Analysis of the cochlear ESTs revealed 788 genetic loci some of which fall

within intervals of mapped deafness loci and represent positional candidates for deafness disorders (http://hearing.bwh.harvard.edu). This comparative sequence analysis led to the identification of the novel gene *OTOR* (Robertson et al, 2000). The alternative strategy combined the approaches of subtractive hybridization and differential screening of the cochlear library and led to identification of genes preferentially expressed in the cochlea (Robertson et al. 1994). As a result of the latter strategy several auditory genes, namely *ATQ1* and *COCH*, of which the latter is novel, have been identified from the cochlear cDNA library (Skvorak et al. 1997; Robertson et al. 2000). *COCH* was further shown to be responsible for a sensorineural deafness and vestibular disorder, DFNA9 (Robertson et al. 1998).

Herein we present characterization of a novel human gene, *PFET1*, identified from the human fetal cochlear cDNA library by subtractive hybridization and differential screening, and the characterization of its mouse homolog, *Pfet1*. We describe expression analyses, chromosomal mapping and immunohistochemical analyses of the human and mouse genes.

MATERIALS AND METHODS

Differential screening of a subtracted cochlear cDNA library

Human *PFET1* was initially identified from a human fetal cochlear cDNA library by subtractive hybridization and differential screening techniques utilized to identify genes important for hearing (Robertson et al. 1994). The original partial cochlear cDNA was designated 2E9. Briefly, a human fetal cochlear cDNA library was subtracted with human fetal brain mRNAs by an avidin-biotin based procedure to enrich for cochlear-expressed

transcripts. Poly (A)+ RNAs from second trimester cochlea and brain cortex were isolated and reverse transcribed to generate ^{32}P-labeled cDNA probes used for differential screening of the subtracted clones to identify those clones expressed at higher levels in the cochlea.

Isolation of cDNA clones

The human *PFET1* partial cDNA, which represents the 3'-most 848 bp of the full-length cDNA, was identified initially from the human fetal cochlear cDNA library. The full-length human *PFET1* cDNA was obtained in two phases. During the first phase, 4.4 kb of the cDNA was obtained by using the insert from the original cochlear cDNA clone as a probe to screen 10^6 recombinant phage from a human fetal brain cDNA library cloned into Lambda ZAP II (Stratagene, La Jolla, CA). Filters were prehybridized and then hybridized at 42°C with a ^{32}P-labeled random-primed (Feinberg and Vogelstein 1984) probe in 10% dextran sulfate, 4X SSC, 7 mM Tris-HCl (pH 7.6), 0.8X Denhardt's solution, and 20 ug/ml sonicated and denatured herring sperm DNA in 40% formamide and 0.5% SDS. Filters were washed in 0.1X SSC in 0.1% SDS at 50°C prior to autoradiography using XAR-5 film (Eastman Kodak Co., Rochester NY) and intensifying screens at –80°C. During the second phase, the remaining 1.7 kb of the 5' end was cloned through a computer search of the accumulated terminal sequence data of human long cDNA libraries of the Kazusa DNA Research Institute (http://www.kazusa.or.jp/huge) (Ohara et al. 1997). The longest clone, which was 6.2 kb in size, was isolated from an adult hippocampus library and is denoted as pg00707.

The mouse *Pfet1* sequence was isolated by using the open reading frame from the human *PFET1* to search the GenBank EST database (http://www.ncbi.nlm.nih.gov/BLAST/, EST database). One EST (GenBank accession number AW230625) was identified with 95%

identity at the nucleotide level and contained 160 bp of the 3' end of the open reading frame and 300 bp of the beginning of the 3' UTR. The AW230625 EST was derived from the 5' end of a mouse IMAGE clone (accession number IMAGE: 2647463) that was obtained from Research Genetics (now Invitrogen Life Technologies, Carlsbad, CA). Together with an overlapping mouse clone (accession number IMAGE: 5012249), the complete sequence of 3' UTR of mouse *Pfet1* was determined. The remainder of the 70% GC-rich open reading frame was cloned from total adult mouse brain RNA using 5' rapid amplification of cDNA ends (RACE; Invitrogen Life Technologies, Carlsbad, CA). Because the ORF is 70% GC-rich, reverse transcription was performed at 50°C in the presence of PCR_x Enhancer Solution (Invitrogen Life Technologies). For amplification of cDNA, the following PCR protocol was performed in the presence of PCR_x Enhancer Solution: initial denaturation at 97°C for 3 minutes; 35 cycles of 96°C for 30 seconds, 62°C for 30 seconds, and 72°C for 2 minutes; and final extension at 72°C for 7 minutes. PCR fragments were TA-cloned (Invitrogen Life Technologies) and sequenced.

Genomic clone

BLAST analysis of the *PFET1* nucleotide sequence identified a 109 kb genomic clone (GenBank accession no. AC000403) corresponding to RPCI-1 PAC clone 264J2, and this PAC was obtained from Research Genetics. PAC 264J2 contains the entire *PFET1* gene.

Sequence analysis

Nucleotide sequence of partial cDNA clones was determined using an ABI PRISM dye-terminator cycle-sequencing system (PE Applied Biosystems, Foster City, CA).

Sequence analysis was performed using the University of Wisconsin Genetics Computer Group software (Devereux et al. 1984) and the Open Reading Frame (ORF) Finder program at the National Center for Biotechnology Information (NCBI; http://www.ncbi.nlm.nih.gov/). The cDNA insert of pg00707 was sequenced using the shotgun strategy according to procedures previously described (Ohara et al. 1997). For DNA sequencing, dye-primer or dye-terminator cycle sequencing reactions were performed using ABI PRISM cycle sequencing kits (PE Applied Biosystems) and the products were analyzed with ABI 373 or 377 DNA sequencers.

Northern blot analysis

Total cellular RNAs were extracted (Chirgwin et al. 1979) from second trimester human fetal organs, adult surgical specimens, and adult mouse tissues. All human organs and specimens were obtained in accordance with guidelines established by the Human Research Committee at Brigham and Women's Hospital. Ten μg of each sample of RNA were electrophoresed in denaturing 1% agarose-formaldehyde gels and capillary-transferred overnight in 10X SSC to GeneScreen Plus membranes (NEN Life Science Products, Inc., Boston, MA; Thomas 1980). Mouse aging brain and mouse embryonic Northern panels were obtained from Seegene, Inc. (Seoul, Korea); each lane contains 20 ug of total RNA isolated from either ICR strain whole mouse embryos at different stages or whole brain at different ages.

Filters were prehybridized for 2 hours and hybridized overnight at 42°C as described above with either ^{32}P-labeled random-primed probe or PCR-generated ^{32}P-labeled probe. Filters were washed in 0.1 X SSC in 0.1% SDS at 42-55°C prior to autoradiography using

XAR-5 film with intensifying screens at -80°C. A human 3' UTR probe was prepared via random labeling from the original 2E9 cochlear clone; a human 3' UTR internal region probe was amplified using the following primers and conditions: upper (5' TGCAAACATGCCAAGTATTTT 3') and lower (5' AGGCAACCAGGTCTCCTTCT 3'); initial denaturation at 97°C for 3 minutes; 35 cycles of 96°C for 30 seconds, 60°C for 30 seconds, and 72°C for 30 seconds; and final extension at 72°C for 7 minutes. To generate radiolabeled PCR fragments representing the beginning (507 bp) and end (462 bp) of the human ORF, the following primers and the same conditions as above were used: upper (5' CCTCTCTGTCATGGCTCTGG 3') and lower (5'TGTTCGGGCTCCGAGTAG 3'), and upper (5' TCCTCTTCCGCTACATCCTG 3') and lower (5' TTGAGGTAATAGCGCGAGGT 3'), respectively.

For generation of a mouse *Pfet1* ORF 460 bp probe (contains 160 bp of the 3' region of the *Pfet1* ORF and 300 bp of the beginning of the 3' UTR) from mouse clone AW230625, the following primers and PCR conditions were used: upper (5' CAGGCCTTCGATAAGCTGTC 3') and lower (5' CGACATCCTGACTCTTGCAT 3'); initial denaturation at 97°C for 3 minutes, 35 cycles of 96°C for 30 seconds, 58°C for 30 seconds, and 72°C for 30 seconds; and final extension at 72°C for 7 minutes. For generation of the mouse *Pfet1* 3' UTR probe 1 (400 bp), the following primers and PCR conditions were used: upper (5' GGCTCATAGGACAGCACCTC 3') and lower (5' GCATGGCTGCACATCAGATA 3'); initial denaturation at 97°C for 3 minutes, 35 cycles of 96°C for 30 seconds, 60°C for 30 seconds, and 72°C for 30 seconds; and final extension at 72°C for 7 minutes. For generation of the mouse *Pfet1* 3' UTR probe 2 (394 bp), the following primers and PCR conditions were used: upper (5'

GAGGGAATCGTTTTGATGTGA 3') and lower (5' CCCAGCAATTTATGGAGTTGA 3'); initial denaturation at 97°C for 2 minutes, 35 cycles of 96°C for 30 seconds, 60°C for 30 seconds, and 72°C for 30 seconds; and final extension at 72°C for 7 minutes.

Gene mapping

A human PAC (246J2, GenBank accession number AC000403) containing the entire *PFET1* gene was obtained from Research Genetics and used to generate a biotin-labeled probe for fluorescence *in situ* hybridization (FISH). About 3 μg of PAC DNA were labeled with dNTPs conjugated with biotin (Boehringer Mannheim, Indianapolis, IN) according to the manufacturer's protocol, precipitated with 6 μg of Cot-1 DNA (Gibco-BRL, Rockville, MD) and resuspended in 30 μl hybridization buffer (50% formamide, 2X SSC). Hybridization of metaphase chromosomes from peripheral blood lymphocytes obtained from a normal male was performed using 0.5 - 1 μg of labeled probe. The biotin-labeled probe was detected using Cy3 avidin (Amersham, Little Chalfont, Buckinghamshire, UK) and chromosomes were counterstained with 4,6-diamidino-2-phenylindole dihydrochloride (DAPI) (Vysis, Downers Grove, IL). The map position of the *PFET1* gene was determined by visual inspection of the signal on the DAPI counterstained metaphase chromosomes. Chromosomes and signals were observed with an Olympus AX70 photomicroscope and photographs were captured using a Photonics CCD camera and Genus software (Applied Imaging, Santa Clara, CA). Mapping of the mouse *Pfet1* gene was performed by using the 3 kb mouse sequence to search for identical sequences in the Celera mouse genome database (Celera, Rockville, MD).

Tissue preparation for immunohistochemistry

Three mice (6-8 weeks), two guinea pigs (less than 3 months), one monkey (unknown age), one adult human (68 years) and one fetal human (20 weeks) cochleas were used in this study. Human fetal tissues were fixed in 4% paraformaldehyde in PBS at 4°C for 2-3 weeks and then decalcified in 0.1 M EDTA in PBS at 4°C for approximately 2 weeks. The human adult temporal bone was retrieved during autopsy; postmortem time is unknown. All tissues were prepared for paraffin sections in the following manner. Animals were anesthetized via intraperitoneal injection of urethane (1.5 g/kg), and exsanguinated through transcardial perfusion of saline with 0.01% sodium nitrite, followed by fixative. Fixatives used were formalin acetic (FA: 10% formalin and 1% acetic acid in PBS) and formalin glutaraldehyde (FG: 10% formalin and 0.1% glutaraldehyde in PBS). The bulla cavity of each animal was quickly exposed and 0.2-0.5 ml of fixative was injected slowly into the scala tympani through the perforated round window. Specimens were kept overnight at 4°C in their respective fixative followed by one week in 120 mM EDTA pH 7 for decalcification. For human specimens, decalcification was performed up to a month. The decalcified specimens were dehydrated in a series of ethanol solutions and xylene baths before embedding in paraffin (Imamura and Adams 1996). Serial 8 μm sections were cut and mounted on glass slides.

Human fetal tissues were obtained following guidelines established by the Human Research Committees at Brigham and Women's Hospital and the Massachusetts Eye and Ear Infirmary. The care and use of animals were in accordance with NIH's "Principles of Laboratory Animal Care" and was approved by the institutional committee on animal care at both institutions.

Immunohistochemical staining

Polyclonal antibody was raised in rabbits against a synthetic peptide corresponding to amino acid residues 256-280 of *PFET1* human sequence, coupled to KLH (keyhole limpet hemocyanin) (Research Genetics). This region of *PFET1* is highly conserved in mouse. Antisera were affinity purified using the pfetin peptide. In order to obtain pfetin as a positive control for Western analysis, the open reading frame of *PFET1* was cloned into vector pET28a to express the protein (Novagen, Madison, WI). Pfetin was also extracted from various adult mouse organ tissues that were shown to contain *PFET1* mRNA through Northern analysis. For a negative control, the pET28a vector only and the pET28a vector with another unrelated ORF were used. All protein was expressed in bacterial cell line BL21 (DES) (Stratagene, La Jolla, CA). Immunostaining of paraffin sections was performed with the biotinylated tyramine (BT) enhancement method (Adams 1992). Paraffin sections containing the cochlear regions were deparaffinzed, hydrated, and rinsed in deionized water and PBS. Sections were blocked with 5% normal horse serum (NHS) in PBS for 30 minutes and then incubated overnight with primary anti-PFET1 antibody diluted between 1:1000 and 1:4000 in 1% NHS-PBS at room temperature in a humid chamber. Sections were rinsed with PBS and incubated for an hour in a 1:1000 dilution of biotinylated goat anti-rabbit IgG (Vector Laboratories, Inc., Burlingame, CA) in 1% NHS-PBS. Sections were rinsed in PBS and incubated with Vectastain ABC reagent (Vector Laboratories). After an hour, sections were rinsed in PBS and incubated with BT diluted 1:100 in 0.01% H_2O_2 for 10 minutes, rinsed in PBS, and incubated with ABC reagent for another 30 minutes. The primary antibody was visualized using 0.05% DAB (3,3' diaminobenzidine) in 0.01% H_2O_2 and 0.1 M phosphate

buffer. Controls for the immunostaining procedures were done with serial dilution of the affinity-purified primary antibody and with 1% NHS-PBS containing no primary antibody.

RESULTS

Identification of human PFET1 by subtractive hybridization and differential screening

To identify genes preferentially expressed in the cochlea, subtractive hybridization and differential screening techniques were performed using a human fetal cochlear cDNA library. Subtracted cochlear clones were differentially screened with ^{32}P-labeled total fetal cochlear and total fetal brain cDNA probes identifying those clones that were highly or preferentially expressed in the cochlea (Robertson et al. 1994). Slot blot analysis revealed that *PFET1* had an increased level of expression in cochlea as compared to brain (data not shown), and led to its selection for further analysis.

Nucleotide and amino acid sequence analysis

To identify the full-length sequence of *PFET1*, human fetal brain and adult hippocampus libraries were screened and yielded several overlapping cDNA clones. The longest clone (6.2 kb) was isolated from the adult hippocampus library and represented the full-length sequence of *PFET1*, containing a predicted full-length open reading frame (ORF) of 325 amino acids encoded by one exon and a 3' UTR of 4996 bases containing twelve polyadenylation consensus sequences (Figs. 1 and 2). The detailed information of the isolated clone is available on a Gene/Protein characteristic table for KIAA1778 of the HUGE database (URL, http://www.kazusa.or.jp/huge). Analysis of the upstream sequence revealed a Kozak

sequence (GCCCGGCCACCN$_8$ATGG) (Fig. 1). The 240 bases 5' to the ORF and the entire ORF are very GC-rich (78% and 70%, respectively) (Figs. 1 and 2). BLAST analysis (dbNR) revealed homology to no known genes in GenBank, identified one partial human fetal brain mRNA clone designated 24475 (GenBank accession number AF052169), and one chromosome 13 PAC clone designated 246J2 (GenBank accession number AC000403). BLAST analysis (dbEST) revealed homology to 279 ESTs from various human libraries, including fetal cochlea (n=31), adult and fetal brain (n=29), adult heart (n=14), adult kidney (n=16), adult lung (n=17), adult ovary (n=17) and adult muscle (n=5). The findings of a consensus Kozak sequence, and that longer transcripts containing additional 5' sequence were not revealed by RT-PCR (data not shown), library screening or computer searching of public databases, suggest that the 6.2 kb clone contains the entire gene.

One mouse EST (AW230625) with 95% identity at the nucleotide level and containing part of the ORF (170 nucleotides of the 3' end of the ORF) was identified from GenBank (mouse dbEST). The remainder of the mouse *Pfet1* ORF was cloned from mouse brain total RNA by performing 5' RACE. The remaining 3.4 kb of the mouse *Pfet1* 3' UTR was obtained by sequencing IMAGE clone 5012249 that overlapped with mouse AW230625 EST (see Materials and Methods). Like its human homolog, the mouse *Pfet1* gene has an unusually long 3' UTR (3700 bp) and contains five putative polyadenylation consensus sequences (Fig. 4).

The protein domain database, Pfam (Bateman et al. 2000), was used to identify protein motifs or domains in the predicted amino acid sequence. A voltage-gated potassium channel tetramerization (T1) domain of 95 amino acids, spanning amino acids 34-129, was identified (E = 7.3e-17) in the amino terminal region (Figs. 1 and 3). No other complete domains were

predicted. A hydropathic profile utilizing the Kyte-Doolittle method revealed four weakly hydrophobic regions of at least 10-15 amino acids (data not shown). The deduced amino acid sequence does not appear to contain any transmembrane spanning domains, as determined by the transmembrane prediction programs TMpred (Hofmann and Stoffel 1993), TMHMM (Sonnhammer et al. 1998), and HMMTOP (Tusnady and Simon 1998).

The human *PFET1* and mouse *Pfet1*genes are 91% identical at the nucleotide level within the ORF and share little sequence similarity outside of the ORF (Fig. 2). The mouse ORF is longer by two amino acids (insertion of proline and histidine at positions 142 and 143, respectively) and the predicted protein differs by eight amino acids (Fig. 2). The human and mouse pfetin are predicted to have 325 amino acids in human and 327 amino acids in mouse and to contain a voltage-gated potassium channel tetramerization domain. The entire human and mouse ORFs are very GC-rich (70%). The tetramerization domain in the mouse *Pfet1* is identical to that of the human *PFET1* except for a phenylalanine to leucine change at position 88 (Fig. 2).

Northern blot analysis

To determine the relative level of expression of human *PFET1* mRNA in various tissues, Northern blot analysis was performed using the original 3' cochlear cDNA clone (0.9 kb of 3' UTR) to probe a panel of human fetal RNA samples (Fig. 5). One transcript (~6 kb) was revealed at high levels in human fetal cochlea and brain, at moderate levels in skeletal muscle, lung, ovary and eye, and at lower levels in thymus, tongue, heart and adrenal gland (Fig. 5A). A Northern blot panel of adult and fetal human organs was hybridized with different *PFET1* probes (Fig. 5 B and D). In contrast to the abundant fetal expression pattern,

the ~6 kb *PFET1* transcript was present at barely detectable levels in adult tissues studied, such as spinal cord, cerebrum, cerebellum, skeletal muscle, lung and lymph node (Fig. 5B). Low expression levels of the *PFET1* transcript were also detected in adult liver, heart and kidney (data not shown). The transcript was also detected in various regions of the fetal brain (Fig. 5C). Other smaller-sized bands, in particular a ~4.7 kb band, were identified by probes made from the *PFET1* ORF (Fig. 5B, ORF probe) and are thought to be due to nonspecific binding since the ORF region is 70% GC-rich and because the 3' internal UTR probe, which would be expected to be present in a transcript of this length, does not identify these bands (see Fig. 5B, 3' UTR internal).

For Northern blot analysis of total RNA from adult mouse tissues, we initially used the "ORF probe" containing part of the 3' ORF region and part of the 3' UTR. A single ~6 kb transcript was revealed at low levels in most adult mouse tissues tested (Fig. 6 A and D). Then, using a probe to a downstream 3' UTR region ("3' UTR probe 1," which overlaps with the "ORF probe"), three transcripts (approximately 4, 4.5 and 6 kb) were identified in samples containing aging mouse brain and whole mouse embryos at different embryonic stages (Figs. 6 B, C and D). The intensity level of the largest *Pfet1* mouse transcript identified during embryogenesis appears to increase between days 11.5 and 15.5, while the intensity level of the smaller mouse transcripts seems to peak earlier, from days 6 to 15.5 (Fig. 6C). In addition, there appears to be a noticeable decrease in expression level of the largest mouse transcript between weeks 2 and 4 of development in mouse brain (Fig. 6B). The smaller transcripts are not as apparent in the adult tissue panel, and most likely reflect the lower concentration of RNA used to prepare that Northern blot. Interestingly, the smallest mouse transcript (~ 4 kb)

was not identified by a probe derived from the 3'-most mouse region (3' UTR probe 2) (data not shown) suggesting the use of an internal polyadenylation sequence.

Northern blot analysis utilizing probes derived from different regions of the human gene gave the same results as obtained with a 3'-most probe, and revealed the presence of no additional transcripts for both the human and mouse genes (data not shown).

Chromosomal mapping in human

Physical mapping of *PFET1* was done to determine its chromosomal position and to access whether it is located within a region of any known deafness loci, making it a positional candidate gene for that deafness disorder. Initially *PFET1* was localized to chromosome 13 by virtue of its sequence homology to a genomic chromosome 13 PAC (GenBank accession no. AC000403, PAC 246J2) and to several chromosome 13 STSs (SHGC-15652, WI-17550 and TIGR-A002N08). PAC 246J2, which contains the entire *PFET1* gene, was FISH-mapped and localized to band q21 on chromosome 13 (Fig. 7). Currently, *PFET1* is not a candidate gene for any known deafness disorder as none have yet been mapped within this chromosomal band (Van Camp and Smith 2003). The mouse *Pfet1* gene was mapped to chromosome 14 near the markers D14Mit8, D14Mit93 and D14Mit145.1 as determined by sequence identity with the Celera sequence GA_x5J8B7W5Y0C. Human 13q21 is contained within a region of homologus synteny in mouse chromosome 14 and thus far, no mouse deafness mutant has been identified near *Pfet1* gene region

Immunohistochemical analysis

Before immunostaining was attempted, the antibody was tested for purity and specificity using Western blot analyses. The analyses of purified pfetin antibody on both bacterially-expressed proteins and tissues extracted from various mouse organs (6 months old brain, heart and skeletal muscle) showed one distinct band between 35 kDa and 47 kDa, the expected size of pfetin, for the positive control but not for either of the negative controls (data not shown).

The mammalian cochlear and vestibular systems consist of various cell types. In the cochlea, the greatest number of immunostained cells were type I fibrocytes in the spiral ligament (Fig. 9). This finding was observed in all species, including human, monkey, mouse, and guinea pig (Fig. 9 and 10B). Immunostaining was also localized in the following cochlear cell classes: types IV and V fibrocytes, Deiters cells, inner and outer pillar cells, inner sulcus cells, interdental cells, supralimbal and limbal fibrocytes (Figs. 9 and 10). Type V fibrocytes, also called suprastrial cells, were positive for immunostaining near the Reissner's membrane in human (Fig. 10D), monkey (Fig. 9C), guinea pig (Fig. 11C) and most of the mouse cochlear sections (Fig. 9B). While immunostaining of limbal fibrocytes and supralimbal cells was observed in mouse, guinea pig, monkey and human cochleas (Fig. 9 and 10), immunostaining in Deiters cells, inner and outer pillar cells and interdental cells was observed only in mouse and guinea pig (Fig. 11A-C). Immunostained neurons included spiral ganglion cells (Fig. 9B), Scarpa's ganglion cells and Purkinje cells in mouse sections containing brain tissues (not shown).

In the vestibular system there was apical immuno-staining of the type I hair cells at the cuticular plate and in the hair cell cytoplasm (Fig. 12G and H). Beneath the sensory

epithelium, connective tissue cells were also immunostained in formalin plus glutaraldehyde-fixed mouse (Fig. 12H) and guinea pig ampulla (Fig. 12 E, F and H). Positively stained fibrocytes extended from beneath the sensory epithelium to the area beneath the vestibular dark cells. Adjacent to the sensory epithelium, transitional cells and cells beneath the vestibular dark cells in human fetal and guinea pig (Figs. 12A, B, E, and F) were positive. In addition, positive cells were present facing the lumen of the semicircular canals in human fetal tissue (Figs. 12C and D) and along with the lumenal and ablumenal surface of formalin plus glutaraldehyde-fixed mouse and guinea pig semicircular canal (Fig. 12E, F and H).

These immunohistochemcial analyses were performed mostly on adult tissues, since fetal tissues were not available at the time of this study. Although Pfetin has a low expression in adult tissues, nonetheless it is expressed in a variety of adult organs and therefore the immunohistochemical analyses on adult organs remains a reasonable initial study to carry out. Immunohistochemical analyses on fetal organs are pertinent and such future analyses will be performed.

DISCUSSION

We have cloned and characterized a novel intronless human gene designated *PFET1* and its mouse homolog, *Pfet1*. The open reading frames of *PFET1* and *Pfet1* are unusually GC-rich (70%); the potential significance of this is not known. The encoded proteins of both genes contain a tetramerization domain characteristic of voltage-gated potassium channel subunits. The 3' untranslated region from the human gene is long (4996 bp) as the average 3' UTR length for human mRNAs deposited in public databases is between 740-755 base pairs

(Pesole et al. 1997; Pesole et al. 2000). The role of the unusually long 3' UTR in this gene is presently unknown. Although 12 putative polyadenylation consensus sequences are predicted in the human sequence, the finding that 5' and 3' probes identified only the largest transcript suggests that the other 11 putative polyadenylation consensus sequences may not be utilized to produce alternatively-sized transcripts. It remains possible that other *PFET1* transcripts of different sizes exist and are at levels below the limits detectable by Northern blot analysis or are expressed in a different temporal or spatial fashion not tested.

PFET1 encodes a single ~6 kb transcript and its mouse homolog encodes three transcripts (4, 4.5 and 6 kb). In humans, a 6 kb *PFET1* transcript is expressed abundantly in a variety of tissues in the fetus and at strikingly lower levels in the adult. The observation that *PFET1* is expressed at much higher levels in fetal organs than in adult organs is intriguing. This expression difference in adult and fetal tissue samples appears also to occur with the mouse *Pfet1* transcripts in brain (compare Fig. 6A, 6B). The disparate expression levels of the *PFET1* 6 kb transcript cannot be explained by the expression of tissue-specific or age-specific alternative transcripts as both 5' (containing part of the ORF) and 3' UTR probes identified only a single transcript, the ~6 kb transcript, in all fetal and adult human tissues tested (see Fig. 5D for position of probes). *PFET1* is the first example to our knowledge of a human cochlear gene with such disparate expression patterns in adult and fetal human organs as late as second trimester developmental age in humans. Similar type of expression has been seem before in other species like mouse, zebrafish, xenopus and chick with genes like GATA3, Pax2, Bmp4, and Bmp7 etc. This type of expression pattern suggests that *PFET1* has a developmental role and thus is required at high levels during embryogenesis and at much lower levels in adulthood. Of note, the human fetal cochlear library from which *PFET1*

was identified represents largely developmental ages of 16-22 weeks, consistent with cochlea that are morphologically adult-like in structure. There is also evidence that the human fetus responds to sound at about this age. In light of these observations, it is interesting that there is a marked difference in expression levels of *PFET1* in the fetus versus the adult, suggesting a potential important role of *PFET1* in further development of the cochlea during later stages of fetal life.

Tetramerization domain

Voltage-gated potassium channels, of which there are multiple families, each consisting of numerous members, are assembled as homomeric and heteromeric tetramers from membrane-integrated α subunits; the *Shaker*-related potassium channel also coassembles with cytosolic β subunits (Jan and Jan 1997; Pongs et al. 1999). The assembly of different subunits to form functional heteromeric tetramers is thought to be determined by the amino acid composition of the tetramerization (T1) domain, and thus contributes to the diversity of electrical responses that a cell can generate in response to changes in membrane potential (Bixby et al. 1999). Therefore, it is not surprising to observe some sequence variations in the conserved regions within K+ channel tetramerization domains amongst family members given the existence of a K+ channel tetramerization domain consensus sequence (Fig. 3). The exact role of the T1 domain remains controversial. Previously, it was shown that the T1 domain is not necessary for K+ channel assembly or function (Kobertz and Miller 1999). Rather, the T1 domain of voltage-gated potassium channel subunits may act more as a segregation domain in that it ensures that tetramerization occurs only among subunits belonging to the same family and that cross-family subunit assembly does not occur

(Li et al. 1992; Shen and Pfaffinger 1995). The T1 domain may also function as a docking station for the β subunit of voltage activated potassium (Kv) channels such that the removal of the T1 domain disrupts β subunit association (Sewing et al. 1996; Gulbis et al. 2000).

Because the predicted ORF of *PFET1* contains a tetramerization domain, it is tempting to speculate that pfetin may be a novel voltage-gated K+ channel subunit that could contribute to tetramer diversity and thus could participate in a variety of electrical responses of the cell. Furthermore, the deduced amino acid sequence of pfetin is predicted to contain four hydrophobic regions of at least 10-15 amino acids in length. However, since *PFET1* is predicted to contain no transmembrane domains, and six are characteristic of voltage-gated potassium channel subunits, it is unlikely that *PFET1* encodes another member of the voltage-gated potassium channel subunits.

Relationship between T1 and POZ domains

The voltage-gated potassium channel tetramerization domain is thought to have a structural and evolutionary relationship to the BTB/POZ (for bric-a-brac, tramtrack, broad complex poxvirus and zinc finger) domain, which is found in a variety of proteins involved in transcriptional regulation, cytoskeletal organization, and development (Aravind and Koonin 1999). The POZ domains of the mammalian transcriptional repressor proteins BCL6 and PLZF (promyelocytic leukemia zinc finger) interact with the transcriptional corepressor proteins mSIN3A and SMRT (silencing mediator of retinoid and thyroid hormone receptor), via a paired amphipathic helix 1 (PAH1) domain (David et al. 1998), and multiple SMRT contacts (Hong et al. 1997), respectively. Chromosomal translocations involved in human leukemias generate fusion proteins, such as RARA-PLZF, containing POZ domains that play

an important role in the pathology of the disease (Hong et al. 1997; Grignani et al. 1998; Lin et al. 1998). The BTB/POZ domain, like the voltage-gated potassium channel T1 domain, is important for protein-protein interactions and allows for dimerization of BTB/POZ domain-containing proteins. However, unlike the voltage-gated potassium channel T1 domain, POZ domains mediate interaction between proteins containing other domains as well. Future studies are necessary to determine if the T1 domain present in PFET1/Pfet1 is functional and possibly acts like a BTB/POZ domain, allowing for the interaction of PFET1/Pfet1 with proteins containing various types of domains.

Immunohistochemistry of pfetin antibody

Perhaps the most numerous cochlear cells that were positive for pfetin were type I fibrocytes of the spiral ligament in the cochlea. Fibrocytes of the ligament are thought to be part of the connective tissue cell gap junction system (Kikuchi et al. 2000) and may play a role in K+ recycling by transporting K+ to the stria vascularis (Spicer and Schulte 1997). The loss of type I fibrocytes of the spiral ligament is the predominant histopathology of DFNA9 (Merchant et al. 2000), a known autosomal dominant, nonsyndromic, progressive sensorineural hearing loss (Robertson et al. 1998) . These are also the cells that are most severely disrupted in the hydropic guinea pig (Ichimiya et al. 1994). The type I fibrocytes, containing enzymes such as intracellular Ca++-ATPase, carbonic anhydrase, aldehyde dehydrogenase and calcium–binding proteins, are thought to be involved in the regulation of cochlear fluid and ion balance (Ichimiya et al. 1994; Spicer et al. 1997). Although the exact function of type I fibrocytes in cochlea has not been clearly defined, it is quite obvious that their loss in DFNA9 show that they play an essential role in normal auditory functions.

Besides type I fibrocytes, pfetin antibody also stains type IV and type V fibrocytes cells in the cochlea across different species tested. Pfetin antibody immunostaining in limbal fibrocytes, supralimbal, Deiter, interdental and pillar cells were less consistent. One possible explanation is species-specific expression of pfetin function in the cochlea. The amount of antigen available for pfetin antibody binding might vary somewhat as well depending on the plane of the section giving certain cellular structure a better exposure. However, the quality of tissue fixation might also have contributed to some of the staining variation. Initial attempts at immunostaining formalin fixed mouse cochlea were negative. Experimentation with other fixatives revealed consistent staining patterns with tissues fixed in formalin plus glutaraldehyde. Although human material that was promptly fixed with formalin plus glutaraldehyde was not available, it seems likely that the immunostaining results from the human sections is credible because of its similarity to the patterns of immunostaining seen in animal tissue where control of fixation was possible. It remains to be confirmed that vestibular hair cells and fibrocytes are pfetin positive in human material.

It is striking that most of the cell classes stained by pfetin antibody in the cochlea have been implicated in the potassium recycling pathway through putative lateral uptake by Deiters cells, forwarding through supporting cells, outer sulcus cells and spiral ligament fibrocytes and on to strial marginal cells. Given the cell types stained by pfetin antibody and their associated function in the cochlea, it is possible that pfetin plays a role in ion transport or ionic content regulation in the cochlea. This hypothesis is especially intriguing given the presence of the T1 domain in pfetin, since this domain is characteristic of K+ channel subunits.

An exciting discovery came from the vestibular sensory epithelium where the cuticular plate and the cytoplasm of the type I hair cells were immunostained. Although the function of this gene product is not yet clear, loss of gene function would likely result in a vestibular phenotype if pfetin plays a key role in hair cell function. Similar to the type I fibrocytes stained in the cochlea, connective tissue cells in the vestibular system show pfetin immunostaining as well. Specifically, immunostaining for pfetin in the human fetal, mouse and some guinea pig vestibular sections reveals a positive signal in a layer of cells underlying the transitional cells and vestibular dark cells. In mouse sections, the connective fibrocytes underneath the vestibular sensory epithelium are prominently stained by pfetin antibody. The functions of these cells are not known. In addition, little is known about the pfetin positive cell layer that lines the lumen of semicircular canals. They form the barrier that faces the endolymphatic space. It is possible that they play some role in ionic content regulation in the vestibule. Because T1 domains are members of the POZ domain superfamily, and some proteins containing these domains are involved in cytoskeletal organization, pfetin may also function, by protein-protein interaction via the T1 domain, in the structural organization of the cochlea and vestibule. Given the presence of pfetin in a variety of cell classes such as sensory cells, nerve cells, epithelial cells and connective tissue cells in the cochlea and vestibular system, it is likely that pfetin could have broad functional roles in inner ear and vestibular system. Additional studies are needed to further elucidate the function of this intriguing novel gene.

REFERENCES

Adams JC (1992) Biotin amplification of biotin and horseradish peroxidase signals in histochemical stains. J Histochem Cytochem 40:1457-63

Aravind L, Koonin EV (1999) Fold prediction and evolutionary analysis of the POZ domain: structural and evolutionary relationship with the potassium channel tetramerization domain. J Mol Biol 285:1353-61

Bateman A, Birney E, Durbin R, Eddy SR, Howe KL, Sonnhammer EL (2000) The Pfam protein families database. Nucleic Acids Res 28:263-6

Bixby KA, Nanao MH, Shen NV, Kreusch A, Bellamy H, Pfaffinger PJ, Choe S (1999) Zn2+-binding and molecular determinants of tetramerization in voltage-gated K+ channels. Nat Struct Biol 6:38-43

Chirgwin JM, Przybyla AE, MacDonald RJ, Rutter WJ (1979) Isolation of biologically active ribonucleic acid from sources enriched in ribonuclease. Biochemistry 18:5294-9

Cohen-Salmon M, El-Amraoui A, Leibovici M, Petit C (1997) Otogelin: a glycoprotein specific to the acellular membranes of the inner ear. Proc Natl Acad Sci U S A 94:14450-5

David G, Alland L, Hong SH, Wong CW, DePinho RA, Dejean A (1998) Histone deacetylase associated with mSin3A mediates repression by the acute promyelocytic leukemia-associated PLZF protein. Oncogene 16:2549-56

Devereux J, Haeberli P, Smithies O (1984) A comprehensive set of sequence analysis programs for the VAX. Nucleic Acids Res 12:387-95

Feinberg AP, Vogelstein B (1984) "A technique for radiolabeling DNA restriction endonuclease fragments to high specific activity". Addendum. Anal Biochem 137:266-7

Gorlin RJ, Toriello HV, Cohen MM (1995) Hereditary hearing loss and its syndromes. Oxford, Oxford University Press.

Grignani F, De Matteis S, Nervi C, Tomassoni L, Gelmetti V, Cioce M, Fanelli M, Ruthardt M, Ferrara FF, Zamir I, Seiser C, Lazar MA, Minucci S, Pelicci PG (1998) Fusion proteins of the retinoic acid receptor-alpha recruit histone deacetylase in promyelocytic leukaemia. Nature 391:815-8

Gulbis JM, Zhou M, Mann S, MacKinnon R (2000) Structure of the cytoplasmic beta subunit-T1 assembly of voltage-dependent K+ channels. Science 289:123-7

Gurish MF, Bell AF, Smith TJ, Ducharme LA, Wang RK, Weis JH (1992) Expression of murine beta 7, alpha 4, and beta 1 integrin genes by rodent mast cells. J Immunol 149:1964-72

Hedrick SM, Cohen DI, Nielsen EA, Davis MM (1984) Isolation of cDNA clones encoding T cell-specific membrane-associated proteins. Nature 308:149-53

Heller S, Sheane CA, Javed Z, Hudspeth AJ (1998) Molecular markers for cell types of the inner ear and candidate genes for hearing disorders. Proc Natl Acad Sci U S A 95:11400-5

Hofmann K, Stoffel W (1993) TMbase - A database of membrane spanning proteins segments. Biol. Chem. Hoppe Seyler. 347:166.

Hong SH, David G, Wong CW, Dejean A, Privalsky ML (1997) SMRT corepressor interacts with PLZF and with the PML-retinoic acid receptor alpha (RARalpha) and PLZF-RARalpha oncoproteins associated with acute promyelocytic leukemia. Proc Natl Acad Sci U S A 94:9028-33

Ichimiya I, Adams JC, Kimura RS (1994) Changes in immunostaining of cochleas with experimentally induced endolymphatic hydrops. Ann Otol Rhinol Laryngol 103:457-68

Imamura S, Adams JC (1996) Immunolocalization of peptide 19 and other calcium-binding proteins in the guinea pig cochlea. Anat Embryol (Berl) 194:407-18

Jacob AN, Manjunath NA, Bray-Ward P, Kandpal RP (1998) Molecular cloning of a zinc finger gene eZNF from a human inner ear cDNA library, and in situ expression pattern of its mouse homologue in mouse inner ear. Somat Cell Mol Genet 24:121-9

Jan LY, Jan YN (1997) Cloned potassium channels from eukaryotes and prokaryotes. Annu Rev Neurosci 20:91-123

Jones DT, Reed RR (1989) Golf: an olfactory neuron specific-G protein involved in odorant signal transduction. Science 244:790-5

Kikuchi T, Adams JC, Miyabe Y, So E, Kobayashi T (2000) Potassium ion recycling pathway via gap junction systems in the mammalian cochlea and its interruption in hereditary nonsyndromic deafness. Med Electron Microsc 33:51-6

Kobertz WR, Miller C (1999) K+ channels lacking the 'tetramerization' domain: implications for pore structure. Nat Struct Biol 6:1122-5

Li M, Jan YN, Jan LY (1992) Specification of subunit assembly by the hydrophilic amino-terminal domain of the Shaker potassium channel. Science 257:1225-30

Lin RJ, Nagy L, Inoue S, Shao W, Miller WH, Jr., Evans RM (1998) Role of the histone deacetylase complex in acute promyelocytic leukaemia. Nature 391:811-4

Merchant SN, Linthicum FH, Nadol JB, Jr. (2000) Histopathology of the inner ear in DFNA9. Adv Otorhinolaryngol 56:212-7

Morton NE (1991) Genetic epidemiology of hearing impairment. Ann N Y Acad Sci 630:16-31

Ohara O, Nagase T, Ishikawa K, Nakajima D, Ohira M, Seki N, Nomura N (1997) Construction and characterization of human brain cDNA libraries suitable for analysis of cDNA clones encoding relatively large proteins. DNA Res 4:53-9

Pesole G, Grillo G, Larizza A, Liuni S (2000) The untranslated regions of eukaryotic mRNAs: structure, function, evolution and bioinformatic tools for their analysis. Brief Bioinform 1:236-49

Pesole G, Liuni S, Grillo G, Saccone C (1997) Structural and compositional features of untranslated regions of eukaryotic mRNAs. Gene 205:95-102

Pongs O, Leicher T, Berger M, Roeper J, Bahring R, Wray D, Giese KP, Silva AJ, Storm JF (1999) Functional and molecular aspects of voltage-gated K+ channel beta subunits. Ann N Y Acad Sci 868:344-55

Resendes BL, Robertson NG, Szustakowski JD, Resendes RJ, Weng Z, Morton CC (2002) Gene discovery in the auditory system: characterization of additional cochlear-expressed sequences. J Assoc Res Otolaryngol 3:45-53

Robertson NG, Heller S, Lin JS, Resendes BL, Weremowicz S, Denis CS, Bell AM, Hudspeth AJ, Morton CC (2000) A novel conserved cochlear gene, OTOR: identification, expression analysis, and chromosomal mapping. Genomics 66:242-8

Robertson NG, Khetarpal U, Gutierrez-Espeleta GA, Bieber FR, Morton CC (1994) Isolation of novel and known genes from a human fetal cochlear cDNA library using subtractive hybridization and differential screening. Genomics 23:42-50

Robertson NG, Lu L, Heller S, Merchant SN, Eavey RD, McKenna M, Nadol JB, Jr., Miyamoto RT, Linthicum FH, Jr., Lubianca Neto JF, Hudspeth AJ, Seidman CE, Morton CC, Seidman JG (1998) Mutations in a novel cochlear gene cause DFNA9, a human nonsyndromic deafness with vestibular dysfunction. Nat Genet 20:299-303

Sewing S, Roeper J, Pongs O (1996) Kv beta 1 subunit binding specific for shaker-related potassium channel alpha subunits. Neuron 16:455-63

Shen NV, Pfaffinger PJ (1995) Molecular recognition and assembly sequences involved in the subfamily-specific assembly of voltage-gated K+ channel subunit proteins. Neuron 14:625-33

Skvorak AB, Robertson NG, Yin Y, Weremowicz S, Her H, Bieber FR, Beisel KW, Lynch ED, Beier DR, Morton CC (1997) An ancient conserved gene expressed in the human inner ear: identification, expression analysis, and chromosomal mapping of human and mouse antiquitin (ATQ1). Genomics 46:191-9

Skvorak AB, Weng Z, Yee AJ, Robertson NG, Morton CC (1999) Human cochlear expressed sequence tags provide insight into cochlear gene expression and identify candidate genes for deafness. Hum Mol Genet 8:439-52

Sonnhammer EL, von Heijne G, Krogh A (1998) A hidden Markov model for predicting transmembrane helices in protein sequences. Proc Int Conf Intell Syst Mol Biol 6:175-82

Soto-Prior A, Lavigne-Rebillard M, Lenoir M, Ripoll C, Rebillard G, Vago P, Pujol R, Hamel CP (1997) Identification of preferentially expressed cochlear genes by systematic sequencing of a rat cochlea cDNA library. Brain Res Mol Brain Res 47:1-10

Spicer SS, Gratton MA, Schulte BA (1997) Expression patterns of ion transport enzymes in spiral ligament fibrocytes change in relation to strial atrophy in the aged gerbil cochlea. Hear Res 111:93-102

Spicer SS, Schulte BA (1997) Golgi-canalicular reticulum system in ion transporting fibrocytes and outer sulcus epithelium of gerbil cochlea. Anat Rec 249:117-27

Tusnady GE, Simon I (1998) Principles governing amino acid composition of integral membrane proteins: application to topology prediction. J Mol Biol 283:489-506

Van Camp G, Smith RJH (2003) Hereditary hearing loss homepage. WWW URL: http://www.uia.ac.be/dnalab/hhh/

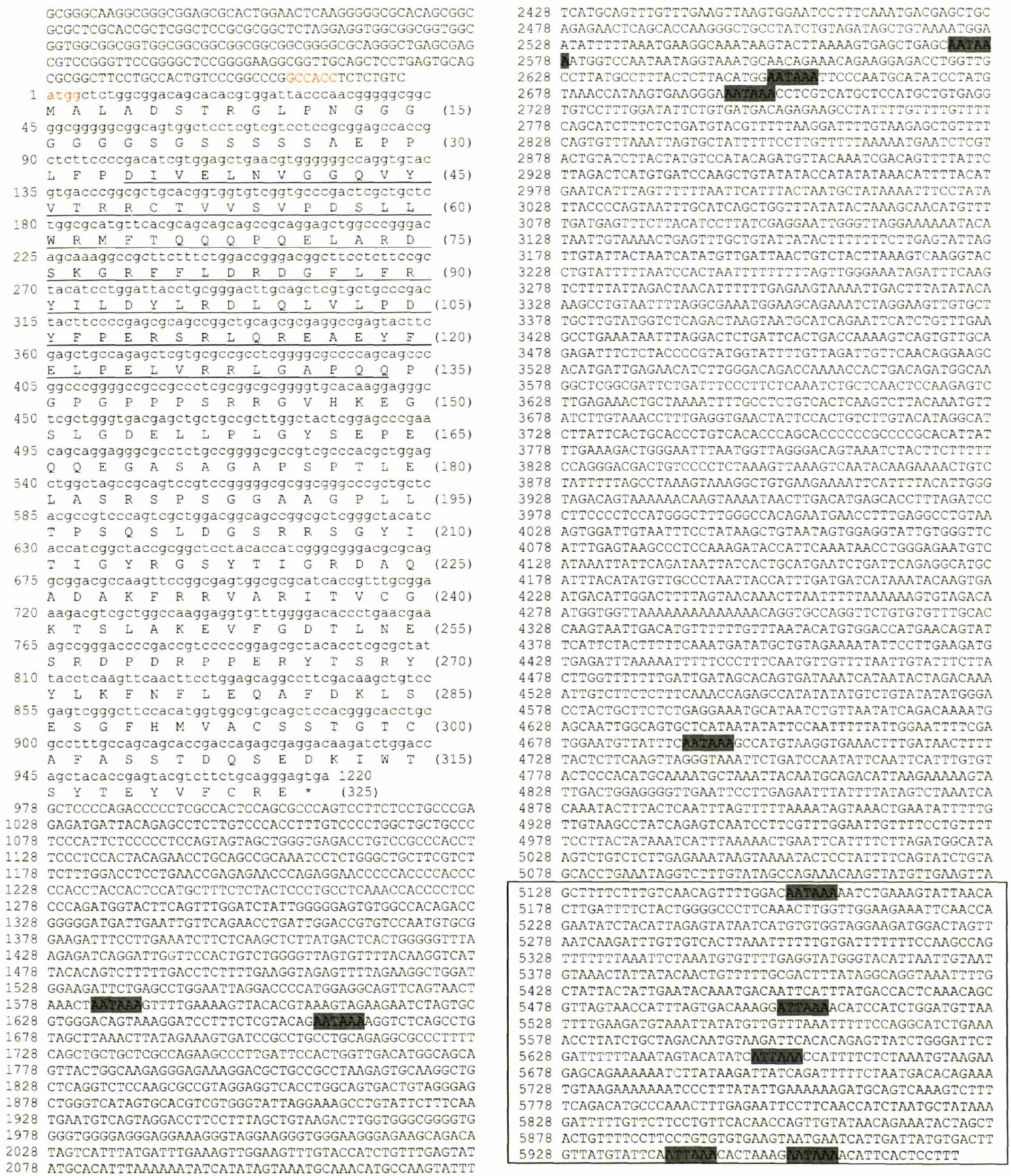

Figure 1. Nucleotide sequence of human *PFET1* cDNA and its deduced amino acid sequence. Nucleotide numbers are shown on the left and amino acid sequence numbers are shown in parentheses on the right. The Kozak consensus sequence is outlined in red. The tetramerization domain is underlined. An asterisk denotes the stop codon. Putative polyadenylation consensus sequences are shaded. The boxed sequence represents the original clone obtained from the cochlear cDNA library.

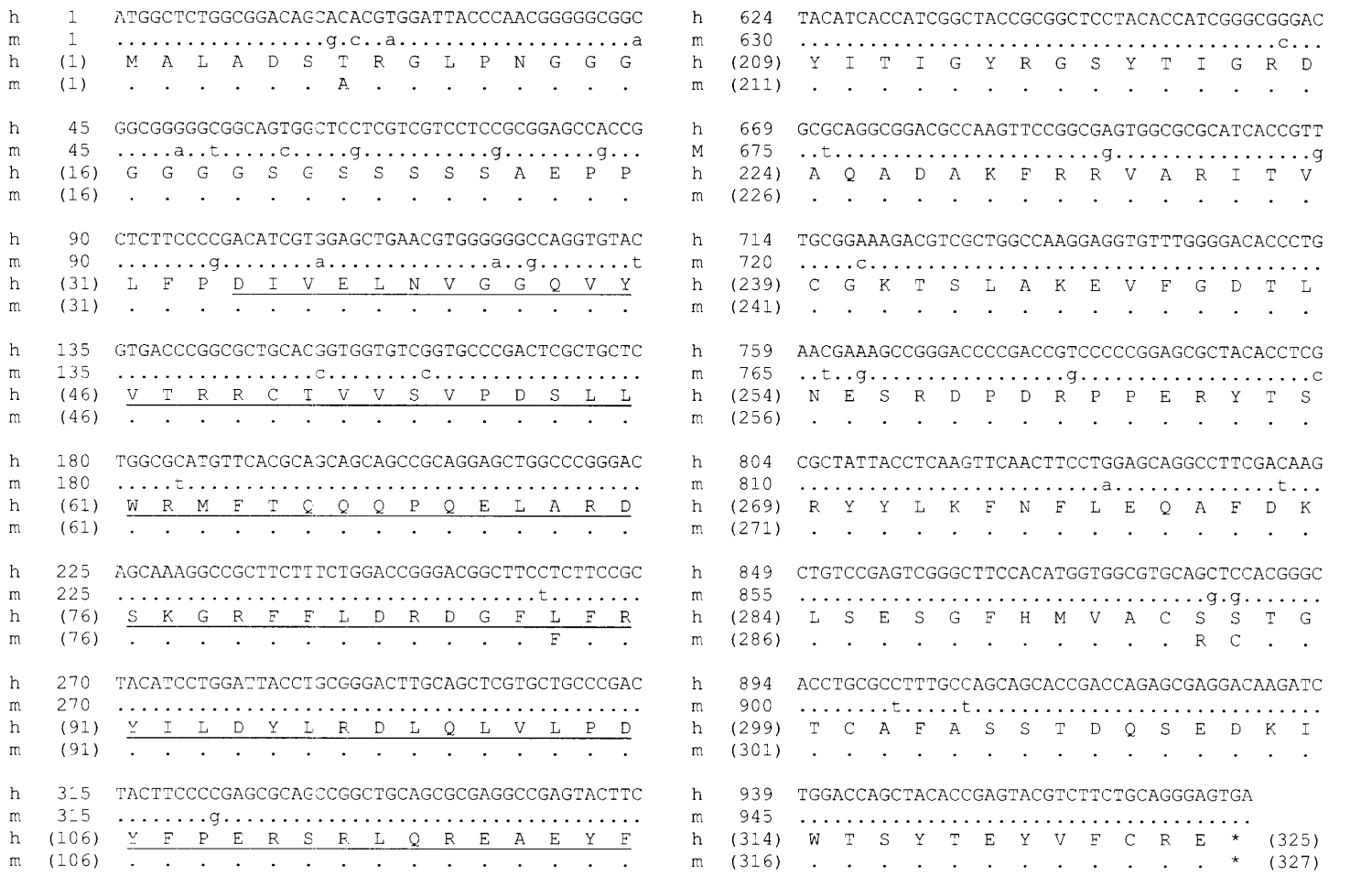

Figure 2. Alignment of the complete deduced sequence of the open reading frames of the human and mouse *Pfet1* genes. The deduced amino acid sequences of the ORFs share 91% similarity and differ by eight amino acids, one of which is within the tetramerization domain (position 88). A high degree of sequence similarity indicates cross-species conservation of the *PFET1* gene. Nucleotide sequence is capitalized for the human *PFET1* gene and in lower case for the mouse *PFET1* gene. Amino acid sequence is capitalized and numbered in parentheses. Dots represent sequence identity between human and mouse genes. Dashes represent gaps introduced to align the sequences. An asterisk denotes the stop codon. The tetramerization domain is underlined.

Figure 3. Nucleotide sequence of mouse *Pfet1* cDNA and its deduced amino acid sequence. Nucleotide numbers are shown on the left and amino acid sequence numbers are shown in parentheses on the right. The Kozak consensus sequence is outlined in red. The tetramerization domain is underlined. An asterisk denotes the stop codon. Putative polyadenylation consensus sequences are shaded.

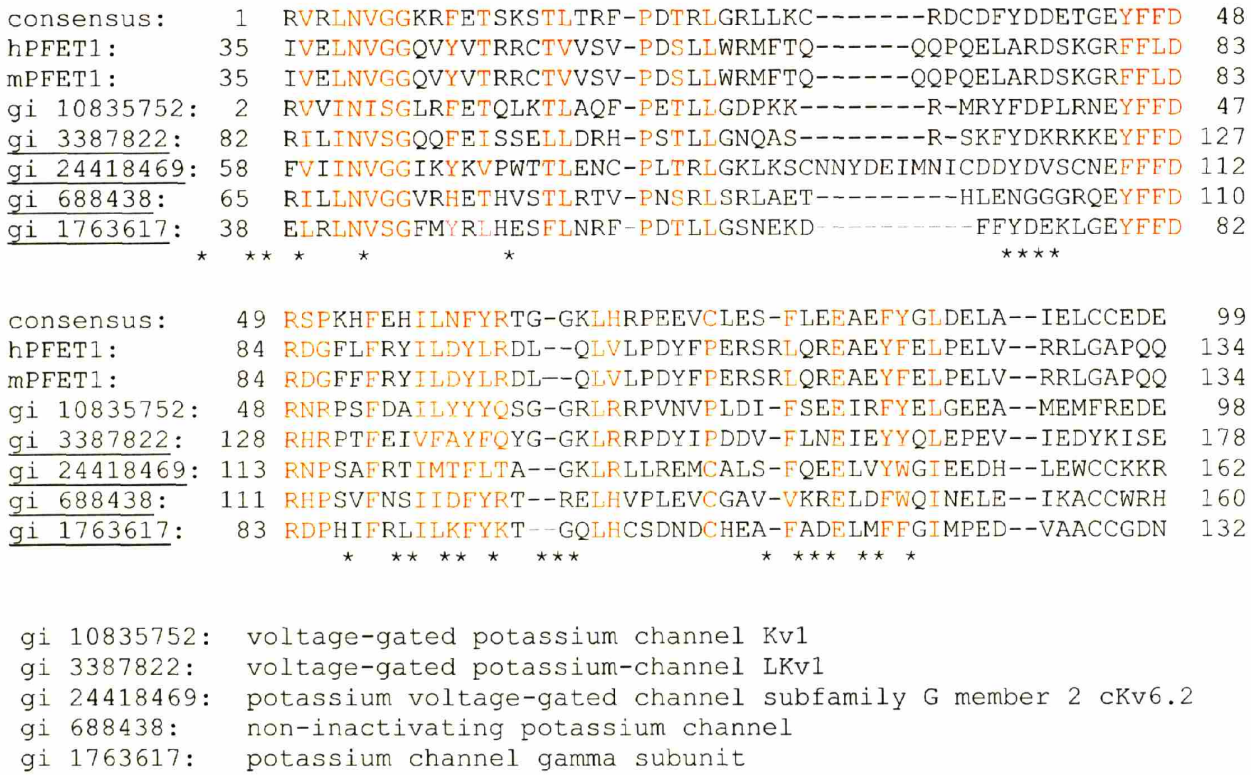

Figure 4. Alignment of the consensus sequence for the tetramerization domain of the voltage-gated K+ channel family (PFAM00214) (Bixby et al. 1999), deduced amino acid sequence of the tetramerization domain from the human and mouse *PFET1* genes, and various potassium channel tetramerization domains. Dashes represent gaps introduced to align the sequences. Asterisks denote amino acids conserved across four subfamilies of voltage-gated K+ channels (Bixby et al. 1999). Red letters represent highly conserved regions across a more diverse group of PFAM00214 family members (only 5 out of 25 were listed) using NCBI's Conserved Domain Database (CDD).

Figure 5A

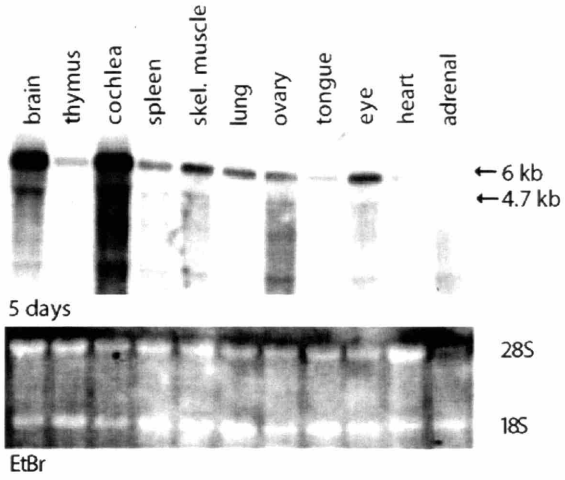

Figure 5B

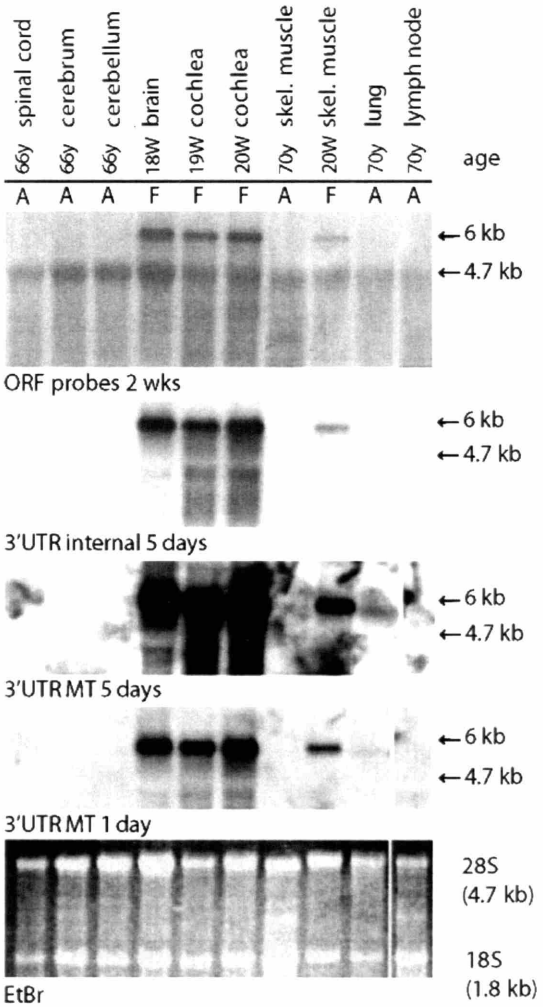

Figure 5C

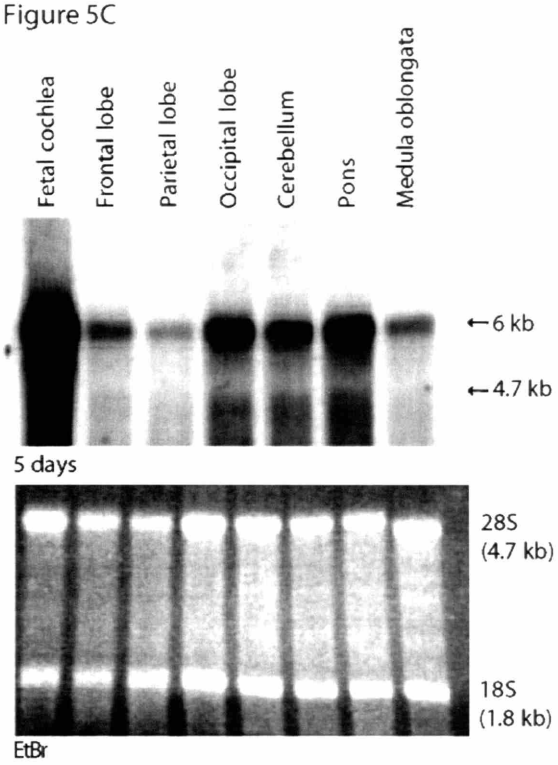

Figure 5A-C. Autoradiographs of Northern blots containing 10 ug per lane of total human RNAs hybridized with radiolabeled *PFET1* fragments. (A) A panel of human fetal tissues probed with the 3'-most UTR *PFET1* probe (MT fragment) demonstrates expression of a single transcript of ~6 kb in most tissues, with highest expression in cochlea and brain. (B) A panel of adult ("A") and fetal ("F") RNAs probed with various *PFET1* probes demonstrates high levels of expression of a single ~6 kb transcript in fetal tissues and barely detectable levels in adult tissues, including spinal cord, cerebrum, cerebellum, skeletal muscle, lung and lymph node. Similar low level expression was observed in the other adult tissues that are not shown, including lung, heart, kidney and liver. (C) A panel of total RNA isolated from different regions of the fetal brain probed with *PFET1*; a single ~6 kb transcript is detected in all samples. A lane of fetal cochlear RNA was included as a positive control. For each Northern blot, a photograph of the EtBr-stained RNA gel is shown. F, fetal; A, adult; Y, years; W, weeks.

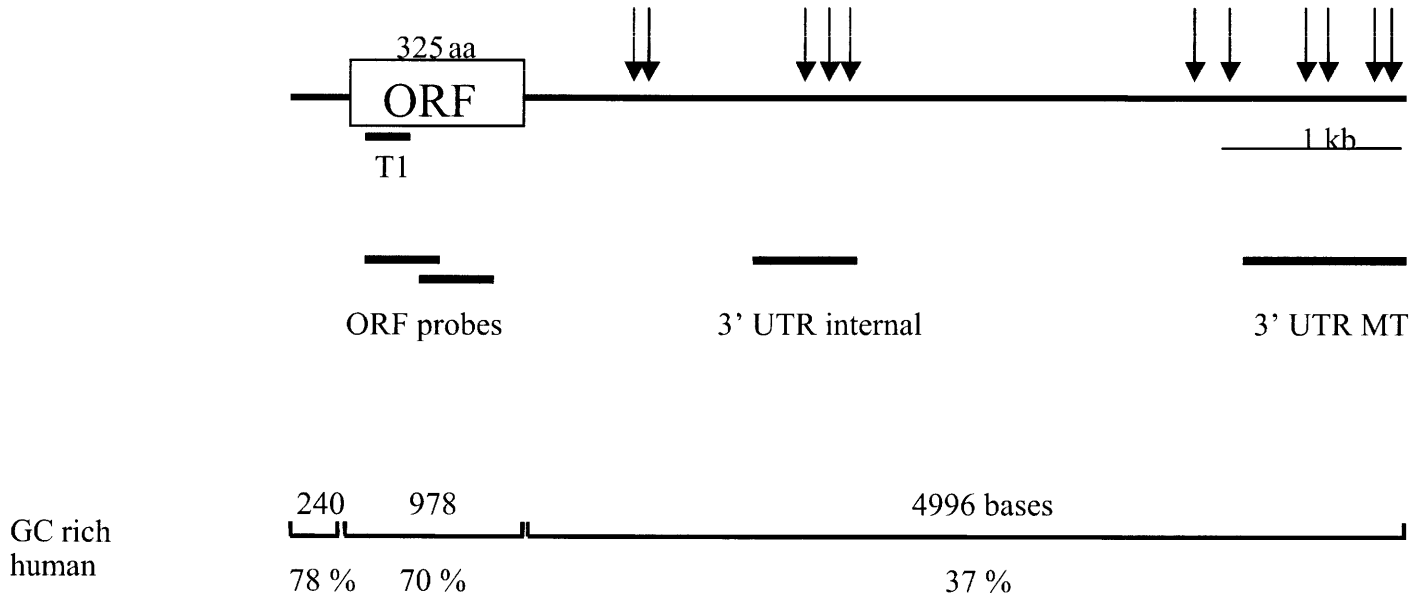

Figure 5D. Schematic of *PFET1* gene. The position of the ORF and the polyadenylation consensus sequences (arrows) are shown relative to each other. The position of the tetramerization domain (T1) is indicated. The positions of 5' and 3' regions of *PFET1* that were amplified by PCR or used for probes are indicated. The "MT" probe is to the 3'-most end of the 3' UTR. The percent GC-richness of various regions within the *PFET1* gene is depicted at the bottom of the diagram.

Figure 6A

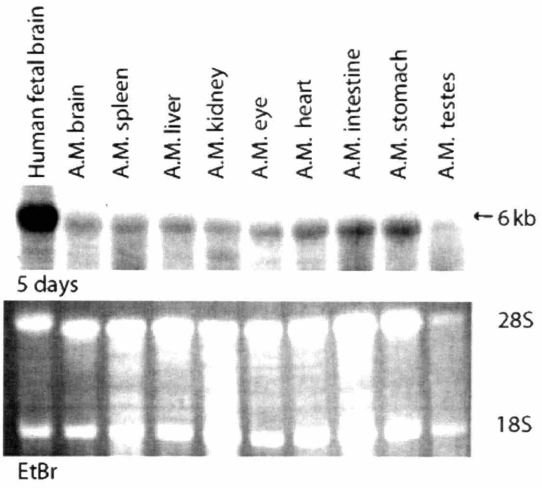

Figure 6B

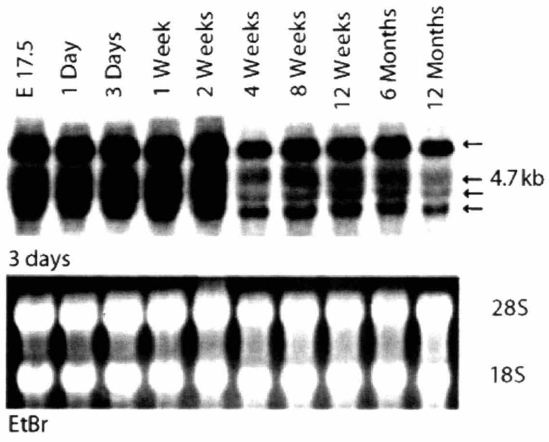

Figure 6C

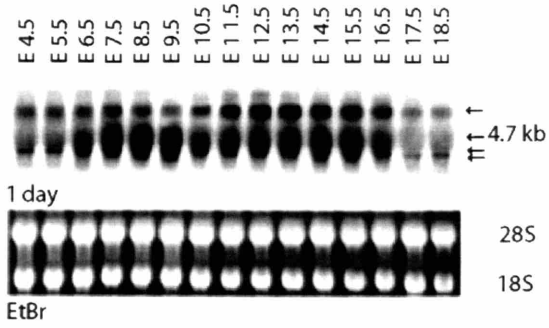

Figure 6A-C. Northern blot analysis of mouse RNA samples hybridized with mouse *Pfet1* radiolabeled fragments. (A) An adult mouse tissue panel containing 10 ug of each sample hybridized with a probe to the 3' end of the ORF reveals low expression levels of a single ~6 kb transcript in adult mouse tissues. A lane containing 10 ug of human fetal brain total RNA is present for comparison. A, adult; M, mouse. (B) A mouse aging brain panel containing 20 ug of each sample hybridized with the 3' UTR probe 1 reveals the presence of a predominate ~6 kb transcript and two smaller and less intense transcripts (~4 and 4.5 kb) in the embryonic and newborn stages. (C) A mouse developmental panel containing 20 ug of each sample hybridized with a probe to the 3' end of the ORF reveals two transcripts. The upper transcript (~6 kb) has a higher level of intensity between days 11.5 and 15.5 while the lower transcripts (~4 and 4.5 kb) have a higher level of intensity between days 6.5 and 15.5. For each Northern blot, a photograph of the EtBr-stained RNA gel is shown.

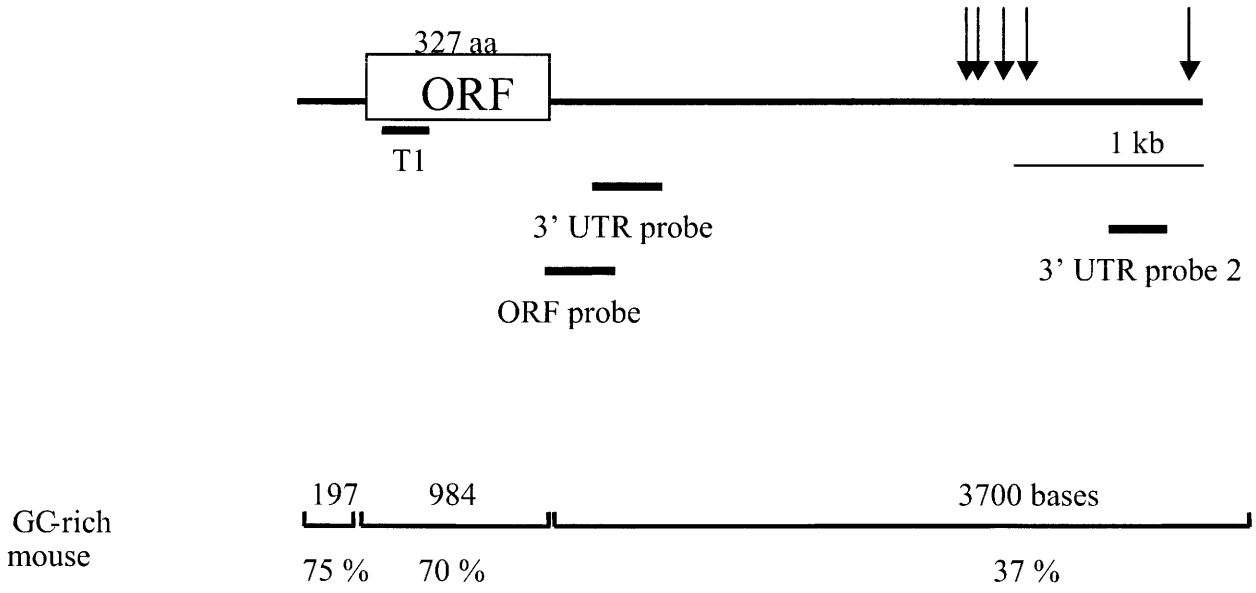

Figure 6D. Schematic of the mouse *Pfet1* gene. The position of the ORF and the polyadenylation consensus sequences (arrows) are shown relative to each other. The position of the tetramerization domain (T1) is indicated. The positions of 5' and 3' regions of *Pfet1* that were amplified by PCR or used for probes are indicated. The percent of GC-richness of various regions within the *Pfet1* gene is depicted at the bottom of the diagram.

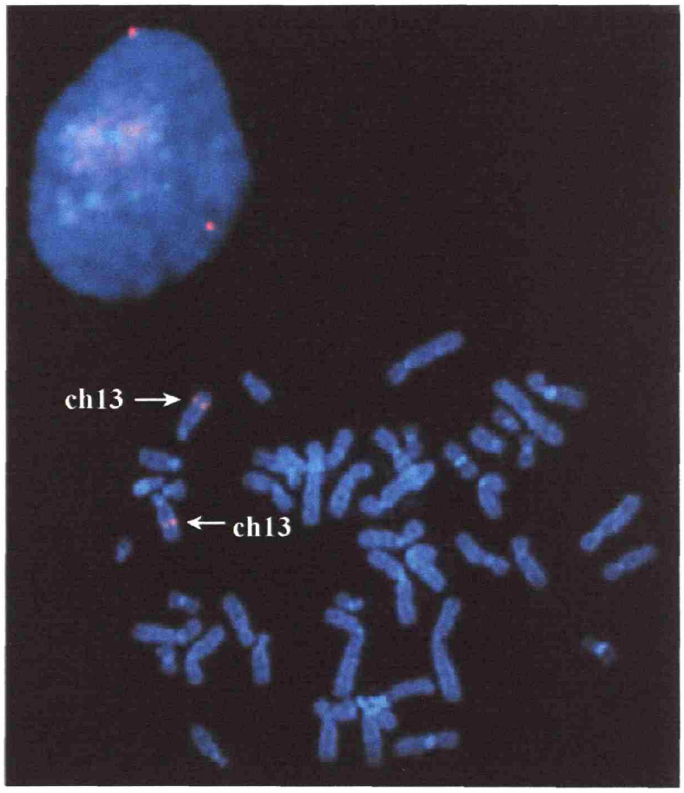

Figure 7. Chromosomal localization by fluorescence *in situ* hybridization (FISH) of a human PAC containing the entire *PFET1* gene. Human metaphase chromosomes are counterstained with DAPI following FISH with PAC 246J2. Arrows indicate the positions of the signals that localize to band q21 on both chromosome 13s.

Figure 8

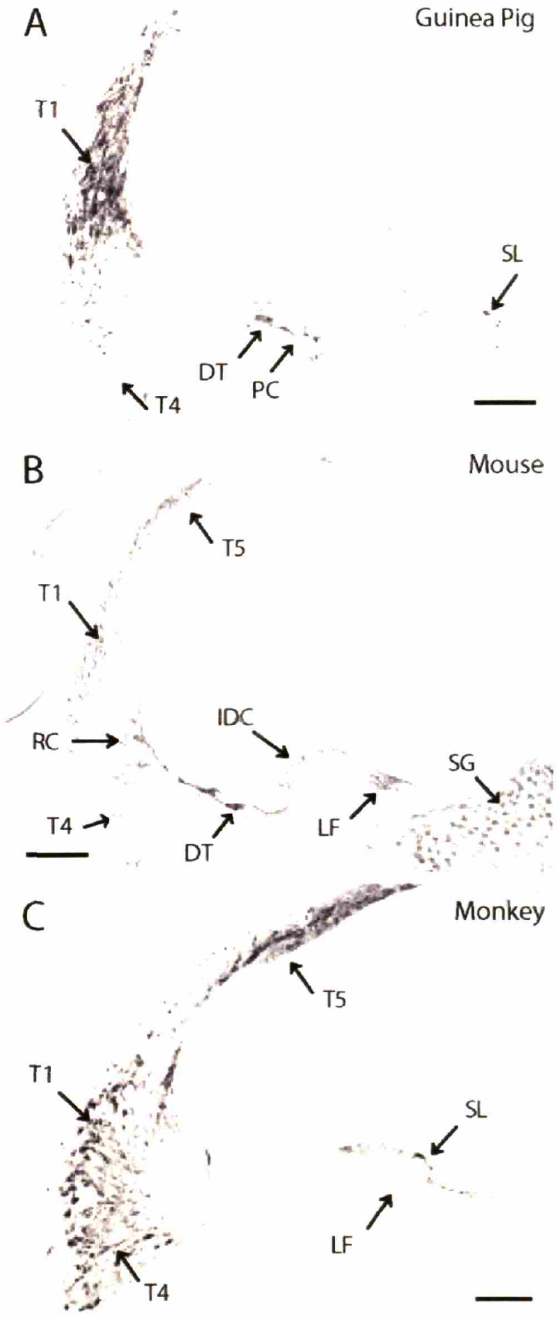

Figure 8. Immunohistochemical staining using pfetin antibody on (A) formalin glutaraldehyde (FG)-fixed guinea pig, (B) FG-fixed mouse, and (C) FA-fixed monkey cochleas. Arrows point to individual cells positive for immunostaining with pfetin antibody. Positive immunostaining is seen as the dark DAB reaction product. Dominant staining is seen in type I fibrocytes of the cochlea. T1, 4, 5 = types I, IV, and V fibrocytes; PC = pillar cell; IDC = interdental cell; ISC = inner sulcus cell; SL = supralimbal cell; LF = limbal fibrocytes; RC = root cells; SG = spiral ganglion cells. Each scale bar represents 100 microns.

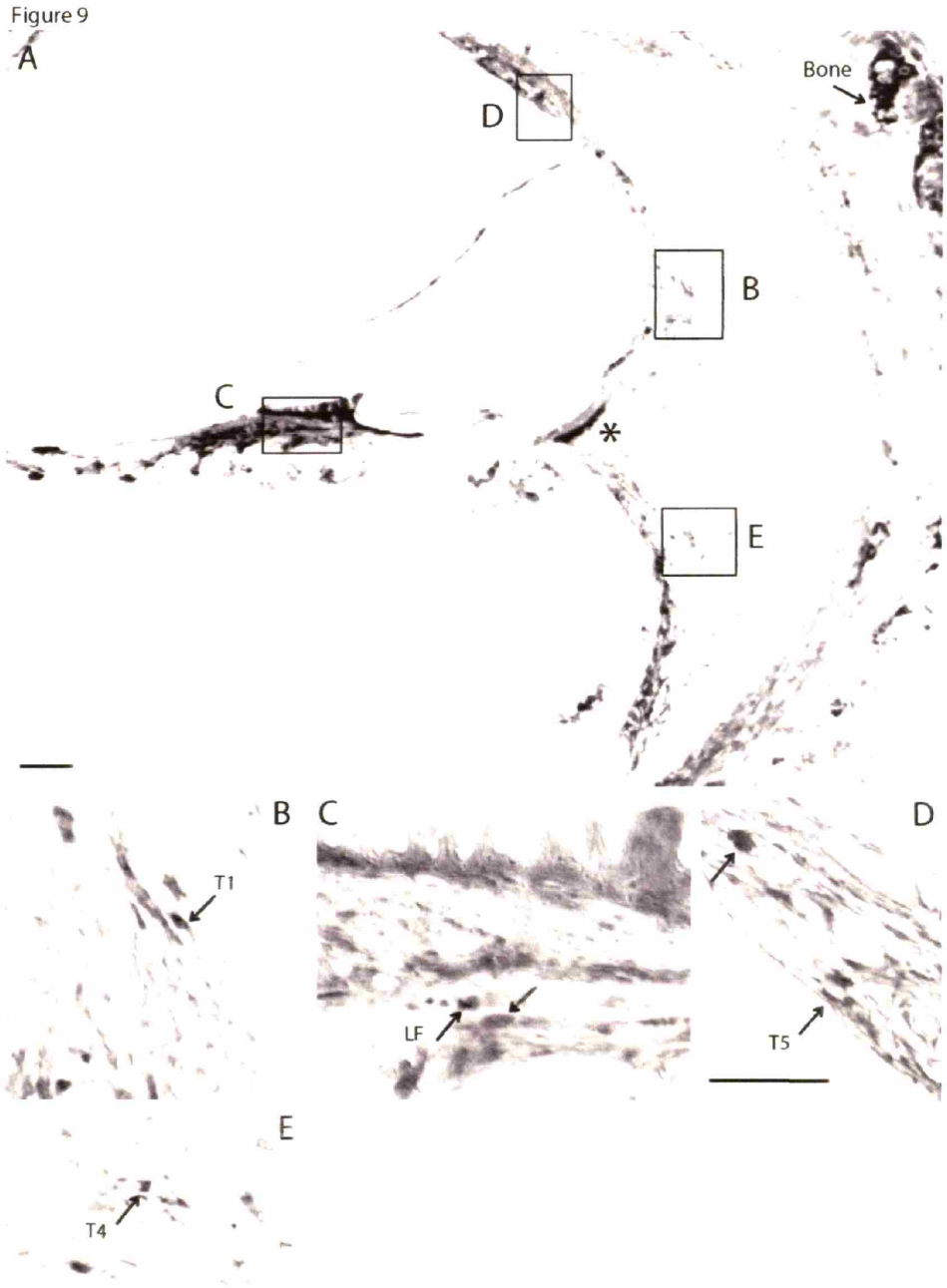

Figure 9. Immunohistochemical staining using pfetin antibody on formalin-fixed adult human cochlea (A). Higher magnification views of the boxed areas are shown in correspondingly lettered images below (B-E). Arrows point to immunostained cells. Immunostaining is present in type I (T1), IV (T4), and V (T5) fibrocytes. LF = limbal fibrocytes; * = extracellular matrix. Each scale bar represents 100 microns. The images in B-E are all the same magnification.

Figure 10

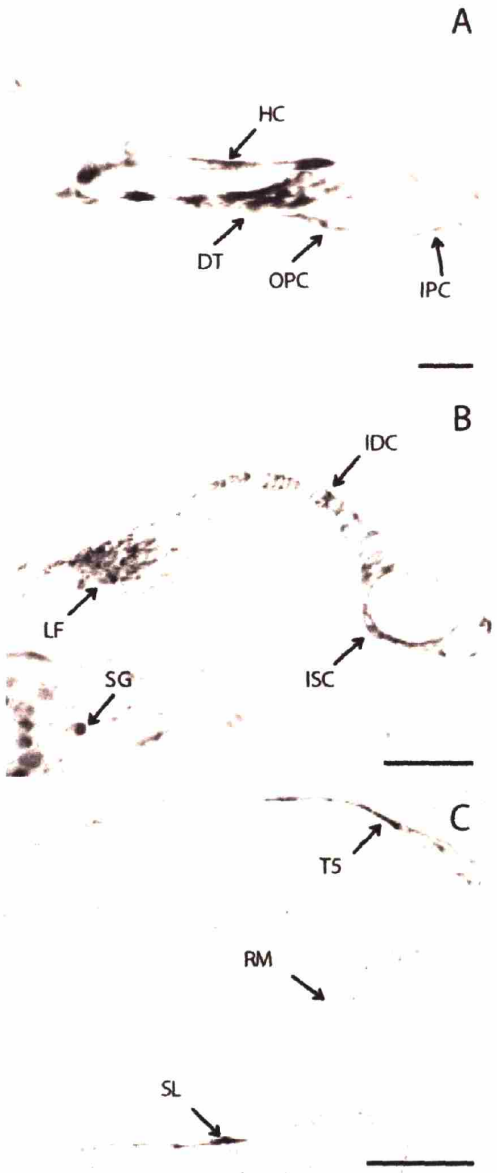

Figure 10. Immunostained formalin plus glutaraldehyde fixed mouse (A and B) and formalin acetic fixed guinea pig (C) cochlea. Panel (A) shows the organ of corti, (B) the spiral limbus and (C) areas contacting Reissner's membrane. IPC, OPC = inner and outer pillar cells; DT = Deiters cells; ISC = inner sulcus cells; IDC = interdental cells; LF = limbral fibrocytes; HC = Hensen cells; SG = spiral ganglion; T5 = Type V fibrocytes (suprastrial cells); SL = supralimbal cells. Each scale bar represents 50 microns.

Figure 11

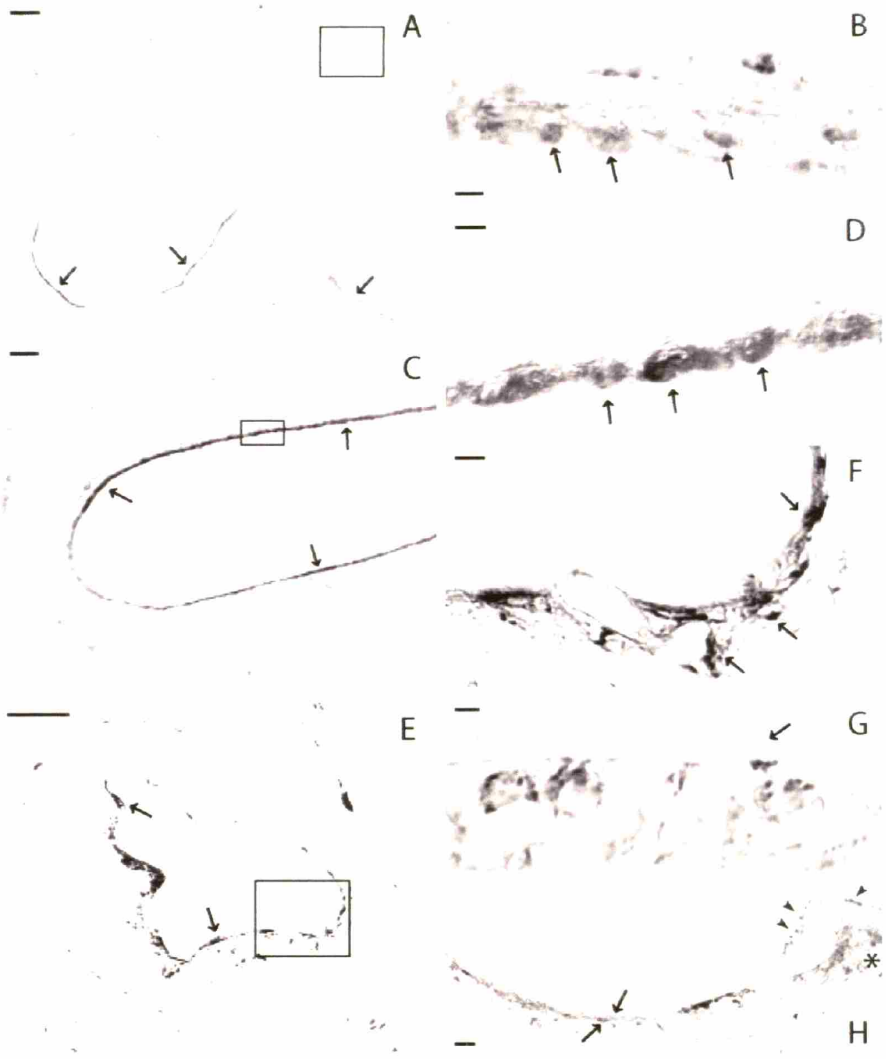

Figure 11. Pfetin immunostaining of vestibular tissue of 20-week human fetus (formalin-fixed)(A-D), guinea pig (formalin plus glutaraldehyde-fixed)(E, F), and mouse (formalin plus glutaraldehyde-fixed)(G, H). The semicircular canal shows (A) a continuous layer of staining (arrow) in the lateral ampulla underlying the transitional cells and vestibular dark cells. (B) Higher magnification of boxed region in (A). Arrows point to individual positive cells. (C) Arrows indicate immunostained cells lining the lumen of the semicircular canal. (D) Higher magnification of boxed region in (C). (E) Guinea pig posterior ampulla with arrows pointing to immunostained cells. (F) Higher magnification of boxed region in (E). (G) Sensory epithelium of the macula of the saccule showing the immunostained type I hair cells. Arrow points to the unstained ciliary bundle extending from the darkly stained cuticular plate. This and adjacent type I hair cells also show granular reaction product within their cytosol. (H) Mouse lateral ampulla with arrows pointing to immunostained lumenal and ablumenal cells. Arrowheads point to cuticular plate staining of type I hair cells. Asterisk indicates staining in the connective fibrocytes underneath the sensory epithelium. Scale bars in Figures 12A, C and E represent 100 microns; in Figures 12B, D, F, and G 10 microns; in Figure 12 H 20 microns.

CHAPTER 3

Functional Characterization of *KCTD12* in Zebrafish

Sharon F. Kuo[1], Jarema Malicki[2*], Cynthia C. Morton[3*]

1)Speech and Hearing Bioscience and Technology, Harvard-MIT Division of Health Sciences and Technology, Boston, MA; 2)Department of Ophthalmology, Harvard Medical School, Boston, MA; 3)Departments of Ob/Gyn and Pathology, Brigham and Women's Hospital, Harvard Medical School, Boston, MA

* Co-last Authors

ACKNOWLEDGMENTS

We thank Drs. Motokazu Tsujikawa and Yoshihiro Omori for sharing their experience and resources in zebrafish *in situ* hybridization and morpholino experiments, Amanda Smith and Dr. Charles Lee for their assistance with the zebrafish fluorescence *in situ* hybridization and chromosome analysis and Dr. Joshua Gamse for kindly providing us with *lov* and *ron* expression constructs and Ron antibody.
This work was supported by the NIH Grants DC03402 (C.C.M.), and T32DC0019 (S.F.K.)

ABSTRACT

KCTD12 (originally described as *PFET1*) was initially isolated from the Morton human fetal cochlear cDNA library with a predominant expression in the fetal cochlea and brain. It is a 6 kb intronless transcript and a member of the newly classified and enlarging potassium channel tetramerization domain containing (KCTD) family containing a single tetramerization domain (T1). Functional characterization of *KCTD12* and its gene product pfetin have been studied in zebrafish with *in situ* hybridization, immunohistochemsitry and morpholino knock-down of the *KCTD12* zebrafish ortholog *right on* (*ron*). *In situ* hybridization revealed expression of *ron* and its encoded protein Ron in the developing zebrafish otic vesicle (OV) and vestibular-cochlear ganglion (VCG). Immunochemical analysis showed co-localization of Ron and an early inner ear marker Islet1 (Isl1) within the VCG. Morpholino knock-down experiments showed correlation between Ron knock-down and Isl1 down-regulation in the VCG during early zebrafish development. Given these observations, we postulate Ron's role as a regulator of neuronal differentiation and identity in the developing inner ear.

KEYWORDS: PFET1, Islet1, Ron, KCTD, Vestibular-Cochlear Ganglion, TNF-alpha,

INTRODUCTION

Previously, we reported the identification of a novel 6kb cochlear transcript, *KCTD12* (gene aliases: *KCTD12*; *C13orf2*), using a combinatorial approach of subtractive hybridization and differential screening of a human fetal cochlear cDNA library. *KCTD12* was determined to be a predominantly fetal expressed gene with a single tetramerization (T1) domain, encoded by a single highly GC-rich (70%) exon, and predicted to contain a full-length ORF of 325 amino acids. Genomic location for *KCTD12* was confirmed by FISH analysis to band q21 on human chromosome 13. Immunohistochemistry with a polyclonal antibody raised against a synthetic peptide to the *KCTD12* sequence reveals expression in a variety of cell types in human, monkey, mouse, and guinea pig cochleas and the vestibular system, including type I vestibular hair cells (Resendes and Kuo 2004). Given its unique preferential expression in fetal cochlea (as late as second trimester developmental age in humans) and the presence of a voltage-gated potassium channel associated T1 tetramerization domain in its ORF, *KCTD12* was chosen for further characterization. Currently, *KCTD12* maps within the vicinity of the AUNA1 locus (13q14–21), responsible for progressive autosomal dominant auditory neuropathy in a large kindred from the United States (Kim et al. 2004).

KCTD12 is the 12th member of the potassium channel tetramerization domain containing (*KCTD*) gene family (Marchler-Bauer et al. 2003). Although the presence of a T1 domain suggests certain functional association with potassium channels and ion transport, familial functional characteristics for KCTD have not been established. Therefore a closer examination of the existing family members should provide insight into deducing certain familial functional traits. To delineate the function of the *KCTD12* encoded protein pfetin in

development, we turned to zebrafish (*Danio Rerio*), a vertebrate animal model for study of the inner ear due to its ease of generation, *in vivo* manipulation, and many similarities to the inner ear of higher vertebrates including humans. Expression analysis through *in situ* hybridization and immunohistochemistry were pursued to provide specific localization information on the zebrafish ortholog of *KCTD12* and morpholino knock-down experiment were performed to facilitate determination of gene function *in vivo*. Through these analyses, the role of *KCTD12* in the vertebrate inner ear has been further elucidated.

MATERIALS AND METHODS

Linkage Group Mapping of *KCTD12* Zebrafish Orthologs

Blast analysis through the Washington University - Zebrafish Genome Resources (http://zfish.wustl.edu/) identified two ESTs, *leftover* (*lov*) (NP_919386, wz39483.2) and *right on* (*ron*) (wz41247.1,) that have largely been studied to date for their asymmetric expression patterns in the habenula (Gamse et al. 2003, 2005). To confirm duplication of the *KCTD12* ortholog in the zebrafish genome, a BAC (zK24H22) containing the entire *ron* genomic sequence was used to generate a biotin-labeled probe for fluorescence *in situ* hybridization (FISH). Given the 75% identity match at the nucleotide level between the two orthologs' ORF, a single probe (zK24H22) was able to identify both *lov* and *ron*. Probe labeling and visualization were carried out using standard protocols (Lee and Smith, 2004).

Real Time RT-PCR

Real time RT-PCR is a sensitive and quantitative tool used for determination of relative RNA expression levels in a gene of interest. Wild-type AB zebrafish embryos were grown until various developmental stages (12, 24, 36, 48, 72 and 96 hours post fertilization). Total RNA was extracted using Trizol and treated with DNAse. RT-PCR reaction was carried out using SuperScript One-Step RT-PCR with a Platinum *Taq* kit (Invitrogen, Carlsbad, CA). Primers and probes for *lov* (NP_919386), *ron* (wz41247.1) and the housekeeping gene *bactin1* (NM131031) were designed with PRIMEREXPRESS software (Applied Biosystem, Foster City, CA). PCR primers used were: upper 5'AAGTCAGATTCAAGGGCCTATTTG3' and lower: 5'TGCAGTGTTCGGAT- GAAGCA3' for *lov*; upper: 5'GAGGCAGAATATTTCCAACTTCAAG3' and lower: 5'TCTGGCAAACCTCCTCGCT3' for *ron*; and upper: 5'AGGTCATCACCATCGG-CAAT3' and lower: 5'ATGAAGTGCGACGTGGACATC 3' for *bactin1*. Probes used were 5'CCCAGATGTGTTTTGTACTCGTTATTCTTTATGCA3' for *lov*; 5'AGCGCC-TGAAACCTGCGGTCAGTAAG3' for *ron*; and 5'CTTCCAGCCTTCCTTCCTGGGT-ATGGAA3' for *bactin1*. Primers were tested using conventional PCR and shown to amplify a single band of approximately 100 bp without production of primer dimers. Real-time PCR, which quantifies the amount of product after each cycle, was carried out on each cDNA sample using an i-cycler (BioRad, Hercules, CA) with Taqman probe. Reactions were heated to 50°C for 15 minutes followed by 95°C for 3.5 minutes. Subsequently, reactions proceeded through 45 cycles at 95°C for 15 seconds and 60°C for 1 minute. The fluorescence level was determined after each cycle, allowing detection of the log phase of amplification. I-cycler software was used to define the cycle in which each sample attained the threshold value of

fluorescence. For a negative control, *Taq* DNA polymerase was substituted for reverse transcriptase. All samples were assessed in duplicate. *Lov* and *ron* mRNA level are expressed as fold increase adjusted for genomic contamination and normalized to *bactin1*.

Developmental *In Situ* Hybridization

Zebrafish (*Danio rerio*) (strain wild-type AB) were kept on a 14/10 hour light/dark cycle according to standard procedures (Westerfield, 1994). Embryos were collected from pairwise timed matings and raised at 28.5°C until the appropriate stage (12, 24, 36, 48, 72, and 96 hours) and then fixed by incubation overnight in 4% paraformaldehyde at 4°C. Embryo medium was supplemented with 1-phenyl-2-thiourea (PTU, 0.003%) prior to 24 hours post fertilization to prevent accumulation of pigment. After fixation, embryos were dehydrated and stored at -20°C in 100% methanol prior to *in situ* hybridization. Nucleotides spanning the ORF of zebrafish *lov* and *ron* were amplified and cloned into a vector derived from pCRII-TOPO (Invitrogen). To generate digoxigenin (DIG)-labeled antisense probes, the DNA plasmid was linearized with *Hind*III or *Xho*I , followed by transcription using SP6/T7 polymerase and DIG RNA labeling mix (Roche, Indianapolis, IN). *In situ* hybridization was then performed according to the high resolution whole-mount *in situ* hybridization protocol (http://zfin.org/zf_info/zfbook/chapt9/9.82.html). The labeling reaction was monitored under a dissecting microscope and the reaction stopped with 1X PBS at pH 5.5. For image recording, embryos were mounted in methyl cellulose for whole mount or embedded in JB-4 resin (Polysciences, Warrington, PA) and sectioned between 4 to 6 micron thicknesses. Images were recorded using a Zeiss Axiocam digital camera (Carl Zeiss, Oberkochen, Germany) and Photoshop software (Adobe, San Jose, CA).

Morpholino Knockdown and Zebrafish Immunohistochemsitry

Morpholino oligonucleotide (MO) knock-downs were performed as described previously (Malicki et al., 2002). MOs are basically synthetic DNA analogues that contain a neutral charged backbone in which the deoxyribose sugar moieties are replaced with morpholino (hydro-1, 4-oxaine) rings. The stability, nuclease-resistance, efficacy, long-term activity, water-solubility, low toxicity and specificity of MOs make them a most ideal gene knockdown reagent. It functions by specific binding to its selected target site to block access of cell components to that target site. MOs can be used to knock down expression of many target genes by sterically blocking the translation initiation complex or modifying and controlling normal splicing events by blocking sites involved in splicing pre-mRNA (Gene Tools, Philomath, OR).

For *ron*, two custom oligonucleotides were used with one targeting the 5' untranslated region (*ron* 5'UTR morpholino) and one targeting the open reading frame region (*ron* ATG morpholino): ron5'UTR, 5'-AGACCTCCAGTGCAATCACAGAACT-3' and ronATG, 5'-GCGCGAGTCTTATCCATCTTTGCAC-3'. Specificity was confirmed by immunofluorescence labeling of frozen tissue sections of both control and anti-*ron* morpholino-injected zebrafish embryos. After the injection of morpholinos, embryos were sacrificed at specified time points and prepared for frozen sections for immunohistochemical analysis with antibody staining (Malicki, 1999; Pujic and Malicki, 2001). The following primary antibodies and dilutions were used: mouse anti-acetylated alpha-tubulin (1:500, Sigma, St. Louis, MO); mouse anti Islet-1/39.4D5 (1:500, Developmental Studies Hybridoma Bank, Iowa City, IA); rabbit anti-Ron (1:500, gift from Dr. Gamse). For frozen section

immunohistochemistry analysis, tissue sections were blocked in 10% goat serum, 0.5% Triton X-100 in PBST for 1 hr and incubated overnight in primary antibody at 4^0C and followed by Alexa 488-conjugated secondary antibody at room temperature for 3 hours. Following three 5 minutes washes in PBST, sections were viewed using a Leica confocal microscope with a Leica HCX APO L40X lens.

RESULTS

Domain Analysis

Blast analysis revealed *KCTD12* to be a member of the KCTD (potassium channel tetramerization domain containing protein) family. Presently, this family consists of 19 members (Table 1) with heterogeneous chromosomal locations, coding regions (225 to 950 amino acids), numbers of exons (1 to 18), and GC content in the ORFs (40 to 70%). Thus far, the lack of any predicted transmembrane domains and the presence of a single tetramerization domain are the salient features shared by members of the KCTD family. Most members of the KCTD family have been recently identified and sequenced. Besides *KCTD12*, only a few other members have been studied: *KCTD10* is a novel PDIP1-related protein that interacts with proliferating cell nuclear antigen and DNA polymerase delta (Zhou et al. 2005), *KCTD11* is a suppressor of Hedgehog signaling (Di Marcotullio et al. 2004), *KCTD3* as an antigen of renal cell carcinoma (Scanlan et al. 1999), and *KCTD13* is a distal target of TNF-alpha activation and a link between cytokine activation and DNA replication (He et al. 2001). As more detailed studies on members of KCTD family become available, further potential unifying functional speculation will be possible.

Table 1. KCTD Family

KCTD family	Predicted ORF in amino acid	Chromosomal Location	Number of predicted exons	ORF GC content (%)
KCTD1	257	18q11.2	5	43
KCTD2	263	17q25.1	6	55
KCTD3	295	1q41	18	42
KCTD4	259	13q14.12	1	40
KCTD5	234	16p13.3	6	59
KCTD6	237	3p14.3	3	45
KCTD7	289	7q11.21	4	60
KCTD8	473	4p13	2	59
KCTD9	389	8p21.2	11	43
KCTD10	313	12q24.11	7	54
KCTD11	232	17p13.1	1	65
KCTD12	235	13q21	1	70
KCTD13	329	16p11.2	6	62
KCTD14	225	11q14.1	2	54
KCTD15	283	19q13.11	7	63
KCTD16	428	5q31.3	4	40
KCTD17	314	22q12.3	9	64
KCTD18	426	2q33.1	7	51
KCTD19	950	16q22.1	16	53

Analysis of *KCTD12* in its Zebrafish Orthologs, *Leftover* and *Right on*

Zebrafish is a good vertebrate animal model for genetic studies because of its high reproductive rate, easy access to embryos of all stages due to external fertilization and transparent development. The zebrafish inner ear also has many similarities to that of mammals with three semicircular canals and a utricle for vestibular function. The saccule and lagena are used for sound detection. Since the embryos are optically transparent, its inner ear and any subsequent staining from experimentation can be easily observed in early developmental stages. As pigment develops in later stages, 1-phenyl-2-thiourea (PTU) can be added to suppress pigment formation. Over a dozen genes have been studied in zebrafish that are pathogenetic for specific defects in the development of the ear (Whitfield et al. 2002).

Linkage Group Mapping of Leftover and Right on

Linkage group mapping showed BAC probe (zK24H22) localization to zebrafish linkage group 8 and 1 only (Fig. 1).

Sequence analysis

Blast analysis has shown *lov* and *ron* to be 75% identical at the nucleotide level within the ORF and share little sequence similarity outside of the ORF. These two *KCTD12* orthologs are also 69% identical at the amino acid level with a protein prediction of the *lov* ORF of 288 amino acids and the *ron* ORF of 271 amino acids. Unlike *KCTD12,* the GC content of *lov* and *ron* ORF each at 53% is not considered to be particularly GC-rich. Similar to *KCTD12,* the tetramerization domain is highly conserved and no transmembrane domains are predicted by TMpred.

Real-Time RT-PCR

Taqman Real-Time RT-PCR revealed the relative RNA expression level of two zebrafish *KCTD12* orthologs (*lov* and *ron*) between developmental stages 12 to 156 hours post fertilization (hpf) (Fig. 2). Expression of these two zebrafish orthologs followed almost an identical expression pattern with an initial peak of expression at 19 hpf and then leveling off after 36 hpf. Several important auditory developmental events occur in this time frame: at 13-14 hours the otic placode (precursor to otic vesicle) becomes visible, at ~18.5 hours the otic vesicles form, at 22 hours the initiation of formation of the statoacoustic ganglion occurs, at 24 hours hair cells start to differentiate, and at 48 hours the semicircular canals first appear (ZFIN, http://zfin.org/zf_info/anatomy/dict/ear/ear.html). Correlations between the time and

intensity of RNA expression could provide valuable insight into possible roles of *lov* and *ron* in auditory development.

Zebrafish *In Situ* Hybridization

Whole-Mount In Situ Hybridization Studies

Based on the RNA expression level of *lov* and *ron* from real-time RT-PCR, we chose to concentrate on establishing the otic placode and vesicle expression pattern of these two zebrafish *KCTD12* orthologs between developmental stages 12 to 96 hpf (Fig. 3). At 12 hpf (data not shown), no significant expression pattern other than similar diffused staining along the entire length of embryo were observed for both *lov* and *ron* riboprobes. By 24 hpf, expression patterns between the two probes began to diverge. The majority of *lov* staining was located at the branchial arches. Distinct *ron* staining was observed at the pectoral fin bud and otic vesicles in addition to branchial arches while diffuse signals appeared across regions of the midbrain and hindbrain. At 48 hpf, both riboprobes detected transcript at the pectoral fin bud, branchial arches and yolk syncytial layer. Diffuse staining remained at the midbrain, hindbrain, and the heart. Individually, distinct signals were observed in the left habenula for *lov*, and otic vesicle and pancreas for *ron*. From 72 hpf on, the difference in expression patterns of *lov* and *ron* riboprobes became more apparent. Detailed expression of *lov* in the brain has been described in detailed previously (Games at al. 2003), and consistent with this report, *lov* seemed to be heavily concentrated in the left habenula in the forebrain region. Additional *lov* expression was observed in the heart whereas signals from *ron* were distributed over the entire cephalic region with some concentration of signals at the habenular and interpeduncular nucleus (IPN) of the midbrain. Faint staining was observed in a layer of cells

inside the eye. No visibly significant signal from either probe was observed near the OV region.

Tissue In Situ Hybridization Studies

Based on the expression pattern of *lov* and *ron* riboprobes in the whole-mount *in situ* hybridization studies, we decided to confirm otic vesicle expression by sectioning regions of whole-mount embryos stages 24 and 72 hpf. Consistent with the whole-mount findings, *lov* antisense probe staining was negative in the otic regions between 24 and 48 hpf (data not shown). For the *ron* probe at 24 hpf, staining extended from within the ventral surface of the otocyst epithilum medially out toward the notochord along the lateral edge of the hindbrain. By 36 hpf, *ron* seemed to be concentrated at the ventral medial edge of the OV where newly formed vestibular-cochlear ganglion (VCG) cells usually reside at this stage. At 48 hpf, *ron* message had formed into a compact mass localizing at the medial edge of the otic vesicle (Fig. 4). By 72 hpf, this expression pattern had shifted more medially, further away from the otic region and became less intense (data not shown). No signals were detected in the OV from the *ron* sense probe.

Right on Morpholino Experiments

Expression pattern of Ron and Isl1 in the Otic Vesicle

In control morpholino-injected embryos, expression of Ron and Isl1 at 48 hpf and 75 hpf followed a similar pattern. Expression of both proteins preceded the anterior start of the otic vesicle (OV) continuing through the anterior macula, followed by gradual diminution upon entering the posterior macula and finally terminating near the posterior edge of the OV.

From the dorsal view, signals from Ron and Isl1 antibody co-localized to the medial edge of the OV (Fig. 5, s1) before the anterior start of the OV. Gradual medial expansion of Ron followed before reaching the anterior and posterior macular junction (s5) and then retreating more laterally and closer to the OV than Isl1. Expression of Ron and Isl1 was at its minimum upon reaching the posterior edge of the OV (s7). The lateral view showed clustering of Ron and Isl1 expression as well. Before entering the OV, Ron expression was slightly more dorsal and overlapped with Isl1 near the region where the OV was about to emerge (Fig. 5, s1). Upon entering the anterior region of the OV, both Ron and Isl1 remained at the same position centered near the ventral side of the OV until after entering the posterior macula (Fig. 5, s6) where the range of expression decreased dramatically. Images captured from the immunohistochemistry staining revealed the majority of Ron and Isl1 signals to be localized in the vestibular-cochlear ganglion (VCG). The two protein signals consistently clustered together in circular patterns symmetrically along the medial edge of the OV. Sparse Isl1 expression was noted in a small population of neurons at the center of the myelencephalon (see white *) for zebrafish at 48 hpf. Similar expression of Ron was observed as well at 75 hpf alongside Isl1. In addition, Isl1 expression was observed in a cluster of neurons located directly medial to the dorsal arotic root and below the VCG (data not shown). For the anti-*ron* morpholino, there was a complete knockdown of Ron and significant reduction of Isl1 expression in the VCG. In the central region of the myelencephalon, Isl1 and Ron were no longer detectable. Isl1 expression was retained in neurons positioned between the dorsal aortic root and VCG at 75 hpf (data not shown).

In summary, co-localization of Ron and Isl1 began before the anterior edge of the OV and then decreased in intensity and distribution upon reaching the posterior macula. The anti-*ron*

morpholino revealed a dramatic knock-down of Ron accompanied by a significant decrease in Isl1 in the VCG.

DISCUSSION

The KCTD Family

KCTD12 is a member of the growing family of potassium channel tetramerization domain-containing genes, recently classified as KCTD and consisting of 19 members. Although all family members possess a single tetramerization domain (T1), the lack of any transmembrane domains excludes KCTD gene products from functioning as classical potassium channels. Phylogenetic mapping of KCTD members confirms that KCTD gene products branch off from the classical potassium channels like the potassium voltage-gated channel shaker-related (KCNA), Shab-related (KCNB), Shaw-related (KCNC) and Shal-related (KCND) subfamilies (Fig. 6). Out of the 19 member family, only four other members of KCTD family (3, 10, 11 and 13) have been characterized in addition to *KCTD12*. Therefore, little is known yet about the functional significance of this KCTD family. However, based on information currently available, there appears to be some emerging similarities between KCTD 3 and 10-13.

KCTD10 and KCTD13 are also members of the PDIP1 family (polymerase delta-interacting protein 1). Although they possess different expression profiles with *KCTD10* mRNA mainly expressed in the lung and *KCTD13* in the kidney and liver, their expression is inducible by TNF-alpha (Zhou et al. 2005, He et al. 2001). KCTD10 and 13 could possibly play a role in TNF-alpha induced DNA replication/repair by interacting with PCNA and

enzymes such as polymerase δ that is involved in DNA replication/repair pathways (Zhou et al. 2005). Similar to KCTD10 and KCTD13, pfetin is also involved in the TNF-alpha pathway by interacting directly with one of TNF-alpha's primary surface receptors, TNFRSF1B (described in Chapter 3 of this thesis). Further experimentation is necessary to determine whether pfetin's expression is also inducible by TNF-alpha.

Akin to *KCTD12*, expression of *REN/KCTD11* is also developmentally regulated in the brain. REN had been proposed to be a novel component of the neurogenic signaling cascade. REN inhibition impairs expression of neurogenin-1 and NeuroD which are members of the bHLH family of transcription factors important for neuronal development and survival (Gallo et al. 2002). Coincidently, knock-out studies from mice genetically deficient in TNF receptors (TNFRSF1A and B) showed increased neuronal vulnerability to excitotoxic and oxidative insults, suggesting a neuroprotective function for both TNF-apha and its receptors (Bruce et al. 1996). In addition, REN may also serve as both a marker and a regulator of neuronal differentiation (Gallo et al. 2002). Data from our morpholino studies suggest that suppression of Ron results in the near complete inhibition of Isl1 expression in the otic vesicle, a marker for newly differentiated neurons (Korzh et al. 1993). Perhaps similar to REN, pfetin/ KCTD12/Ron could potentially serve as a regulator of neuronal differentiation in addition to being a component in some TNF signaling pathway involving neuronal protection and survival.

Ron and Isl1's Role in the Inner Ear

Expression analysis via whole-mount *in situ* hybridization reveals distinct labeling of the zebrafish OV by the anti-*ron* probe. *In situ* sections and immunohistochemical analysis

on zebrafish frozen sections confirm the expression of both *ron* and its gene product in the VCG.

Initial characterization of the anti-*ron* morpholino injection suggests suppression of Ron may down-regulate expression of Isl1 mostly in the zebrafish VCG. With Isl1 commonly serving as a marker for newly differentiated neurons, the implication is that Isl1 suppression (regulated by Ron) could possibility lead to improper neuronal differentiation potentially jeopardizing the survival of neurons in the VCG. To understand the effect of Ron on VCG, the role of Isl1 in inner ear neuronal development warrants examination.

Isl1(alias: Lim-homeodomain protein Islet1, islet-1) is a member of the LIM-HD transcription factors that function as key regulators in developmental pathways such as specification of neuronal cell fate in the vertebrate nervous system (Bachy et al. 2001). Isl1 was initially identified as a protein binding to the rat insulin gene enhancer (Karlsson 1990). It is expressed in a variety of tissues including thyroid, pituitary, kidney, spinal cord, heart, brain and inner ear. Mice lacking Isl1 do not survive past E11.5. Loss of Isl1 perturbs the generation of motor neurons, and differentiation of many of the cell types that normally express the protein, including sensory neurons of dorsal root and cranial sensory ganglia and cells of the endocrine pancreas (Pfaff et al. 1996)

The functional domains of LIM-HD transcription factors consisting of two tandem LIM domains followed by a homeodomain (HD) are capable of forming tetrameric and hexameric interactions with other transcriptional regulators and creating an array of transcriptional regulating complexes. It is perhaps this flexibility that enables them to regulate transcription in a tissue-specific manner and participate in a variety of developmental events including establishing neuronal subtype identity (Hobert and Westphal 2000, Shirasaki and

Pfaff 2002). In regard to this particular role, LIM-HD may partner with the basic helix-loop-helix (bHLH) transcription factors in the determination of neural identity.

During the multistep process of neurogenesis, bHLH proteins have traditionally been classified as proneural factors involved in activation of neurogenesis during which neuronal precursor cells gradually adopt neuronal characteristics and become committed to neuronal lineage; the LIM-HD proteins would act specifically on postmitotic neuronal cell subtype identity after neuronal cells have undergone terminal differentiation and on their way to becoming more mature neurons. And these two processes, originally thought to happen at different stages of neurogenesis, were shown to work in a synchronous fashion as in the case of motor neuron subtype identity where bHLH transcription factors NeuroM and E47 cooperate with LIM-HD complexes (NLI, Isl1 and Lhx3) to specify motor neuron subtype identity (Lee and Pfaff 2003).

New evidence suggests that this form of cooperation might also take place in the determination of inner ear neuronal lineages. In the developing chicken inner ear, islet-1 is expressed in cells of the ventral part of the otic placode where auditory and vestibular neurons originate, demonstrating islet-1 as one of the earliest markers of inner ear neural precursors (Li et al. 2004). Similar expression was shown within the region of the mouse otocyst that gives rise to both the auditory sensory organ (the organ of Corti) and the sensory ganglion neurons (SG) increasing the likelihood of Isl1 as a common step in the early development of both sets of cells in inner ear development (Radde-Gallwitz et al. 2004). In cells giving rise to the neuronal lineage, Isl1 expression co-localized with NeuroD, an inner ear neuronal marker expressed during early development. Subsequent expression showed maintenance of Isl1

expression in the neuronal lineage and down-regulation in the sensory lineage upon initiation of hair cell differentiation.

NeruoD as a potent neuronal differentiation factor is vital for survival of inner ear sensory neurons during differentiation. Mice lacking NeuroD protein exhibit no auditory evoked potentials, reflecting a profound deafness due to failure of inner ear sensory neuron survival during differentiation in development. (Kim at al. 2001). Mice lacking Isl1 do not survive past E11.5. However if Isl1 and NeuroD were truly to cooperate in the confirmation of inner ear-specific neuronal or sensory competency/identities, then Isl1 would be as vital to the survival of inner ear neurons as NeuroD making pfetin/Ron a potentially important regulator of inner ear neurons.

REFERENCES

Bachy I, Vernier P, Retaux S (2001) The LIM-homeodomain gene family in the developing Xenopus brain: conservation and divergences with the mouse related to the evolution of the forebrain. J Neurosci 21:7620–7629

Bruce AJ, Boling W, Kindy MS, Peschon J, Kraemer PJ, Carpenter MK, Holtsberg FW, Mattson MP (1996) Altered neuronal and microglial responses to excitotoxic and ischemic brain injury in mice lacking TNF receptors. Nat Med 2(7):788-94

Di Marcotullio L, Ferretti E, De Smaele E, Argenti B, Mincione C, Zazzeroni F, Gallo R, Masuelli L, Napolitano M, Maroder M, Modesti A, Giangaspero F, Screpanti I, Alesse E, Gulino A (2004) REN(KCTD11) is a suppressor of Hedgehog signaling and is deleted in human medulloblastoma. Proc Natl Acad Sci USA 101(29):10833-8

Gallo R, Zazzeroni F, Alesse E, Mincione C, Borello U, Buanne P, D'Eugenio R, Mackay AR, Argenti B, Gradini R, Russo MA, Maroder M, Cossu G, Frati L, Screpanti I, Gulino A (2002) REN: a novel, developmentally regulated gene that promotes neural cell differentiation. J Cell Biol 158(4):731-40

Gamse JT, Thisse C, Thisse B, Halpern ME (2003) The parapineal mediates left-right asymmetry in the zebrafish diencephalon. Development 130(6):1059-68

Gamse JT, Kuan YS, Macurak M, Brosamle C, Thisse B, Thisse C, Halpern ME (2005) Directional asymmetry of the zebrafish epithalamus guides dorsoventral innervation of the midbrain target. Development 132(21):4869-81

He H, Tan CK, Downey KM, So AG (2001) A tumor necrosis factor alpha- and interleukin 6-inducible protein that interacts with the small subunit of DNA polymerase delta and proliferating cell nuclear antigen. Proc Natl Acad Sci USA 98(21):11979-84

Hobert O, Westphal H (2000) Functions of LIM-homeobox genes. Trends Genet 16(2):75-83

Karlsson O, Thor S, Norberg T, Ohlsson H, Edlund T (1990) Insulin gene enhancer binding protein Isl-1 is a member of a novel class of proteins containing both a homeo- and a Cys-His domain. Nature 344(6269):879-82

Kim TB, Isaacson B, Sivakumaran TA, Starr A, Keats BJ, Lesperance MM (2004) A gene responsible for autosomal dominant auditory neuropathy (AUNA1) maps to 13q14-21. J Med Genet 41(11):872-6

Kim WY, Fritzsch B, Serls A, Bakel LA, Huang EJ, Reichardt LF, Barth DS, Lee JE (2001) NeuroD-null mice are deaf due to a severe loss of the inner ear sensory neurons during development. Development 128(3):417-26

Korzh V, Edlund T, Thor S (1993) Zebrafish primary neurons initiate expression of the LIM homeodomain protein Isl-1 at the end of gastrulation. Development 118(2):417-25

Lee SK, Pfaff SL (2003) Synchronization of neurogenesis and motor neuron specification by direct coupling of bHLH and homeodomain transcription factors. Neuron 38(5):731-45

Lee C, Smith A (2004) Molecular cytogenetic methodologies and a bacterial artificial chromosome (BAC) probe panel resource for genomic analyses in zebrafish. Methods Cell Biol 77:241-54

Li H, Liu H, Sage C, Huang M, Chen ZY, Heller S (2004) Islet-1 expression in the developing chicken inner ear. J Comp Neurol 477(1):1-10

Malicki J (1999) Development of the retina. Methods Cell Biol 59:273-99

Malicki J, Jo H, Wei X, Hsiung M, Pujic Z (2002) Analysis of gene function in the zebrafish retina. Methods 28(4):427-38

Marchler-Bauer A, Anderson JB, DeWeese-Scott C, Fedorova ND, Geer LY, He S, Hurwitz DI, Jackson JD, Jacobs AR, Lanczycki CJ, Liebert CA, Liu C, Madej T, Marchler GH, Mazumder R, Nikolskaya AN, Panchenko AR, Rao BS, Shoemaker BA, Simonyan V, Song JS, Thiessen PA, Vasudevan S, Wang Y, Yamashita RA, Yin JJ, Bryant SH (2003) CDD: a curated Entrez database of conserved domain alignments. Nucleic Acids Res 31(1):383-7

Pfaff SL, Mendelsohn M, Stewart CL, Edlund T, Jessell TM (1996) Requirement for LIM homeobox gene Isl1 in motor neuron generation reveals a motor neuron-dependent step in interneuron differentiation. Cell 84(2):309-20

Pujic Z, Malicki J (2001) Mutation of the zebrafish glass onion locus causes early cell-nonautonomous loss of neuroepithelial integrity followed by severe neuronal patterning defects in the retina. Dev Biol 234(2):454-69

Radde-Gallwitz K, Pan L, Gan L, Lin X, Segil N, Chen P (2004) Expression of Islet1 marks the sensory and neuronal lineages in the mammalian inner ear. J Comp Neurol 477(4):412-21

Resendes BL, Kuo SF, Robertson NG, Giersch AB, Honrubia D, Ohara O, Adams JC, Morton CC (2004) Isolation from cochlea of a novel human intronless gene with predominant fetal expression. J Assoc Res Otolaryngol 5(2):185-202

Scanlan MJ, Gordan JD, Williamson B, Stockert E, Bander NH, Jongeneel V, Gure AO, Jager D, Jager E, Knuth A, Chen YT, Old LJ (1999) Antigens recognized by autologous antibody in patients with renal-cell carcinoma. Int J Cancer 83(4):456-64

Shirasaki R, Pfaff SL (2002) Transcriptional codes and the control of neuronal identity. Annu Rev Neurosci 25:251-81

Westerfield M. (1994). "The Zebrafish Book." University of Oregon press, Eugene, OR.

Whitfield TT, Riley BB, Chiang M-Y, Phillips B (2002) Development of the zebrafish inner ear. Dev Dyn 223(4):427-458

Zhou J, Ren K, Liu X, Xiong X, Hu X, Zhang J (2005) A novel PDIP1-related protein, KCTD10, that interacts with proliferating cell nuclear antigen and DNA polymerase delta. Biochim Biophys Acta 1729(3):200-3

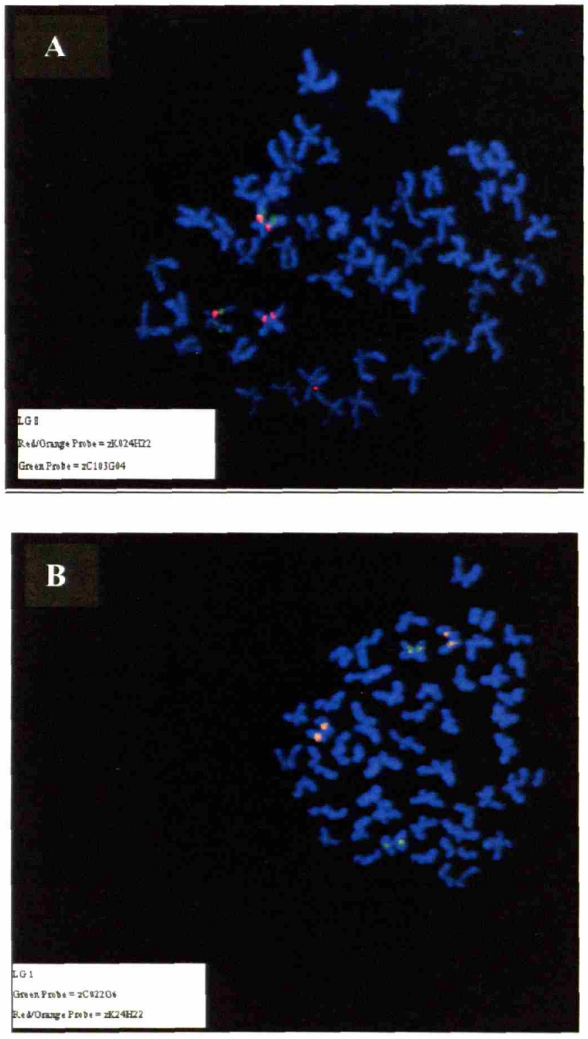

Figure 1. FISH of zebrafish metaphase chromosomes for localization of *leftover* (A) and *right on* (B). A. Centromeric probe to linkage group 8, zC103G04 (green), and BAC probe, zK24H22 (red), co-localize to the same zebrafish linkage group. B. Centromeric probe to linkage group 1, zC00206 (green), and BAC probe, zK24H22 (red/orange), co-localize (yellow) to the same zebrafish linkage group.

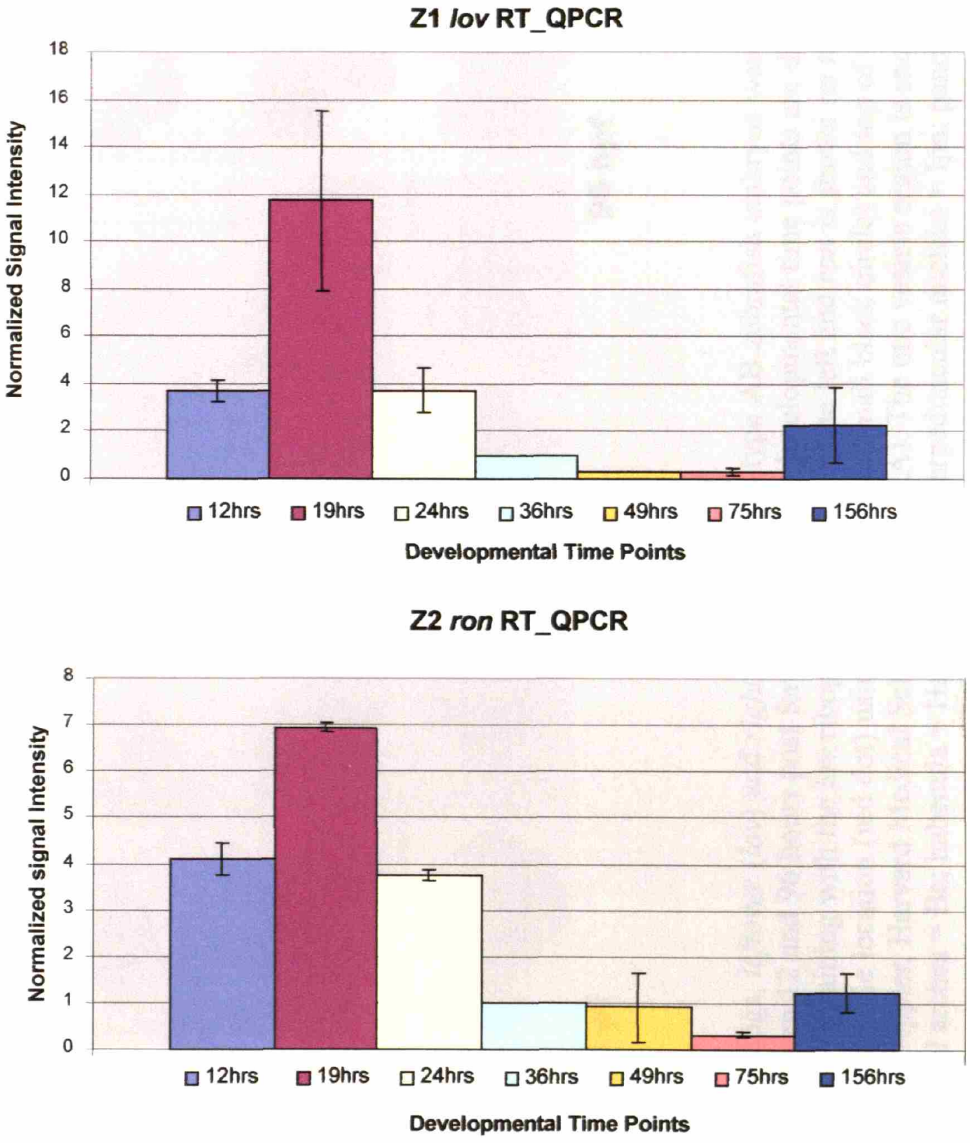

Figure 2. RNA expression levels of *leftover* and *right on.* Different developmental time points are presented in various colors. The Y axis represents the expression level (with standard deviation) normalized against the housekeeping gene *bactin1* across all developmental time points.

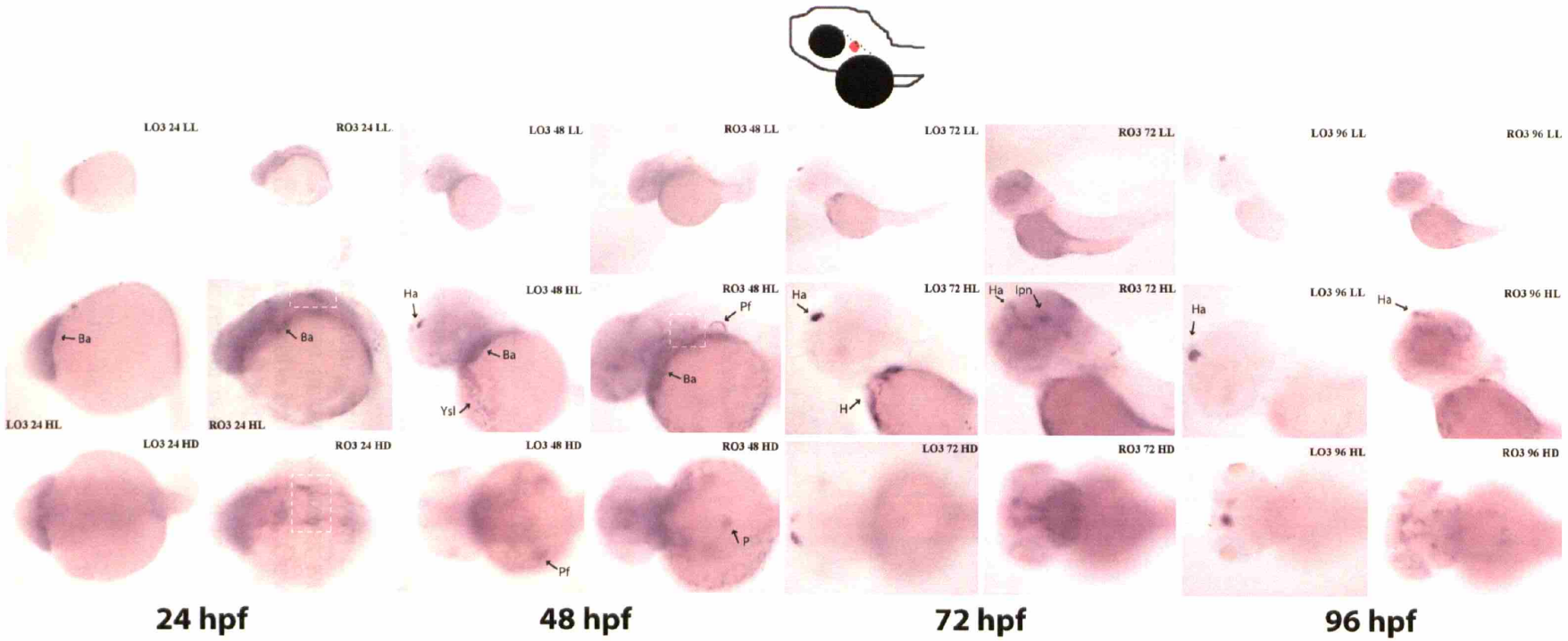

Figure 3. Localization of *KCTD12* zebrafish orthologs, *leftover* (*lov*) and *right on* (*ron*). Wild-type AB zebrafish embryos were grown in egg media and harvested at various stages between 12 and 96 hours post fertilization. Four developmental time points are displayed from left to right in four panels. Within each panel, staining with the *lov* riboprobe is shown on the left and *ron* is shown on the right. Located at the top is a schematic diagram of otic vesicle location (red dot) using top of the eye (small black circle) and top of the yolk (larger black circle) for landmark (courtesy of Dr. Appler, Harvard Medical School, Boston, MA). The otic vesicle region is enclosed in the area indicated by the dashed line box; branchial arches = Ba; habenula = Ha; heart = H; interpeduncular nucleus = Ipn; pancreas = P; pectoral fin = Pf; yolk syncytial layer = Ysl.

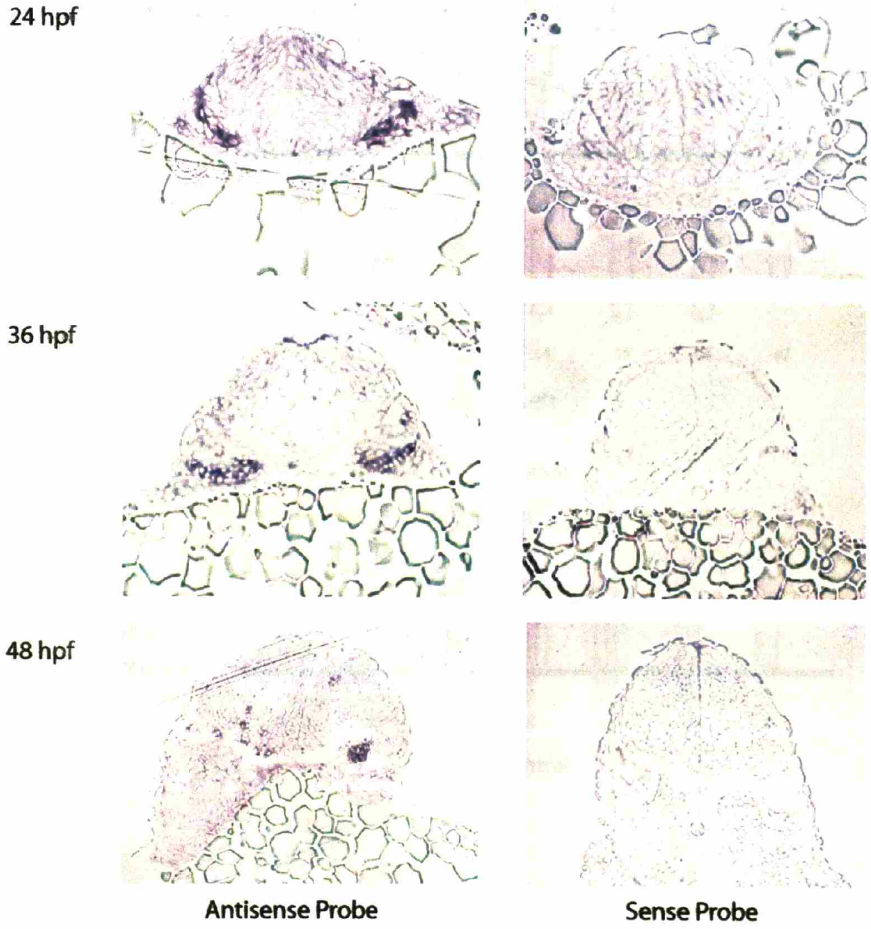

Figure 4. Expression pattern of *ron* riboprobe in zebrafish sections. Images are presented in two columns with the *ron* antisense probe on the left and sense probe on the right. Developmental stages from top to bottom are 24 hpf, 36 hpf and 48 hpf. Probe signal is in dark purple. The otic vesicle region is enclosed in the area indicated by the dashed line box

Figure 5

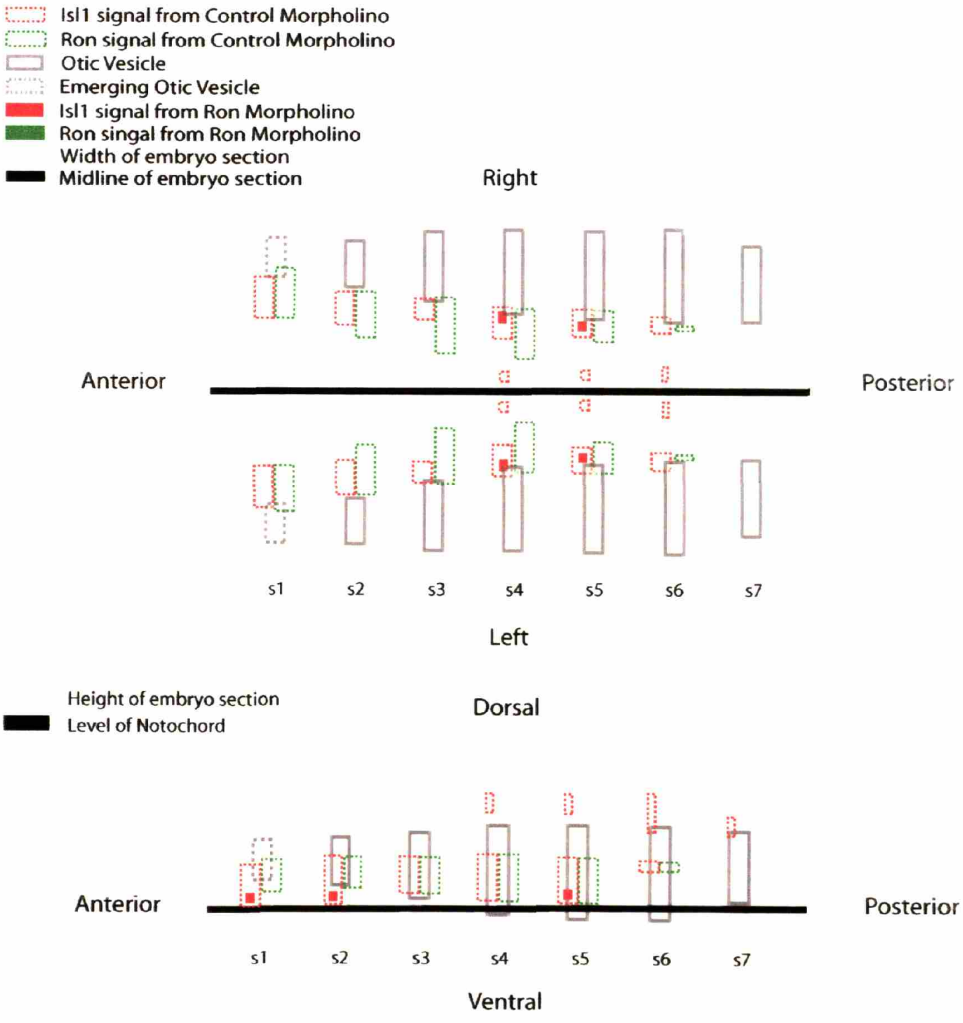
Isl1 signal from Control Morpholino
Ron signal from Control Morpholino
Otic Vesicle
Emerging Otic Vesicle
Isl1 signal from Ron Morpholino
Ron singal from Ron Morpholino
Width of embryo section
Midline of embryo section
Right
Anterior
Posterior
s1
s2
s3
s4
s5
s6
s7
Left
Height of embryo section
Level of Notochord
Dorsal
Anterior
Posterior
s1
s2
s3
s4
s5
s6
s7
Ventral

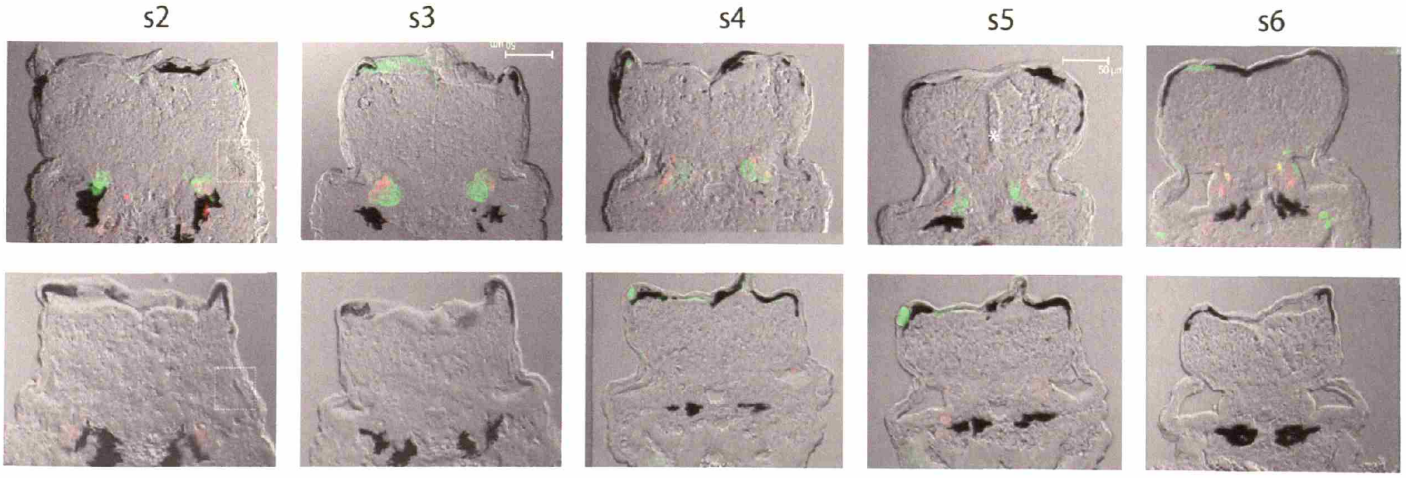
s2
s3
s4
s5
s6

Figure 5. Expression pattern of Ron and Isl1 in the otic vesicle. Two schematic diagrams are presented detailing the expression pattern of Ron and Isl1 in the OV around 48 hpf, one dorsal view and the other lateral view. Gray vertical columns represent 12-14μm thick serial sections from morpholino-injected embryos stained with Ron and Isl1 antibody, covering the OV region. Columns are labeled as sections one through seven (s1-s7) from anterior to posterior. Ron antibody is visualized in green and Isl1 in red. The expression pattern of Ron and Isl1 is represented on either side of each column denoting expression within the same section. Corresponding immunohisto-section images are listed below for reference with control morpholino embryo sections on the top row and ron morpholino embryos on the bottom. All images are given at the same magnification with the scale bar denoting 50μm.

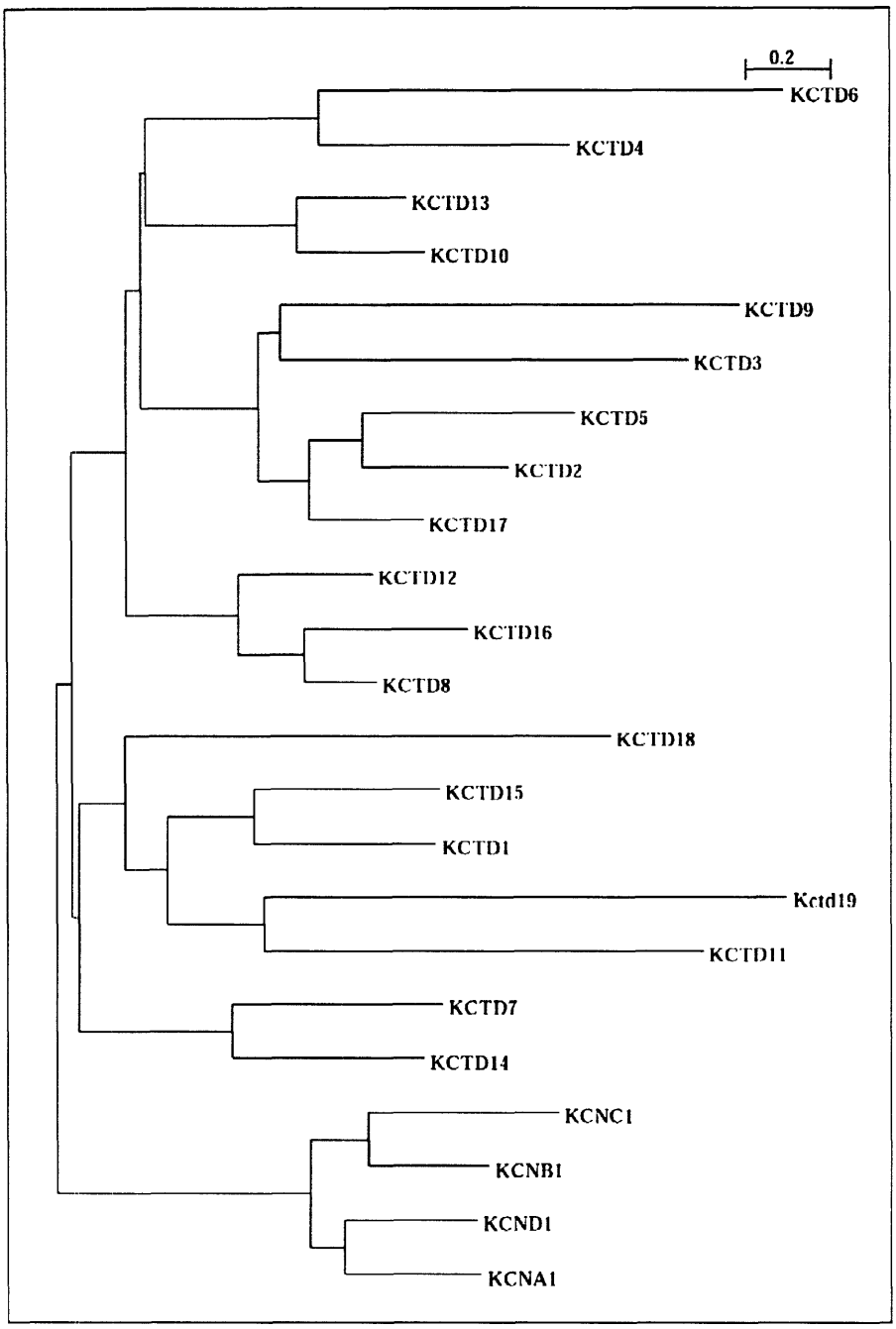

Figure 6. Phylogenetic tree of KCTD family members. Multiple alignments of complete amino acid sequence of human KCTD proteins were performed using ClustalX 1.83 and the resulting tree was visualized using NJplot. Four classical potassium channel proteins (KCNA1, KCNB1, KCNC1, KCND1) were used as a reference. Branch length is denoted in the scale bar.

CHAPTER 4

Genomic and Proteomic Characterization of *KCTD12* and Pfetin

Sharon F. Kuo[1], Weining Lu[2,3], Chinweike Ukomadu[2,3], Arti Pandya[4], Walter E. Nance[4], Cynthia C. Morton[3,5]

1)Speech and Hearing Bioscience and Technology, Harvard-MIT Division of Health Sciences and Technology, Boston, MA; 2)Department of Medicine, Brigham and Women's Hospital and 3) Harvard Medical School, Boston, MA; 4)Department of Human Genetics, Medical College of Virginia, Virginia Commonwealth University, Richmond, VA; 5)Departments of Ob/Gyn and Pathology, Brigham and Women's Hospital and Harvard Medical School, Boston, MA

ACKNOWLEDGMENTS

We thank Dr. Zheng-Yi Chen and MingQian Huang for performing the GeneChip analysis and Drs. Marco Ramoni and Gil Alterovitz for their assistance with Human Massome Database and Ingenuity System Analysis.
This work was supported by the NIH Grants DC03402 (C.C.M.), and T32 DC0019 (S.F.K.).

ABSTRACT

KCTD12, a member of KCTD gene family, was identified as a 6 kb cochlear transcript containing a single exon with a particularly GC-rich ORF. Previous *in situ* hybridization and immunohistochemical expression studies in revealed localization of *KCTD12* and its gene product pfetin in the vestibular-cochlear ganglion of zebrafish otic vesicle, and a variety of cell types in the human, mouse and guinea pig cochlea. In this study, further characterization of *KCTD12* and its gene product pfetin is detailed through mutation screening of the GC-rich *KCTD12* in a series of DNAs from multiplex kindreds with hearing loss, gene expression profiling using GeneChip technology, a database search for protein interaction and immunoprecipitation for pfetin binding profile. Although, the screen of 88 individuals with an increased likelihood of genetic etiology for hearing loss revealed no mutations within the ORF of *KCTD12*, the protein interaction search defined two major pfetin binding partners, TNFRSF1B and RelA, both belonging to the TNF-α/NF-κB signal transduction pathway, suggesting potential pfetin involvement in this signal cascade.

Keywords: KCTD12, pfetin, TNF-alpha/NF-κB, TNFRSF1B, RelA

INTRODUCTION

KCTD12 was previously characterized as a predominantly fetal cochlear transcript with expression spanning the auditory systems of human, mouse, guinea pig and zebrafish. *KCTD12* belongs to a family of KCTD genes all containing a single the potassium channel tetramerization (T1) domain. To date, this T1 domain, however, has provided little information on the actual function of this gene family. In addition, the ORF of *KCTD12* is particularly GC rich (70%) which is of note as CpG dinucleotides have the highest mutation rate in humans due to deamination (Ducan and Miller, 1980) and making it worthwhile to pursue a mutation screen in the *KCTD12* ORF in human populations susceptible to genetic hearing loss.

Advances in both genomic and proteomic technologies have opened new means for the study of hearing and deafness associated genes. Microarray technologies can be used to rapidly determine the expression pattern of tens of thousands of genes from the inner ear. The derived expression profiles may reveal genes with similar or differential expression patterns, and analysis of such gene clusters may help infer underlying functional pathways (Corey and Chen, 2002). In addition, technologies are available for large scale protein-protein interaction studies involving the two-hybrid system, co-purification of affinity tagged complexes coupled with mass spectrometry protein identification, and protein microarrays (de Hoog and Mann, 2004). One way to deduce a protein's function is to identify its interacting partners, because proteins interacting with one another are often involved in the same cellular processes.

With advances in the automation of genomic and proteomic technologies such as automated sequencing, microarrays, and mass spectrometry, an enormous amount of data have been generated available in public databases. This rapid generation of data has spurred

advancements in computational methods to keep pace with analysis of this rapid expansion of new information and full integration with existing knowledge. Many bioinfomatic tools are available and are under continues development to access and interpret expression patterns, protein interactions, signaling and molecular pathways (123 Genomics website, http://www.123genomics.com/). Genomic and proteomic information already available in public databases is combined herein with bench-top experimental data to investigate the expression pattern, interaction partners and functional pathways of *KCTD12* and its gene product pfetin.

MATERIALS AND METHODS

Mutation Screening of Deafness Individuals from Multiplex Kindreds

Genomic DNAs from a panel of 88 multiplex kindreds were obtained from Dr. Arti Pandya (Medical College of Virginia, Virginia Commonwealth University). Given the high GC content (i.e., 70%) of the *KCTD12* ORF, the GC-RICH PCR System from Roche Applied Science (Indianapolis, IN) was used for amplification of the target region (~1 kb containing the entire *KCTD12* ORF). The following primers and PCR conditions were used: upper (5'-CGGTTGCAGCTCCTGAGT-3') and lower (5'-GTAATCATCT CTCGGGCAGG-3'); initial denaturation at 95°C for 3 minutes; amplification by 15 cycles of 95°C for 30 seconds, 62°C for 30 seconds, and 72°C for 56 seconds, 24 cycles of 95°C for 30 seconds, 62°C for 30 seconds, and 72°C for 60 seconds; and final extension at 72°C for 7 minutes. PCR products were gel purified, sequenced and compared against the wild type *KCTD12* gene sequence

using Blast 2 Sequences software from NCBI (http://www.ncbi.nlm.nih.gov/blast/bl2seq/wblast2.cgi).

Affymetrix Chip and Ingenuity System Analysis

GeneChip Microarray

Microarray technology offers a fast and efficient approach to study gene expression and interaction. It can be used in cross-tissue comparisons for identification of genes with unique expression patterns, and cluster analysis to identify genes of similar expression. Coepxression can be suggestive of functional pathways, identifying interactions amongst known or novel genes. There are different forms of microarray technology, but they are all based on the general principle of a massively parallel analysis: immobilize multiple targets (*e.g.*, cDNAs, oligonucleotides, tissues) on the surface of a solid support, apply a sample (*e.g.*, cDNA, DNA, antibody) to the targets and quantify all signals.

Dr. Zheng-Yi Chen's lab has done extensive expression analysis of cochlear transcripts using both human and mouse Affymetrix GeneChip microarrays, human U95 and mouse MOE430 (Affymetrix, Santa Clara, CA). Briefly, mouse utricles of developmental stages E10.5 to P12 were dissected and RNA extracted, followed by cDNA and cRNA synthesis, and then hybridization of fragmented cRNA to individual GeneChip. Subsequent data analysis was performed using GeneChip Analysis Suite V3.0 (Chen and Corey, 2002). One probe set, 1434881_s_at matching to the 3' region of the *KCTD12/Kctd12* brain transcript (gi 47578122 and gi26082764), was confirmed to be on mouse MOE430 GeneChip array. Utilizing Dr. Chen's database, we sought to identify genes co-regulated with *KCTD12*.

Ingenuity Software Analysis

The data output from the GeneChip analysis was further analyzed through the use of Ingenuity Pathways Analysis (Ingenuity® Systems, www.ingenuity.com) to seek out potential mechanisms and functional pathways associated with *KCTD12* expression. One representation of the data analysis output is in the form of a network graph. A network/My Pathways is a graphical representation of the molecular relationships between genes/gene products. Genes or gene products are represented as nodes, and the biological relationship between two nodes is represented as an edge (line). All edges are supported by at least one reference from the literature, from a textbook, or from canonical information stored in the Ingenuity Pathways Knowledge Base. Human, mouse, and rat orthologs of a gene are stored as separate objects in the Ingenuity Pathways Knowledge Base, but are represented as a single node in the network. Nodes are displayed using various shapes that represent different functional classes of the gene product.

Immunoprecipitation (IP)

KCTD12 Expression Construct, Cell Culture and Cell Transfection

Human *KCTD12* cDNA (GenBank Accession No. AF359381) containing its entire protein coding region (327 amino acid residues) was cloned into a modified form of pcDNA3 (Invitrogen, Carlsbad, CA) that permits expression of polypeptides with three C-terminal hemagglutinin (HA) tags. COS7 (African green monkey kidney) cells were cultured in Dulbecco's modified Eagle's medium (DMEM) supplemented with 10% fetal calf serum (FCS), 100 units of penicillin, and 100 μg of streptomycin in 60 mm dishes (for immunoprecipitation analysis or Permanox Lab-Tek chamber slides (Nalge Nunc, Naperville,

IL) (for immunocytochemistry). Cells were transiently transfected in the absence of antibiotics with the *KCTD12* HA-tagged construct using Lipofectamine 2000 transfection reagent according to the manufacturer's protocols (Invitrogen). The negative control for transfection experiment was performed without addition of the *KCTD12* construct.

Immunoprecipitations and [^{35}S]Methionine Labeling

An [^{35}S]methionine labeling immunoprecipitation reaction was performed prior to the large scale non-radioactive IP reaction to estimate the size of pfetin binding aggregates. For [^{35}S]methionine labeling, the radioactive isotope [^{35}S]methionine was obtained from PerkinElmer Life Sciences (Boston, MA). Once cells reached 90% confluency, medium was removed and cells were washed twice in phosphate-buffered saline prior to incubation in methionine-free medium for one hour. Cells were labeled for four hours in methionine-free medium, supplemented with 5% dialyzed fetal calf serum, 25 μCi/ml [^{35}S]methionine (specific activity, 1175 Ci/mmol). Proteins were extracted with lysis buffer as above and separated in precast Tris–Bis gradient gels (Invitrogen, Carlsbad, CA). For the subsequent non-radioactive IP reaction, transfected cells were treated with lysis buffer supplemented with 50 mM NaF and 1 mM Na_3V0_4. Cell lysates were immunoprecipitated with anti-HA bound to beads (Santa Cruz Biotechnology, Inc., Santa Cruz, CA) for one hour. Beads were washed three to five times in lysis buffer, followed by solubilization of adsorbed proteins with SDS-PAGE loading buffer with β-mercaptoethanol (β-ME) at 95–100°C for five minutes and then separated by 10% SDS-polyacrylamide gel electrophoresis. After silver staining the gel, gel bands present only in the positive transfection lane were excised and sent for sequencing by the Taplin Biological Mass Spectrometry Facility (Harvard Medical School, Boston, MA).

Human Massome Database

The Human Massome of protein interactions is a newly developed public database (www.chip.org/proteomics/massome.html) containing a network of over 134,000 protein interactions integrated from multiple existing sources in a non-redundant manner. They are stored in a common format, and can be presented in various forms for analysis. This database seeks to combine the strengths of the two main approaches used in proteomics (mass-based proteomics and interaction based proteomics) to create a better protein interaction database. The interactions are searchable by the masses of the interaction participants (including both cleavage products and mutant proteins). It also facilitates protein identification for many mass spectrometry technologies such as High-Throughput Mass Spectrometric Protein Complex Identification (HMS-PCI) and SELDI (Alterovitz et al. 2005).

RESULT

Mutation Screen

To detect potential pathogenetic sequence variants within the *KCTD12* ORF (given the 70% GC-richness of the *KCTD12* ORF and the associated bias towards deamination of CpG dinucleotides as a common molecular cause of mutations in humans), a panel of DNAs was sequenced from individuals likely to have a genetic etiology for their hearing loss. This panel, consisting of 88 probands from multiplex sibships, was provided by Dr. Arti Pandya and Walter Nance at Virginia Commonwealth University, Richmond, VA. This multiplex panel

was prepared from a repository of DNA samples obtained from over 2,000 deaf probands prescreened for common genetic etiologies of hearing disorders such as the connexins. Primers were designed to produce a single PCR product spanning the entire *KCTD12* ORF. The ORF of all 88 probands was cloned and sequenced. Three individuals were found to have a synonymous base change (776C>G) which does not present any new splice site. Search of the NCBI SNP database (http://www.ncbi.nlm.nih.gov/SNP/) revealed a single synonymous change (215A>G). No other sequence variations were noted. As new appropriate individuals are collected and become available from this DNA repository, they will be sequenced for possible mutations.

Expression Profile on Affymetrix Chip and Ingenuity System Analysis

GeneChip analysis demonstrated that *KCTD12*, along with 38 other genes, share similar changes of expression during mouse utricle development (Fig. 1). In this gene cluster, elevation in expression begins around E12.5, maximum expression is reached between E17.5 and P3, followed by a steady decrease until P12 when expression is minimal. This list of 38 genes was then evaluated through the Ingenuity System for gene interaction and pathway analysis.

Gene interactions were mapped between all members of the cluster (Fig. 2). The largest group of gene interactions involved eight members of the 38 cluster genes. *LMO2* (LIM domain only 2), *PF4* (chemokine (C-X-C motif) ligand 4), *KDR* (kinase insert domain receptor), *TGFB1I1* (transforming growth factor beta 1 induced transcript 1), *IGFBP2* (insulin-like growth factor binding protein 2), *BGN* (biglycan), *COL5A2* (collagen type V alpha 2) and *CSPG4* (chondroitin sulfate proteoglycan 4). This group of genes seemed to be

centered around *ITGB1* and *3* (integrin beta subunits 1 and 3). Integrin family members are membrane receptors involved in cell adhesion and participate in a variety of cell-surface mediated signaling including embryogenesis, hemostasis, tissue repair, immune response and metatastatic diffusion of tumor cells (NCBI www.ncbi.nlm.nih.gov/entrez/query.fcgi?db=gene). There were several smaller gene interaction clustered around *COL4A1* (collagen type IV alpha 1), *SLIT2* (slit homolog 2 (*Drosophila*)), *ABCC9* (ATP-binding cassette, sub-family C (CFTR/MRP), member 9), *C3AR1* (complement component 3a receptor 1) and *F13A1* (coagulation factor XIII, A1 polypeptide). However, no interactions direct or indirect were found between *KCTD12* and any other members of the 38 gene cluster and no significant match to canonical pathways was detected.

Immunoprecipitation (IP) and Human Massome Database

Given the presence of the T1 domain and its association with potassium channels which are vital for both the function and maintenance of the inner ear, it is important to determine pfetin's binding partner and begin to delineate the exact role it plays in auditory function.

Immunoprecipitation is one of the traditional approaches to finding interaction partners. COS7 cells were transfected with a *KCTD12* construct to express HA-tagged pfetin. Cells were harvested and protein extract passed through an HA-conjugated column to collect tagged pfetin and its associated proteins. IP products from both positive and negative transfection reactions were electrophoresed in a 10% Bis-Tris gel. Four bands at 200, 70, 41, and 35 kDa (only present in the positive transfection reaction) were excised from the gel post

silver staining. Table 1 represents post sequencing results of the best-matched proteins identified at each band size.

Table 1. Putative Interactors of Pfetin

200 kDa	CAD protein, fatty acid synthase, polyubiquitin
70 kDa	heat shock or heat shock-related protein (hsp70-1/hsp70-2), stress-70 protein, mitochondrial [Precursor] , calcium-binding mitochondrial carrier protein Aralar1 and 2 (CMC1/CMC2), ATP-dependent DNA helicase II (70 kDa subunit), 78 kDa glucose-regulated protein [Precursor], CTP synthase, UQHUB polyubiquitin 3, Probable RNA-dependent helicase p72
41 kDa	pfetin, ER-associated Hsp40 co-chaperone, actin, cytoplasmic 1
35 kDa	pfetin, B cell receptor-associated protein BAP37, guanine nucleotide-binding protein beta subunit 2-like 1, L-lactate dehydrogenase A and B chain, putative deoxyribose-phosphate aldolase, ELAV-like protein 1, mitochondrial 39S ribosomal protein L39, sideroflexin 3, calponin-2

In addition to performing IP, we took advantage of the vast information already available in the public protein interaction databases and performed a search using the newly developed Human Massome (www.chip.org/proteomics/massome.html). It revealed two major protein to protein interaction partners for pfetin. They are tumor necrosis factor receptor superfamily member 1B (TNFRSF1B) and v-rel reticuloendotheliosis viral oncogene homolog A, nuclear factor of kappa light polypeptide gene enhancer in B-cells 3 (RelA).

TNFRSF1B (aliases: p75, TBPII, TNFBR, TNFR2, CD120b, TNFR80, TNF-R75, p75TNFR, TNF-R-II) is a member of the TNF-receptor superfamily whose function is closely associated with tumor necrosis factor (TNF) superfamily member 2 (aliases: TNF-α DIF, TNFA, TNFSF2). Information from Entrez Gene, NCBI's database for gene-specific information (www.ncbi.nlm.nih.gov/entrez/query.fcgi?db=gene), indicates that TNF-α encodes a multifunctional proinflammatory cytokine that functions through its receptors

TNFRSF1A and TNFRSF1B in a variety of processes such as cell proliferation, differentiation, apoptosis, lipid metabolism, and coagulation. This cytokine has been implicated in a variety of diseases, including autoimmune diseases, insulin resistance, and cancer.

RelA (aliases: p65, NFKB3) is one of the five structurally related subunits that make up the NF-kappa B (NF-κB) family of transcription factors. Together, these subunits form various homodimeric and heterodimeric combinations to create NFKB complexes that function as transcription regulators (activators and repressors) in multiple cellular processes such as inflammation, cell cycle regulation, apoptosis and oncogenesis (Arlt and Schafer 2002). Other family members include NF-κB1/p50, NF-κB2/p52, RelB and c-Rel with p50:p65 (RelA) being the most abundant of the NF-κB complexes (Ghosh et al. 1998)

DISCUSSION

Expression analysis using the Affymetrix mouse genome array revealed a developmental regulation of *KCTD12* in the mouse utricle with peak expression centering between embryonic day 17.5 and postnatal day 3, along with 38 other genes in the cluster. Unfortunately, gene cluster analysis did not reveal any interaction between *KCTD12* and any other members of the cluster. However, interactions mapped here were based on research data published prior to June 2005 (date of gene cluster analysis). Therefore, it is possible that as more and more data become available in the public domain and new connections determined, it will be possible in the near future to delineate the functional significance of this cluster of genes with similar expression regulation in the mouse developing utricle.

A search for protein interaction using Human Massome with pfetin identified TNFRSF1B, one of TNF-alpha's major receptor and RelA, a member of the NF-κB complex as its binding partners. TNF-α is a multifunctional cytokine, which participates in a wide variety of biological activities such as cell proliferation, differentiation, apoptosis, lipid metabolism, and coagulation. Knock-out studies in mice have suggested a neuroprotective function for this cytokine.

Both of pfetin's binding partners are involved in cell signal transduction regulating the cell cycle (*e.g.*, proliferation, differentiation). They are also functionally connected in the TNF-α/NF-κB pathway. In fact, this pathway is initiated by the binding of TNF-α to its receptors TNFRSF1A and TNFRSF1B at the cell surface, requiring many protein complexes to implement the intracellular signal cascade which eventually leads to activation of the NF-κB complex and its targeted genes (Bouwmeester et al. 2004). Knock-out mice studies from both TNF-α and TNFRSF1B have suggested neuroprotective function (Bruce et al. 1996). Inappropriate activation of NF-κB has been associated with a number of inflammatory diseases while persistent inhibition of NF-κB leads to inappropriate immune cell development or delayed cell growth (Ghosh 2002).

Immunoprecipitation identified a number of candidate binding partners for pfetin. Some proteins ubiquitously expressed in the cell were most likely immunoprecipitated as part of the experimental background noise (*e.g.*, heat shock and heat shock related proteins). However, two of pfetin's binding candidates also showed ties to the TNF-α/ NF-κB pathway. PHB2 (prohibitin 2) (aliases: REA, p22, Bap37, BCAP37, PNAS-141) is a novel histone deacetylase-associated protein that functions putatively as a mediator of transcription (Kurtev et al. 2004). It also interacts with RelA, another pfetin interactor, and plays a part in the TNF-

α trigged signaling cascade of activation of NF-κB (Bouwmeester et al. 2004). The other pfetin interactor CAD (carbamoyl-phosphate synthetase 2, aspartate transcarbamylase, and dihydroorotase) is a multifunctional protein that initiates and regulates mammalian *de novo* pyrimidine biosynthesis (Sigoillot et al. 2005). CAD also interacts with TRADD (TNFRSF1A-associated via death domain adaptor protein) which in turn interacts with one of TNF-α's major receptors, TNFRSF1A, and mediates programmed cell death signaling and NF-κB activation (Sandu et al. 2005).

The TNF-α/NF-κB pathway is an elaborate pathway that forms the basis for numerous physiological and pathological processes involving a network of 680 non-redundant proteins (Bouwmeester et al. 2004). Interactions of pfetin with many members of the TNF-α/NF-κB pathway suggest possible involvement in cellular processes inducible via TNF-α. However, the exact manner in which pfetin interacts and functions with members of this complex signalling cascade awaits further investigation.

REFERENCES

Alterovitz G (2005) A Bayesian Framework for Statistical Signal Processing and Knowledge Discovery in Proteomic Engineering. Ph.D. thesis, Massachusetts Institute of Technology, Cambridge, MA, USA.

Arlt A, Schafer H (2002) NFkappaB-dependent chemoresistance in solid tumors. Int J Clin Pharmacol Ther. 40(8):336-47

Bouwmeester T, Bauch A, Ruffner H, Angrand PO, Bergamini G, Croughton K, Cruciat C, Eberhard D, Gagneur J, Ghidelli S, Hopf C, Huhse B, Mangano R, Michon AM, Schirle M, Schlegl J, Schwab M, Stein MA, Bauer A, Casari G, Drewes G, Gavin AC, Jackson DB, Joberty G, Neubauer G, Rick J, Kuster B, Superti-Furga G (2004) A physical and functional map of the human TNF-alpha/NF-kappa B signal transduction pathway. Nat Cell Biol 6(2):97-105

Bruce AJ, Boling W, Kindy MS, Peschon J, Kraemer PJ, Carpenter MK, Holtsberg FW, Mattson MP (1996) Altered neuronal and microglial responses to excitotoxic and ischemic brain injury in mice lacking TNF receptors. Nat Med 2(7):788-94

Chen ZY, Corey DP (2002) An inner ear gene expression database. J Assoc Res Otolaryngol 3(2):140-8

Chen ZY, Corey DP (2002) Understanding inner ear development with gene expression profiling. J Neurobiol 53(2):276-85

de Hoog CL, Mann M (2004) Proteomics. Annu Rev Genomics Hum Genet 5:267-93

Ducan, B.K and Miller, J.H. (1980) Mutagenic deamniation of cytosine residues in DNA. Nature, 287, 560-561

Ghosh S, May MJ, Kopp EB (1998) NF-kappa B and Rel proteins: evolutionarily conserved mediators of immune responses. Annu Rev Immunol 16:225-60

Ghosh S, Karin M (2002) Missing pieces in the NF-kB puzzle. Cell 109 (Suppl.):S81–S96

Kurtev V, Margueron R, Kroboth K, Ogris E, Cavailles V, Seiser C (2004) Transcriptional regulation by the repressor of estrogen receptor activity via recruitment of histone deacetylases. J Biol Chem 279(23):24834-43

Sigoillot FD, Kotsis DH, Serre V, Sigoillot SM, Evans DR, Guy HI (2005) Nuclear localization and mitogen-activated protein kinase phosphorylation of the multifunctionalprotein CAD. J Biol Chem 280(27):25611-20

Sandu C, Gavathiotis E, Huang T, Wegorzewska I, Werner MH (2005) A mechanism for death receptor discrimination by death adaptors. J Biol Chem 280(36):31974-80

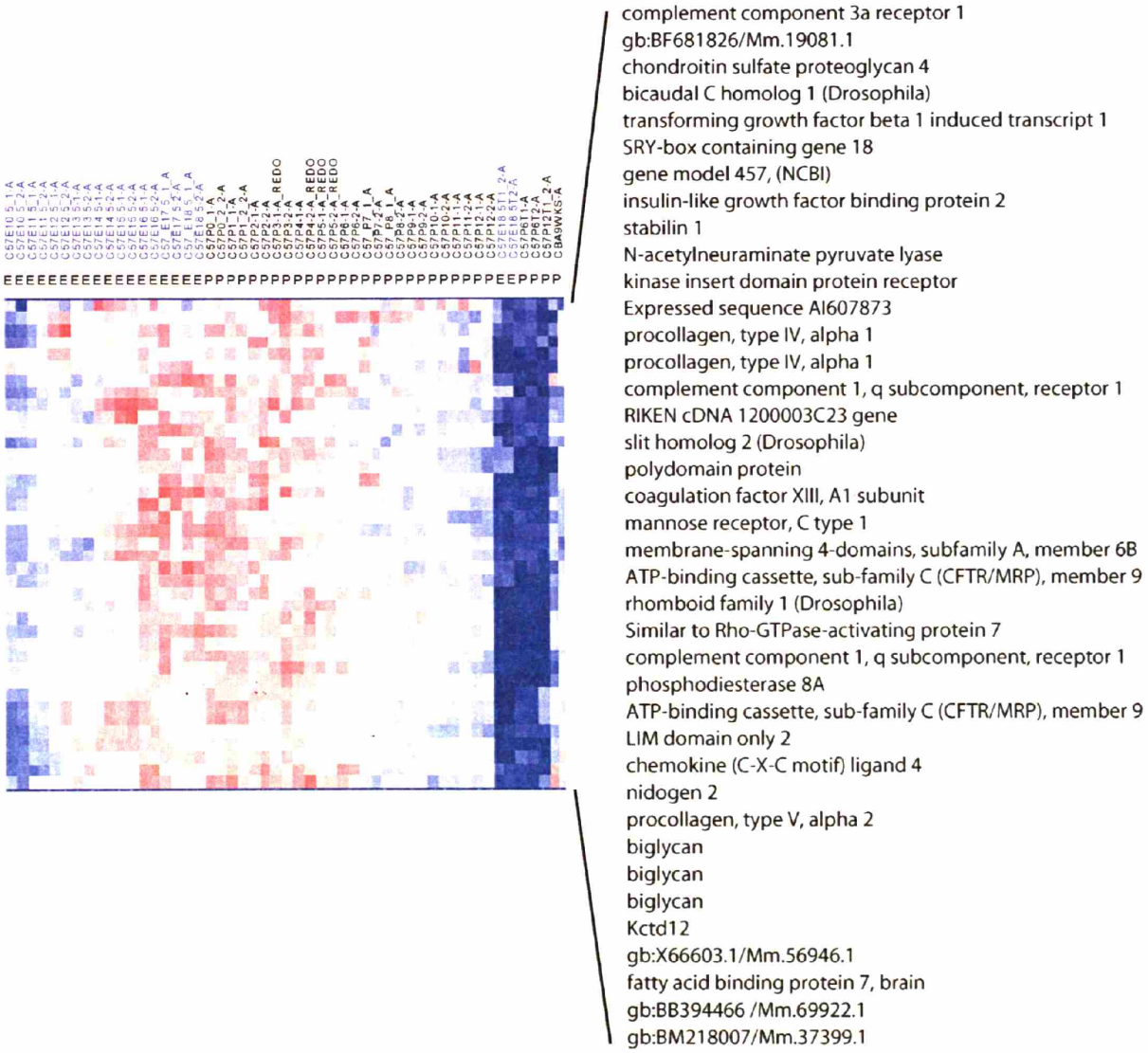

Figure 1. Expression of *Pfet1/Kctd12* in Affymetrix Mouse Genome 430 Array. The left column is a heat map showing the hierarchical clustering of 38 probe sets that reveal a similar expression pattern as *Pfet1/Kctd12*. Each probe set is presented by one row along the Y axis and the samples (mouse developmental stages from embryonic day (E) 10.5 to post-natal day (P)12 are presented in duplicate on the top along the X axis from left to right. The expression level of each probe set is standardized against itself across different developmental stages and is shown in color spectrum from red (high) to blue (low). The column on the right lists the genes associated with each probe set.

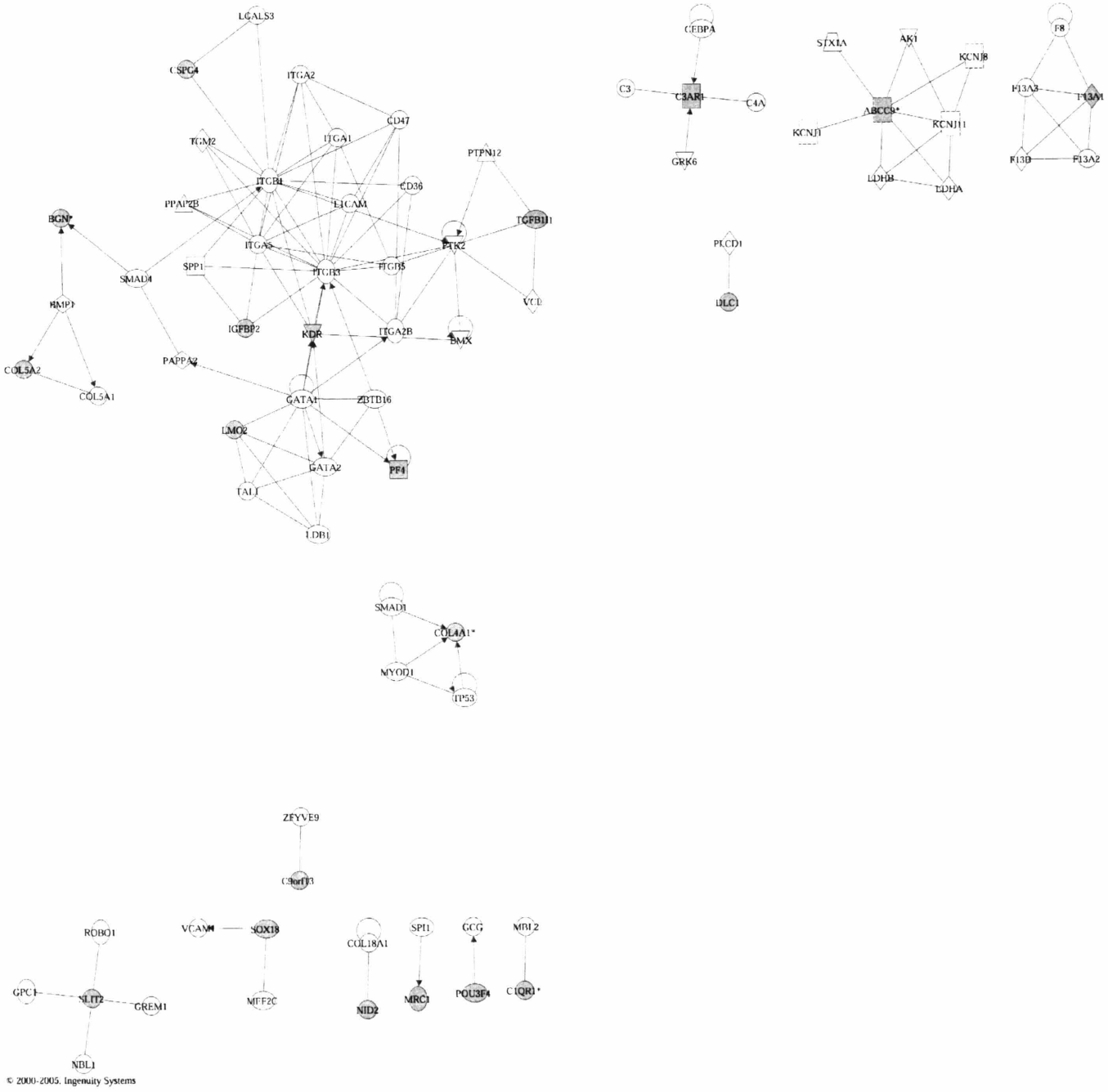

Figure 2. Network graph of 38 cluster genes from Affymetrix Chip analysis. Genes or gene products are represented as nodes, and the biological relationship between two nodes is represented as an edge (line). Filled in nodes represent members of the 38 gene cluster. Gene/Protein IDs marked with an asterisk indicate that multiple identifiers from the input list mapped to a single gene in the Global Molecular Network.

CHAPTER 5

SUMMARY

The cochlea is a complex organ comprised of dozens of cell types and specialized regions required for the normal process of hearing. Of the genes responsible for hearing and deafness, many of the encoded proteins have been shown to be expressed in the cochlea with a variety of functions including transcription factors, potassium ion channels, gap junctions, and extracellular matrix components. As a part of the continuing effort in finding genes important for hearing and deafness, a novel cochlear transcript with a predominantly fetal expression containing a single tetramerization domain (*PFET1*, HUGO-approved symbol *KCTD12*) was identified from the Morton fetal cochlea cDNA library. This thesis reports characterization of this novel human gene and its encoded protein pfetin in relation to its role in auditory function.

KCTD12 was selected through subtractive hybridization and differential screening of human fetal cochlear cDNA clones. *KCTD12/Kctd12* is an evolutionarily conserved intronless gene encoding a 6 kb transcript in human and three transcripts of approximately 4, 4.5 and 6 kb in mouse. The protein, pfetin, is predicted to contain a voltage-gated potassium channel tetramerization (T1) domain. Expression of *KCTD12/Kctd12* or its encoded protein pfetin was characterized in several species including human, monkey, mice, guinea pig, and zebrafish. Of particular interest are the time course and regions of expression in the inner ear. Initial findings demonstrated a striking preferential expression of the human 6 kb transcript in a variety of second trimester human fetal tissues (including brain and cochlea) with dramatically lower expression levels in adult tissues. GeneChip analysis also revealed developmental upregulation of expression of *Kctd12* in the mouse utricle along with a cluster of 38 other genes between stages E13.5 and P6. Real Time RT-PCR substantiated

upregulation of *right on* and *leftover* (*ron* and *lov*: *KCTD12* zebrafish orthologs) during the first 24 hours post fertilization (hpf) of embryo development. Immunohistochemistry with a polyclonal antibody raised against a synthetic peptide to the *KCTD12* sequence revealed immunostaining in a variety of cell types in human, monkey, mouse, and guinea pig cochleas (notably types I, IV and V fibrocytes and spiral ganglion cells) and the vestibular system, including type I vestibular hair cells (Chapter 2). Mouse developmental immunohistochemical analysis demonstrated a dramatic increase in the expression of pfetin in postnatal cochlea. Both *in situ* hybridization with a *ron* riboprobe and immunohistochemistry with a Ron antibody revealed expression of the pfetin zebrafish ortholog in the vestibular-cochlear ganglion (VCG) of the developing zebrafish otic vesicle (Chapter 3).

These observed expression patterns strongly suggest a developmental role for *KCTD12* and its encoded protein. Most of the upregulation in RNA expression was seen spanning or overlapping crucial inner ear developmental milestones. The emergence of otic placode (mouse E8.5, zebrafish 13-14 hpf), the formation of otic vesicles (mouse E9.5, zebrafish ~18.5 hpf), the initiation of auditory hair cells differentiation (mouse E14, zebrafish 24 hpf), and hair cell transduction (mouse E16, zebrafish 36 hpf) all occur during the first 36 hours post zebrafish embryo fertilization and first 16 to 17 days post observation of a vaginal plug in the mouse. Similarly by 20-22 weeks gestational age, the human fetus developed a functional ear to detect sound in its surroundings. Both zebrafish and mouse RNA expression persisted after these inner ear developmental milestones had occurred. There was down-regulation of *Kctd12* in mouse utricle after P6 and of *ron* expression in the zebrafish after 72 hpf. However, there was never any complete secession of expression, at least into early adulthood. In mouse, expression persisted until 12 months (Chapter 2, Fig. 6B) and zebrafish

until after 6 days post fertilization (dpf) (Chapter 3, Fig. 2). In humans, data are not available for *KCTD12* expression during young adulthood. By late adulthood, the 6 kb *KCTD12* transcript has disappeared from various regions of adult brain (Chapter 2, Fig. 5B) perhaps as the result of the ageing process.

Given the expression level from various Northern blot analyses and RT-QPCR experiments, it is difficult to extrapolate from the overall expression level of the whole embryo and whole brain to the expression near the auditory sense organ. Sections from zebrafish *in situ* hybridization provided one of the confirmations of *KCTD12/ron* expression in the developing auditory sense organ (Chapter 3, Fig. 4). Immunohistochemical analysis provided additional evidence in support of the importance of the *KCTD12*-encoded protein pfetin in the developing auditory sense organ with immunostaining signals observed from Ron (pfetin zebrafish ortholog) labeling vestibular-cochlear ganglion (VCG), and immunostaining signals detected from various cells within the mouse cochlea. Immunohistochemical analysis of the human fetal cochlea was inconclusive due to technical issues arising from the fixation of available tissue for study. The common fixative used to preserve fetal tissue can interfere with the binding of antibody to its antigen. Therefore, it is not clear when pfetin begins to be expressed in early human cochlear development.

The developmental protein expression from mouse and zebrafish did not follow the exact time course as that of RNA expression. This is not unusual given the fact that the relationship between RNA and protein expression for many genes is not necessarily well correlated. In fact, the commencement of mouse and zebrafish protein expression lagged behind their respective peak RNA expression and after most of the key inner ear developmental milestones have passed. In zebrafish, protein expression in the VCG region

commenced around 24 hpf and persisted well after 75 hpf (data not shown). In mouse, protein expression in the cochlea commenced postnatally (Appendix to Chapter 2) and then continued well into adulthood (Chapter 2, Fig. 8B). This protein expression time course suggests that perhaps pfetin/Ron might be necessary for the continuing growth and health of the inner ear.

Morpholino experiments further revealed the potential importance of the presence of Ron in the developing VCG by demonstrating a correlation between Ron knock-down and Isl1 (early inner ear neuronal marker) down-regulation in the VCG during early zebrafish development. Isl1 has been postulated to cooperate with NeuroD in the confirmation of inner ear-specific neuronal or sensory competency/identities (Radde-Gallwitz et al. 2004). Therefore, pfetin/Ron could potentially function as an important regulator in the development of inner ear neurons.

The genomic location for *KCTD12* was confirmed by FISH analysis to band q21 on chromosome 13 which presently maps within the vicinity of the *AUNA1* locus (13q14–21) responsible for progressive autosomal dominant auditory neuropathy (Kim et al. 2004). There are no known deafness loci mapped in close proximity to the *KCTD12* mouse ortholog, *Kctd12,* on chromosome 14 or the zebrafish ortholog *right on* on linkage group 1. No pathogenetic sequence variants were detected within the 70% GC-rich *KCTD12* ORF from mutation analysis of a panel of DNAs from individuals from multiplex kindreds without a recognized genetic etiology for their hearing loss. Although much has been learned about *KCTD12* and its encoded protein pfetin through this thesis research, much remains to be known. The discovery and characterization of each new gene expressed in the ear takes us

ever closer to attaining a more complete understanding of this intricate and wonderful life-enhancing process that is human hearing.

REFERENCES

Hao A, Novotny-Diermayr V, Bian W, Lin B, Lim CP, Jing N, Cao X (2005) The LIM/homeodomain protein Islet1 recruits Janus tyrosine kinases and signal transducer and activator of transcription 3 and stimulates their activities. Mol Biol Cell. 16(4):1569-83.

Kim TB, Isaacson B, Sivakumaran TA, Starr A, Keats BJ, Lesperance MM (2004) A gene responsible for autosomal dominant auditory neuropathy (AUNA1) maps to 13q14-21. J Med Genet. 41(11):872-6.

Radde-Gallwitz K, Pan L, Gan L, Lin X, Segil N, Chen P (2004) Expression of Islet1 marks the sensory and neuronal lineages in the mammalian inner ear. J Comp Neurol. 477(4):412-21.

Van Camp G, Smith RJH (2005) Hereditary hearing loss homepage. WWW URL: http://www.uia.ac.be/dnalab/hhh/

APPENDIX

Appendix to Chapter 2:

Isolation from Cochlea of a Novel Human Intronless Gene with Predominant Fetal Expression

Mouse Developmental Immunohistochemistry

Materials and Methods

Tissue preparation and immunohistochemical staining procedures were performed as previously described (Resendes et al., 2004). ICR mice were crossed to produce embryos. The day the vaginal plug was found was identified as E0.5. Cochleas from mouse developmental ages embryonic stages 13.5 and 17.5, and postnatal day 1 and 10 were collected for this study. Primary anti-PFET1 antibody was diluted between 1:200 and 1:500.

Result/Discussion

Similar to the expression pattern observed in adult mouse cochlea in postnatal days 1 and 10 mouse cochlear sections, immunostained cells included various fibrocytes (predominately types I and IV) in the spiral ligament, limbal fibrocytes and supralimbal and interdental cells in the limbus, and spiral ganglion cells. Unlike the adult cochlear expression, immunostaining was observed in almost all cell types within the cochlea at postnatal day 1. Immunostaining of individual cell types became distinguishable by postnatal day 10. However, no pfetin immunostained cells were observed in embryonic mouse cochlea. Although Northern blot analysis revealed early *Kctd12* expression in developing embryonic mouse whole brain and embryo tissues, it is well known that the relationship between RNA and protein expression for many genes is not necessarily well correlated, and appears to be the situation observed here for *Kctd12*. Immunohistochemical analysis of developing mouse

cochlea indicated a dramatic up-regulation of the expression of pfetin during transition from the embryonic to postnatal stage. Such tightly regulated yet widely distributed expression of pfetin in mouse cochlea during the early postnatal stage lends further support to the importance of *Kctd12* during cochlear development.

REFERENCES:

Resendes BL, Kuo SF, Robertson NG, Giersch AB, Honrubia D, Ohara O, Adams JC, Morton CC (2004) Isolation from cochlea of a novel human intronless gene with predominant fetal expression. J Assoc Res Otolaryngol 5(2):185-202. (co-first authors)

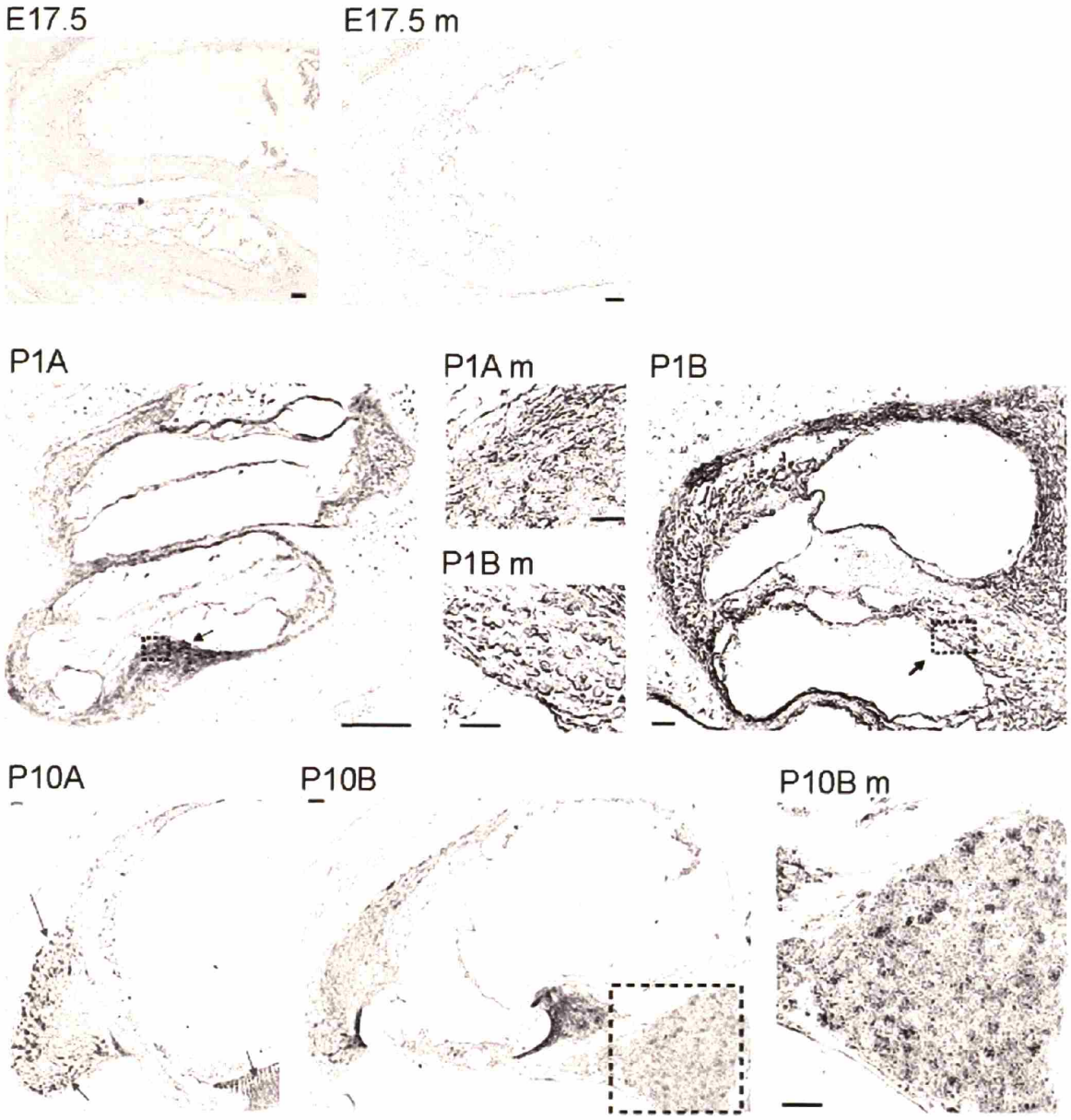

Figure Caption.
Pfetin immunostaining of developmental mouse cochleas E17.5, P1 and P10. Developing E17.5 mouse cochlea is shown at the top. Higher magnification of the boxed region for E17.5 is shown to its right labeled as E17.5m. Higher magnification of the boxed regions for P1 are shown in the center labeled as P1A m and P1B m (m for magnification). The arrows in P1 point to immunostained acoustic ganglions in the developing modiolus. Arrows in P10 point to immunostained types I and IV fibrocytes (left up and down) and limbal fibrocytes (right). Higher magnification of the boxed region for P10B is shown to the right labeled as P10B m. All scale bars represent 25μm, except for P1A which is 250μm. E = embryonic, P= postnatal